UNIVERSITY OF THE
WITWATERSRAND,
JOHANNESBURG

THE EFFECTS OF ACUTE LPS-INDUCED INFLAMMATION ON CARDIAC MORPHOLOGY, GEOMETRY AND FUNCTION IN SPONTANEOUSLY HYPERTENSIVE RATS

by

Kealeboga Mme Fako

A dissertation submitted to the Faculty of Health Science, University of the Witwatersrand, Johannesburg, in fulfilment of the requirements for the degree of Master of Science in Medicine

June 2024

Declaration

I, Kealeboga Mme Fako, declare that this dissertation is my own work, except where I indicated in the acknowledgements section. It is being submitted for the degree of Master of Science in Medicine in the School of Physiology, Faculty of Health Sciences, University of the Witwatersrand, Johannesburg. The work contained in this dissertation has not been submitted before for any degree or examination at this or any other university.

I hereby certify that the study contained in this dissertation has been approved by the Animal Research Ethics Committee, University of the Witwatersrand, Johannesburg. The ethics approval number is 2022/05/03/C.

……

Kealeboga Mme Fako

Signed on 12th day of June 2024

……

Assoc Prof Aletta Millen

12th day of June 2024

……

Assoc Prof Frederic Michel

12th day of June 2024

Abstract

It has been established that systemic inflammation negatively impacts myocardial structure and function, especially in individuals with comorbidities such as hypertension. Acute exposure to lipopolysaccharide (LPS), resulting in acute high-grade inflammation, has been demonstrated to induce cardiomyocyte oedema and apoptosis in the short-term, resulting in left ventricular (LV) systolic and diastolic dysfunction. While exposure to LPS-induced inflammation causes LV dysfunction in the short-term, the long-term consequences of exposure to acute high-grade inflammation on the structure and function of the heart remain unclear. Therefore, the current study aimed to ascertain the immediate and long-term effects of a single exposure to LPS on the structure and function of the heart and its potential compounding effects in a hypertensive model.

Wistar-Kyoto rats (WKY, n=36) and spontaneously hypertensive rats (SHR, n=38) were randomly divided into two groups per rat strain. The control groups (WKY-control and SHR-control) received one injection of saline (1 ml/kg, i.p.). The LPS groups (WKY-LPS and SHR-LPS) received one injection of LPS (1 mg/kg, i.p.). Animals were then terminated either 24 hours (WKY, n=11; SHR, n=16) or 6 weeks (WKY, n=25; SHR, n=22) after the saline or LPS injections. Prior to termination, conventional and speckle-tracking echocardiography were performed on all animals under anaesthesia to ascertain the effects of LPS on LV geometry, systolic and diastolic function. Following termination, heart tissues were removed and weighed prior to storage. Total collagen content in the left ventricle was determined using the Picrosirius red stain. A mixed model two-way analysis of variance (ANOVA) was used to ascertain differences in echocardiographic parameters, the inflammatory cytokine

and fibrosis, followed by a Tukey's *post hoc* test. Pearson's correlation was used to determine associations between collagen volume and echocardiographic parameters.

After 24 hours, LPS administration significantly increased interleukin (IL)- 1β concentrations in WKY-LPS ($p = 0.02$), and SHR-LPS ($p = 0.03$) groups compared to their respective control groups. LPS-induced inflammation resulted in impaired LV diastolic function as indicated by impaired LV relaxation (E/A, septal and average e') in SHR-LPS compared to SHR-control (all $p < 0.05$). LV passive stiffness (e'/a') increased significantly in WKY-LPS compared to WKY-control ($p = 0.05$). However, heart weight was significantly higher in SHR-LPS compared to WKY-LPS due to hypertension, not inflammation ($p = 0.02$).

LPS-induced inflammation also significantly decreased LV systolic function in the short-term, as indicated by a reduced left ventricular outflow tract (LVOT) velocity time integral (VTI, $p = 0.0004$) and LVOT peak velocity (V_{max}, $p = 0.008$) in SHR-LPS compared to SHR-control. Hypertension significantly decreased left ventricular ejection fraction (LVEF, $p = 0.02$) and endocardial fractional shortening ($FS_{end,}$ $p = 0.03$), which are markers of global systolic function, in SHR-LPS compared to WKY-LPS. LVOT VTI ($p = 0.02$) and V_{max} ($p = 0.03$) were significantly lower in the SHR-LPS compared to WKY-LPS in response to hypertension.

LPS administration significantly reduced circumferential ($p = 0.03$) and longitudinal strain ($p = 0.02$), which are markers of early systolic dysfunction, in SHR-LPS compared to SHR-control. Hypertension significantly reduced circumferential ($p = 0.0004$) and longitudinal strain ($p = 0.01$), in SHR-control compared to WKY-control, and in SHR-LPS compared to WKY-LPS (both $p < 0.0001$). There were also reductions in circumferential strain rate in SHR-control compared to WKY-control ($p = 0.01$), and

in both circumferential ($p < 0.0001$) and longitudinal strain rate ($p = 0.0005$), in SHR-LPS compared to WKY-LPS.

In the animals that were terminated 6 weeks after LPS exposure, there were no differences in IL- 1β (all $p > 0.05$). LPS-induced inflammation had no effect on any of the LV diastolic or systolic function parameters in any of the groups (all $p > 0.05$). However, heart weight ($p = 0.03$) and normalised heart weight ($p = 0.02$) were significantly higher in SHR-control compared to WKY-control due to hypertension. Similarly, heart weight ($p = 0.02$) and normalised heart weight ($p = 0.0006$) were significantly higher in SHR-LPS compared to WKY-LPS in response to the effect of hypertension. Hypertension significantly impaired LV relaxation (reduced septal e') in SHR-control compared to WKY-control ($p = 0.04$) and in SHR-LPS compared to WKY-LPS ($p = 0.04$).

LPS-induced inflammation had no significant effects on LVOT VTI and LVOT V_{max} (all $p > 0.05$). Hypertension significantly reduced LVEF ($p = 0.03$) and FS_{end} ($p = 0.04$) in SHR-control compared to WKY-control, as well as LVOT VTI in SHR-control compared to WKY-control ($p = 0.04$). LPS administration had no significant consequences on circumferential and longitudinal strain as well as circumferential and longitudinal strain rate (all $p > 0.05$). Hypertension significantly decreased circumferential ($p = 0.005$) and longitudinal strain ($p < 0.0001$) in SHR-control compared to WKY-control, and longitudinal strain in SHR-LPS compared to WKY-LPS ($p = 0.002$). There were also reductions in circumferential ($p = 0.01$) and longitudinal strain rate ($p < 0.0001$) in SHR-control compared to WKY-control, and in longitudinal strain rate in SHR-LPS compared to WKY-LPS ($p = 0.002$) due to hypertension.

In the short-term groups, inflammation was significantly associated with impaired LV relaxation and passive stiffness, while collagen volume was significantly associated with impaired LV relaxation and myocardial deformation. In the long-term groups, inflammation was associated with impaired LV relaxation, passive stiffness, myocardial deformation and collagen volume, while collagen volume was significantly associated with impaired LV relaxation.

In conclusion, acute LPS-induced high-grade inflammation resulted in impaired LV diastolic and systolic function after 24 hours. These changes were worsened in the animals predisposed to hypertension. Although majority of the LV systolic and diastolic function variables were reversed after six weeks, alterations in morphological and myocardial deformation were not reversed. Therefore, a single dose of LPS administration may impact structural remodelling and myocardial strain in rats predisposed to hypertension in the long-term.

Acknowledgements

I would like to sincerely express my gratitude and appreciation to my supervisors, Prof Aletta Millen and Prof Frederic Michel, who went above and beyond to ensure that we met the submission deadline. Thank you for your support and guidance, for your technical assistance, your valuable advice and constructive comments throughout the study and during the write-up process. I would also like to thank Ms Leandrie Pienaar and Ms Tiiso Maluleke, for assisting with data collection, animal feeding and terminations when I was not available to do so. I would like to express my gratitude to the National Research Foundation, Integrated Molecular Physiology Research Initiative and the University of the Witwatersrand for funding of this project and my studies. I would like to express my gratitude to Dr Monica Gomes for performing the enzyme-linked immunosorbent assay and assisting with the histological staining. I am grateful to the Wits Research Animal Facility staff for assisting in taking care of the rats utilised in this study. Thank you to my family (especially my mother and sister), friends and accountability buddy, Nkhluleko, for their constant support and motivation throughout the course of this degree. Lastly, thank you to my partner, who has been my biggest source of inspiration and greatest supporter.

Table of contents

List of figures

List of tables

List of abbreviations

A	late mitral valve inflow velocity
a'	late annular tissue lengthening velocity
ANOVA	analysis of variance
AREC	Animal research ethics committee
ATP	adenosine triphosphate
Ca^{2+}	calcium
cGMP	cyclic guanosine monophosphate
COVID- 19	coronavirus disease- 19
CS	circumferential strain
CSR	circumferential strain rate
CVD	cardiovascular disease
CVF	collagen volume fraction
E	early mitral valve inflow velocity
e'	early annular tissue lengthening velocity
E/A	ratio of early to late mitral inflow velocity
e'/a'	ratio of early to late annular tissue velocity
E/e'	ratio of early mitral inflow velocity to early annular tissue velocity
ECM	extracellular matrix
ELISA	enzyme-linked immunosorbent assay
FS	fractional shortening
FSend	endocardial fractional shortening
FSmid	mid-wall fractional shortening
Heart mass/BW	heart mass normalised to body weight

HFmrEF	heart failure with a mid-range ejection fraction
HFpEF	heart failure with a preserved ejection fraction
HFrEF	heart failure with a reduced ejection fraction
i.p.	intraperitoneal
i.v.	intravenous
IL- 1β	interleukin-1β
IL- 6	interleukin-6
IQR	interquartile range
IVSd	interventricular septal wall thickness at end-diastole
IVSs	interventricular septal wall thickness at end-systole
LPS	lipopolysaccharide
LS	longitudinal strain
LSR	longitudinal strain rate
LV	left ventricle
LV mass/BW	left ventricular mass normalised to body weight
LVEDD	left ventricular end-diastolic diameter
LVEDV	left ventricular end-diastolic volume
LVEF	left ventricular ejection fraction
LVESD	left ventricular end-systolic diameter
LVESV	left ventricular end-systolic volume
LVOT Vmax	left ventricular outflow tract peak velocity
LVOT VTI	left ventricular outflow tract velocity time integral
LVPWd	left ventricular posterior wall thickness at end-diastole
LVPWs	left ventricular posterior wall thickness at end-systole

Na^+	sodium
NF- κB	nuclear factor- κB
NO	nitric oxide
PKG	protein kinase-G
RWT	relative wall thickness
s'	early systolic mitral annular velocity
SD	standard deviation
SERCA	sarcoplasmic reticulum Ca2+-ATPase
SHR	spontaneously hypertensive rat
STE	speckle tracking echocardiography
TLR- 4	toll-like receptor- 4
TNF- α	tumour necrosis factor- α
WKY	Wistar Kyoto rats
WRAF	Wits research animal facility

Chapter 1: Introduction

One of the leading causes of morbidity and death globally is hypertension, which is a significant risk factor for cardiovascular disease (CVD) (Mills *et al.*, 2020). In 2019 alone, hypertension caused approximately 10.8 million deaths worldwide (Micklesfield *et al.*, 2022). The prevalence of high blood pressure has been steadily increasing worldwide (Mills *et al.*, 2020), with World Health Organisation estimating 1.3 billion people living with hypertension globally (Geneva: World Health Organization (WHO), 2023).

In South Africa, hypertension causes more burden than in high-income countries, such as the United Kingdom and Canada (Mills *et al.*, 2020). Although antihypertensives are readily available in low-income countries, which can effectively reduce blood pressure, the disease control still remains suboptimal (Schutte *et al.*, 2021). Only 24% of adults with hypertension in South Africa are diagnosed, undergo treatment and have their hypertension under control (World Health Organization (WHO), 2023). The increased burden of hypertension emphasises the need for further investigations regarding its pathophysiology and improved control.

Hypertension, along with other risk factors such as age, influence the pathogenesis of heart failure with a preserved ejection fraction (HFpEF) (Borlaug, 2020). HFpEF is a clinical condition characterised by the inability of the heart to adequately fill with blood during diastole, leading to symptoms of congestion (Bozkurt *et al.*, 2021). Half of all heart failure cases are accounted for by HFpEF, and its prevalence is continuing to increase (Nair, 2020). Therefore, investigating the risk factors and how they interact in the progression of HFpEF is imperative.

It was shown recently that sepsis increased the risk of developing myocardial infarction, congestive heart failure and stroke up to 5 years after recovering from the

condition (Kosyakovsky *et al.*, 2021). Indeed, sepsis plays an independent role in the increased risk of CVD development (Angriman *et al.*, 2022). According to The Third International Consensus Definitions task force, sepsis is defined as uncontrolled inflammatory host response to infection, that is life-threatening and targets the organs, including the heart (Singer *et al.*, 2016). Sepsis is characterised by an imbalanced immune response, that results in a hyper-inflammatory state accompanied by a suppressed immune system (van der Poll *et al.*, 2017). The increased inflammation causes all the harmful effects seen in sepsis patients (van der Poll *et al.*, 2021). The incidence of sepsis was 233.6 per 100 000 people in 2016, compared to 175.9 in 2011 (Kang *et al.*, 2024). In a six-year sepsis study, 47% of the hospitalised patients diagnosed with sepsis had pre-existing hypertension (Kang *et al.*, 2024). Therefore, the pathogenesis and management of inflammation need to be further elucidated. Furthermore, the mechanisms by which an increased inflammatory response causes myocardial dysfunction in sepsis patients years after recovery ought to be investigated.

The present dissertation commences with a literature review in chapter 2, that outlines the most recent findings on HFpEF, hypertension and inflammation. Chapter 2 will also provide the knowledge gaps and inconsistencies in the development of LV diastolic and systolic dysfunction that emphasise the need for conducting this study. The methods are described in chapter 3 and the findings are presented in chapter 4. Chapter 5 discusses the findings from this study in context to the previous findings, and chapter 6 concludes and lists the limitations and potential future implications of the present study.

Chapter 2: Literature review

2.1 Heart failure

Heart failure is a heterogeneous condition characterised by the inability of the heart to maintain metabolic demands of the body, resulting in exhaustion, breathing difficulties and oedema (Kemp & Conte, 2012). Heart failure affects 1-3% of adults, which significantly contributes to the burden of disease worldwide (Groenewegen *et al.*, 2020). Heart failure can be classified into subtypes according to left ventricular (LV) ejection fraction (EF) (Savarese *et al.*, 2022). A LVEF below 40% describes heart failure with a reduced LVEF (HFrEF), while LVEF equal or greater than 50% describes heart failure with a preserved LVEF (HFpEF) (Bozkurt *et al.*, 2021). LVEF between 40% and 50% describes heart failure with a mid-range LVEF (HFmrEF) (Bozkurt *et al.*, 2021; Savarese *et al.*, 2022).

The cause of heart failure is multifactorial, and different events or risk factors are linked to the different classifications of heart failure (Savarese *et al.*, 2022). For instance, an impaired pump capacity and reduced systolic function characterise HFrEF, which is largely caused by a significant loss of functional cardiomyocytes due to injury or damage (Van Heerebeek *et al.*, 2006). In contrast, an impaired ability of the LV to relax during diastole and fill with blood characterises HFpEF, which has been ascribed to the stiffening of the myocardium (Yamamoto *et al.*, 2002). Although both HFrEF and HFpEF have similar physiological symptoms, their aetiology, management and treatment are very different (Simmonds *et al.*, 2020). In this regard, the aetiology of HFrEF has been well described and treatment and management strategies have been effective (Balmforth *et al.*, 2019). In contrast, the aetiology of HFpEF is poorly understood and is believed to be heterogeneous (Tschöpe & Van Linthout, 2014; Lewis *et al.*, 2017). Hence, it is not surprising that the therapy of HFpEF has puzzled

the cardiovascular scientific community for some time (Lewis *et al.*, 2017). Moreover, HFpEF is becoming more prevalent and accounts for more than half of heart failure occurrences (Dunlay *et al.*, 2017). Therefore, in the next chapters, I will discuss some of the aspects contributing to HFpEF and identify areas of uncertainty that were investigated in this research.

2.2 Heart failure with a preserved ejection fraction

As mentioned above, in HFpEF, the heart is unable to adequately relax and fill with blood during diastole (Savarese *et al.*, 2022). HFpEF is often preceded by LV diastolic dysfunction, a preclinical change in cardiac function that is characterised by impaired relaxation (Redfield *et al.*, 2003), and increased LV stiffness (Borbély *et al.*, 2005). This impaired relaxation and stiff ventricle prevent adequate LV filling during diastole (Zile *et al.*, 2004). Therefore, even though pump and systolic function is adequate, decreased LV end-diastolic volume results in a low cardiac output, and hence the characteristic heart failure symptoms (Hamdani *et al.*, 2013; Tan *et al.*, 2017).

2.2.1 Characteristics and measures of LV diastolic dysfunction

During diastole, the ventricles relax to ensure adequate filling of the LV with blood for the subsequent cardiac cycle (Savarese *et al.*, 2022). As mentioned in the preceding section, impaired LV relaxation and elevated passive stiffness are the hallmarks of LV diastolic dysfunction. Hence, it is suggested that both passive and active processes contribute to myocardial relaxation (Borlaug & Kass, 2006). The passive processes are important for diastolic relaxation as they facilitate adequate compliance, which allows the LV to recoil (Biesiadecki *et al.*, 2014). LV diastolic

dysfunction arises when structural or functional LV abnormalities prevent the myocardium to recoil, and hence prevents adequate LV filling during diastole (Kapila & Mahajan, 2009). On the other hand, active processes require adenosine triphosphate (ATP) to facilitate the removal of calcium (Ca^{2+}) from the cytosol to allow for the dissociation of the cross-bridges formed during LV contraction (Biesiadecki *et al.*, 2014). Based on these two processes, the fundamental features of LV diastolic dysfunction are raised LV end-diastolic as well as left atrial pressures (Chinnaiyan *et al.*, 2007; Lewis *et al.*, 2017).

Structural and functional changes in LV diastolic dysfunction are routinely diagnosed by echocardiography (Chu *et al.*, 2019). Two-dimensional (2D) or M-mode echocardiography is used to determine LV internal chamber diameter and wall thickness in systole and diastole, which together determine the presence of structural remodelling (Shah *et al.*, 2019). The internal chamber diameter relative to the wall thickness are utilised to determine the relative wall thickness (RWT) and LV mass, which are both indices of concentric or eccentric LV hypertrophy patterns (Nistri *et al.*, 2008). Concentric LV hypertrophy is a mild and early alteration in heart geometry and is linked to LV diastolic dysfunction (Cuspidi *et al.*, 2002). Nevertheless, substantial morphological heterogeneity has been reported in LV diastolic dysfunction and hence not all patients present with concentric hypertrophy or increased LV mass (Lewis *et al.*, 2017).

In addition to structural and geometric remodelling, echocardiography is often used to assess functional diastolic measures (Zile *et al.*, 2004; Abhayaratna *et al.*, 2006). Pulsed-wave Doppler is used to measure early (E) or late (A) mitral inflow velocities, and the ratio of E/A indicates LV relaxation (Kasner *et al.*, 2011). Tissue

Doppler imaging measures rate of tissue lengthening at the mitral annulus during early (e') or late (a') diastole (Redfield *et al.*, 2003). One of the early markers of poor relaxation is impairments in the early mitral annulus lengthening velocity (e') (Nagueh *et al.*, 1997), while the e'/a' ratio indicates LV stiffness (Redfield *et al.*, 2003). LV filling pressures are measured as E/e' (Kasner *et al.*, 2011). Indeed, these echocardiographic measures of impaired relaxation (E/A and e'), increased stiffness (e'/a') and elevated filling pressures (E/e'), are reported in patients with LV diastolic dysfunction (Andersen *et al.*, 2017), and are linked to HFpEF pathogenesis (Wachtell *et al.*, 2000; Kasner *et al.*, 2011).

2.2.2 Characteristics and measures of LV systolic dysfunction

Besides diastolic function, systolic function is also routinely measured by echocardiography (Shvilkina & Shapiro, 2023). As mentioned above in section 2.2.1, chamber sizes and volumes can be measured using either M-mode echocardiography or using more sophisticated volumetric techniques, such as Simpson's biplane (Bellenger *et al.*, 2000). These measures are used to calculate endocardial (FS_{end}) or mid-wall fractional shortening (FS_{mid}) and LVEF (Schussheim *et al.*, 1998; Shah *et al.*, 2019). However, these measures are global measures of pump function and contractility, and are largely influenced by heart rate, afterload, preload as well as changes in the cardiac geometry (Stokke *et al.*, 2017). In this regard, LVEF may remain normal with the presence of concentric hypertrophy regardless of decreased stroke volume or cardiac output (Tan *et al.*, 2017; Chu *et al.*, 2019). Therefore, due to geometric influence, LVEF does not accurately reflect the more sensitive measures of systolic function in HFpEF (Stokke *et al.*, 2017).

Besides diastolic abnormalities, subclinical myocardial systolic dysfunction has been documented in HFpEF patients (Guan *et al.*, 2019). Recently in our lab, we have shown in a model of LV diastolic dysfunction induced by inflammation, that despite normal LVEF and FS_{end}, rats present with subclinical systolic dysfunction (Mokotedi *et al.*, 2020; Denga *et al.*, 2023). In this regard, two-dimensional speckle tracking echocardiography (STE) is a novel, precise technique used in measuring myocardial strain, which is used to assess subclinical LV systolic function (He *et al.*, 2021). Myocardial strain is a measurement of length and velocity of LV segments in the longitudinal or circumferential planes in different axes over several cardiac cycles (Stokke *et al.*, 2017). STE measures myocardial strain with increased sensitivity and precision (Chu *et al.*, 2019), providing an advantage over the use of conventional echocardiographic determination of systolic function. Another method of measuring LV systolic function that outperforms LVEF is left ventricular outflow tract (LVOT) velocity time integral (VTI), which is an index for stroke volume and measures the amount of blood ejected (Nistri *et al.*, 2008). LVOT VTI has been used to predict disease severity in hospitalised patients with HFpEF (Omote *et al.*, 2020). In addition, LVOT V_{max} is the maximal velocity of blood that flows through the LVOT, and together with LVOT VTI ascertain the capacity of the LV to pump blood, and hence a more precise method in assessing LV pump function (Nistri *et al.*, 2008).

While echocardiography has been a major tool in achieving consensus regarding the definition of LV diastolic dysfunction, it is established that this syndrome includes a sizable group of individuals with various comorbidities (Paulus & Tschöpe, 2013). However, as mentioned above, the underlying disease mechanisms of LV diastolic dysfunction are partially misunderstood. The many cellular pathways involved

in LV diastolic dysfunction are responsible for the incomplete comprehension around its pathogenesis. (Lewis *et al.*, 2017). In the following section, I will briefly highlight some of the known molecular pathways that lead to LV diastolic dysfunction.

2.2.3 Molecular mechanisms of LV diastolic dysfunction

The pathogenesis of LV diastolic dysfunction has been linked to several molecular mechanisms, making its management challenging (Simmonds *et al.*, 2020). Different molecular mechanisms are believed to contribute to the passive and active processes implicated in LV diastolic dysfunction (Franssen & González Miqueo, 2016). With regards to increases in LV stiffness, it is suggested that both extracellular matrix (ECM) remodelling and changes in the functional properties of cardiomyocytes contribute to its development (Borbély *et al.*, 2005; Zile *et al.*, 2015).

The myocardial ECM consists of a network of fibres of structural or non-structural proteins, including collagen and elastin, and several cells such as fibroblasts, leukocytes as well as cardiac myocytes and vascular cells (Rienks *et al.*, 2014). The structural protein collagen comprises the majority of the ECM content and provides support and strength to the myocardium (Pauschinger *et al.*, 1999). Cardiac collagen is produced and broken down to maintain a stable balance and consistent volume in the ECM (Zile *et al.*, 2015). The overall amount of collagen in the ECM is the result of balancing collagen production and degradation, post-translational modifications and post-synthetic processing (López *et al.*, 2012; Zile *et al.*, 2015). Increased rate of collagen synthesis in relation to the rate of degradation leads to an increased collagen volume (González *et al.*, 2018*b*). In addition, when collagen degradation is increased through the action of matrix metalloproteinases, whose

function is to degrade extracellular matrix components, the degraded products in turn stimulate the production of collagen (Li *et al.*, 2000). However, this stimulation often leads to disorganised collagen synthesis as well as a change in the collagen isoform (Westermann *et al.*, 2011; López *et al.*, 2012).

Indeed, collagen exists in two isoforms; the more rigid collagen type I and the more compliant collagen type III (Pauschinger *et al.*, 1999). Based on the isoform that dominates the ECM, collagen may affect the ECM structural properties (Kasner *et al.*, 2011). Besides increased collagen turnover, post-synthetic processes such as collagen cross-linking play a further role in fibrotic formation, and hence the altered ECM properties (López *et al.*, 2012). Several pathological conditions have shown to disrupt the balance of collagen turnover and cross-linking, which may lead to cardiac fibrosis (Westermann *et al.*, 2011). Various comorbidities including diabetes mellitus, obesity and hypertension, have been linked to a disruption in the homeostasis of collagen, which is highly prevalent and an important contributor to HFpEF development (Paulus & Tschöpe, 2013; Zile *et al.*, 2015). Indeed, myocardial biopsies of HFpEF patients had higher collagen content, with a shift in the isoform from the compliant collagen type III to the rigid collagen type I and increased cross-linking between collagen fibres (Paulus & Zile, 2021). These changes in collagen volume and isoform have been strongly associated with LV passive stiffness in LV diastolic dysfunction (Westermann *et al.*, 2011).

As previously mentioned in section 2.2, although the definition of HFpEF suggests that the condition is characterised by diastolic abnormalities, evidence suggests that the existence of HFpEF-related impaired LV systolic cardiac function

(Fukuta & Little, 2007). However, the current cellular mechanisms underlying these observations are limited and indirect (Nagueh, 2021). Nevertheless, it is suggested that ECM changes and interstitial fibrosis are the most plausible contributors to impaired regional systolic dysfunction, as it may interfere with contraction force generation and transmission (Tyagi, 2000; Maragiannis *et al.*, 2018; Frangogiannis, 2021). Considering that systolic dysfunction in HFpEF patients is a sign of a worse clinical outcome (Omote *et al.*, 2020), better comprehension of the mechanisms involved in systolic dysfunction in HFpEF is necessary.

Besides ECM remodelling, it has been proposed that changes in the properties of the cardiomyocytes also contribute to increased LV passive stiffness (Borbély *et al.*, 2005). In cardiomyocytes, LV passive stiffness depends largely on titin, a giant cytoskeletal protein which acts as a molecular spring in the sarcomere (Fukuda *et al.*, 2005). In the adult myocardium, titin exists in two isoforms; namely, the N2B isoform, which is shorter and stiffer, and the N2BA isoform, which is longer and more compliant (Fukuda *et al.*, 2005; Zile *et al.*, 2015). The myocardium co-expresses both the N2B and N2BA isoforms in a balanced ratio in healthy persons (Zile *et al.*, 2015). However, in HFpEF patients, there is a shift towards the expression of the N2B isoform, which is responsible for the increased LV passive stiffness (Van Heerebeek *et al.*, 2006). Besides the changes in the titin isoform, LV passive stiffness is further regulated by the phosphorylation status of titin (Paulus & Tschöpe, 2013). Several molecular pathways, including cyclic guanosine monophosphate (cGMP)-dependent protein kinase-G (PKG) have been proposed to regulate titin phosphorylation (Krüger *et al.*, 2009). Indeed, in patients with HFpEF low levels of PKG and hypophosphorylation of

the N2B subunit of titin have been strongly associated with the increased LV passive stiffness (Borbély *et al.*, 2009; Van Heerebeek *et al.*, 2012).

During systole, cytosolic Ca^{2+} facilitates cross-bridge formation that results in cardiac contraction (Grossman, 1991). Following contraction, the myocardium needs to relax and reduce the LV pressure, to allow the opening of the mitral valve to adequately fill the LV with blood for the subsequent cardiac cycle (Grossman, 1991). The process of active relaxation largely depends on mitochondrial function to produce ATP that is needed by the sarcoplasmic reticulum Ca^{2+}-ATPase (SERCA) pump for the reuptake of Ca^{2+} into the sarcoplasmic reticulum (Griffiths & Rutter, 2009). In LV diastolic dysfunction, it has been proposed that increased cytosolic Ca^{2+} concentrations during diastole caused prolonged actin-myosin cross-bridge activation, resulting in increased resting tension, and thus impaired LV relaxation (Selby *et al.*, 2011; Kilfoil *et al.*, 2020). In this regard, Ca^{2+} leaking into the cytosol from the sarcoplasmic reticulum via dysfunctional sodium (Na^{+}) - Ca^{2+} exchanger have been suggested to contribute to an inability of the LV to relax during diastole (Selby *et al.*, 2011). Others have suggested that abnormalities in the SERCA pump function lead to impaired Ca^{2+} reuptake from the myocardial cells, also contributing to impaired relaxation (Kilfoil *et al.*, 2020). Similarly, others have suggested that changes in LV passive stiffness may be the main contributor in the development of LV diastolic dysfunction (Sakata *et al.*, 2013). Nevertheless, further research is needed to better understand the pathophysiological mechanisms underlying the development of LV diastolic dysfunction.

Since it is well known that LV diastolic dysfunction has several heterogeneous phenotypes (Redfield *et al.*, 2003), it is important to further consider the risk factors

that are associated with its development. In this regard, a variety of comorbid conditions have been linked to the pathogenesis of LV diastolic dysfunction including obesity, ageing and diabetes mellitus (Franssen *et al.*, 2016). However, hypertension is still considered a primary factor involved in the decline of LV diastolic function and HFpEF (Hicklin *et al.*, 2020).

2.3 Contribution of hypertension to LV diastolic dysfunction

In South Africa, as of 2019, there are at least 45% of people who live with hypertension (Geneva: World Health Organization (WHO), 2023). Hypertension is classified as systolic blood pressure greater than 140 mmHg and diastolic blood pressure greater than 90 mmHg (Szelényi *et al.*, 2015). It has been shown that if hypertension is poorly managed, there is a 36% likelihood that it will ultimately result in LV diastolic dysfunction or HFpEF (De Simone *et al.*, 2005; Border *et al.*, 2007; Rayner, 2010). In this regard, there are several physiological mechanisms whereby hypertension can lead to LV diastolic dysfunction (Wachtell *et al.*, 2000). However, the most well documented consequences of hypertension that contribute to LV diastolic dysfunction are LV remodelling and fibrosis (González *et al.*, 2018*a*).

Long-standing high blood pressure leads to LV remodelling which includes changes in the size, shape, structure and function of the LV (De Simone *et al.*, 2005; Zile *et al.*, 2011). One of the main characteristics of hypertension-induced LV structural remodelling is LV hypertrophy (Izzo & Gradman, 2004). Briefly, an increased blood pressure increases the afterload, and hence the workload of the LV (Grossman *et al.*, 1975). To maintain an adequate stroke volume against the increase in LV afterload, there is a compensatory increase in myocardial wall thickness to maintain the force of contraction (Grossman *et al.*, 1975). Increased wall thickness without a change in

chamber volume results in the development of pressure-dependent concentric hypertrophy (Izzo & Gradman, 2004). LV concentric hypertrophy maintains LV systolic function, however, the increased LV wall thickness due to the pressure overload may ultimately reduce LV compliance, thus leading to impaired LV relaxation (De Simone *et al.*, 2005). There are several pathological changes that were found present in hypertensive patients presenting with LV hypertrophy (Drazner, 2011). In a model of pressure overload, increased myocyte size and fibrosis of the perivascular space were associated with the presence of hypertrophy in mice (Matsusaka *et al.*, 2006). Indeed, changes in ECM protein composition and arrangement cause the progression of hypertension to LV hypertrophy (Berk *et al.*, 2007).

Despite the fact that LV diastolic dysfunction is linked to concentric LV hypertrophy, hypertension can cause cardiac dysfunction without affecting cardiac geometry (Zile *et al.*, 2011). In fact, concentric LV hypertrophy is not seen in all individuals with heart failure induced by hypertension (Ganau *et al.*, 1992). Similarly, studies showed that hypertensive patients may present with LV diastolic dysfunction, without concentric LV hypertrophy (Zile *et al.*, 2011; Lee *et al.*, 2015; Yucel *et al.*, 2015). As mentioned in section 2.2.3, excess synthesis of collagen fibres and cross-linking results in myocardial fibrosis (Westermann *et al.*, 2011). The functional properties of collagen fibres include LV passive stiffness, solubility and the ability to be degraded (Brower *et al.*, 2006). In contrast to the normal collagen present in healthy cells, collagen cross-linking produces collagen fibres that have increased LV passive stiffness, are insoluble and cannot easily be degraded (López *et al.*, 2012). Taken together, the quantity and quality of the collagen contribute to myocardial fibrosis.

Fibrosis increases wall tension, and subsequent impairments in LV relaxation and increased LV passive stiffness, which are linked to LV diastolic dysfunction (Lew *et al.*, 2014). Finally, long-standing pressure overload has also been shown to activate pro-fibrotic pathways without cardiomyocyte cell death (Kong *et al.*, 2014).It is well accepted that there is a strong relationship between hypertension, myocardial fibrosis and LV diastolic dysfunction. However, the molecular mechanisms involved in the progression of hypertension to LV remodelling, remain under investigation. In this regard, hypertension-induced systemic inflammation has recently been suggested as one of the mechanisms that may contribute to the development of hypertension induced cardiac structural and functional changes (Paulus & Tschöpe, 2013).

2.4 The role of inflammation in LV diastolic dysfunction and HFpEF

Inflammation occurs as a general immune response to infection, injury or stress and can be classified as acute or chronic (Asgharzadeh *et al.*, 2018*a*; Asgharzadeh *et al.*, 2018*b*). Acute inflammation is a short-term process that is activated within a few minutes to hours after exposure to the insult and usually resolves within hours to days (Asgharzadeh *et al.*, 2018*b*). In contrast, chronic inflammation happens in response to long-term inflammatory stress, such as comorbid conditions or when the immune system does not resolve the acute inflammatory process adequately (Ortega-Gómez *et al.*, 2013; Asgharzadeh *et al.*, 2018*b*). In the sections below, I will highlight the current knowledge regarding the contribution of both chronic and acute inflammation to LV diastolic dysfunction.

2.4.1 The role of chronic inflammation in the development of LV diastolic dysfunction

Studies have demonstrated a systemic inflammatory state in heart failure patients, as evidenced by increased circulating levels of interleukin (IL)- 6 and tumour

necrosis factor (TNF)- α (Collier *et al.*, 2011). Additionally, IL- 1β was shown to cause cardiac remodelling, thus leading to LV diastolic dysfunction (Harouki *et al.*, 2017). Indeed, increased levels of inflammatory cytokines are strongly associated with LV diastolic dysfunction and HFpEF in adults (Torre-Amione *et al.*, 1996; Deswal *et al.*, 2001). As previously mentioned, chronic exposure to comorbid conditions induces chronic low-grade systemic inflammation (Asgharzadeh *et al.*, 2018*b*). In this regard, studies showed that chronic low-grade systemic inflammation has deleterious effects on cardiac structure and function (Lew *et al.*, 2013; Asgharzadeh *et al.*, 2018*a*).

Furthermore, in diseases characterised by chronic systemic inflammation such as auto-immune disorders, there is increased risk for the development of HFpEF compared to the overall populace (Breunig *et al.*, 2018). In our lab, we demonstrated in a collagen-induced arthritis rat model, characterised by chronic systemic inflammation, that circulating and tissue inflammatory markers, including TNF- α, IL- 6 and IL- 1β are consistently associated with the development of altered cardiac geometry, abnormal LV pump function and contractility as well as subclinical systolic dysfunction, using STE (Mokotedi *et al.*, 2020; Manilall *et al.*, 2021; Le Roux *et al.*, 2022). Increased levels of circulating inflammatory markers cause a decline in subclinical systolic function, as indicated by decreased myocardial strain, (Ikonomidis *et al.*, 2009). However, what evidence is there that inflammation contributes to the molecular mechanisms associated with LV diastolic dysfunction development?

A decade ago, in a seminal paper, Paulus & Tschöpe (2013) proposed that comorbid-induced inflammation is strongly implicated in the development of LV diastolic dysfunction and its progression to HFpEF (Paulus & Tschöpe, 2013). It was suggested that chronic low-grade inflammation leads to myocardial structural and

functional changes via microvascular endothelial dysfunction, (Paulus & Tschöpe, 2013; Franssen *et al.*, 2016). In this regard, increased expression of vascular adhesion molecules leads to the activation, adhesion and migration of circulating leukocytes through the endothelium into the ECM (Westermann *et al.*, 2011; Szelényi *et al.*, 2015). The activated leukocytes increase the expression of transforming growth factor-β, which mediates the differentiation of cardiac fibroblasts into myofibroblasts in the ECM (González *et al.*, 2011). Myofibroblasts stimulate deposition of collagen into the ECM, resulting in increased collagen volume, an increase in the collagen type I compared to collage type III expression and increased collagen cross-linking (Kasner *et al.*, 2011; López *et al.*, 2012). As previously mentioned, these alterations in collagen regulation lead to fibrotic tissue formation, resulting in increased myocardial LV passive stiffness and impaired LV relaxation, and finally LV diastolic dysfunction (Kasner *et al.*, 2011; Manilall *et al.*, 2021).

Furthermore, it has been proposed that chronic inflammation caused by comorbid conditions is linked to altered myocardial relaxation via changes in titin phosphorylation and cardiac Ca^{2+} handling (Franssen & González Miqueo, 2016). In response to the inflammation-induced changes in the microvascular endothelium, the bioavailability of endothelial nitric oxide (NO) is reduced (Paulus & Tschöpe, 2013). This reduced NO bioavailability impacts the adjacent cardiomyocytes, as it causes a reduction of cGMP production, thus leading to the decreased activation of PKG in the cardiomyocytes (Szelényi *et al.*, 2015; Manilall *et al.*, 2021). Reduced cGMP-dependent PKG results in titin hypophosphorylation, and subsequent increase in myocardial LV passive stiffness (Borbély *et al.*, 2009).

Besides the influence of inflammation on LV passive stiffness, studies have also proposed that it impacts active relaxation processes (Sturgess *et al.*, 2021). Some studies have suggested that chronic inflammation may impair the SERCA pumps and cause increased cytosolic Ca^{2+} concentrations in the myocardium, leading to impaired LV relaxation (Joulin *et al.*, 2009). However, this was not supported by prior studies in our (Manilall *et al.*, 2023), and other laboratories (Pironti *et al.*, 2018).

Taken together, there is clear evidence that chronic inflammation, induced by comorbid conditions, is important in the pathogenesis of LV diastolic dysfunction as well as preclinical systolic dysfunction. Moreover, independent of hypertension, our lab has consistently shown a strong association between inflammation and LV diastolic and systolic dysfunction (Mokotedi *et al.*, 2020; Le Roux *et al.*, 2022), and the molecular mechanisms driving its development (Manilall *et al.*, 2021; Manilall *et al*., 2023). However, based on the model of chronic inflammation established in our laboratory, it seems that inflammation-induced LV diastolic dysfunction is largely driven by changes in LV passive stiffness, especially changes in ECM remodelling (Manilall *et al.*, 2021).

Despite the important role of chronic inflammation in LV diastolic dysfunction development, the recent coronavirus diseases (COVID)- 19 pandemic has highlighted the devastating cardiovascular consequences of an acute onset of high-grade systemic inflammation (Peng *et al.*, 2021). In this regard, systemic inflammation induced by COVID-19 has been associated with the development of LV diastolic dysfunction, especially in patients with associated comorbid conditions, such as hypertension (Zaccone *et al.*, 2021). Moreover, in patients with existing LV diastolic dysfunction, inflammation induced by COVID-19 was associated with the progression

to HFpEF (Zaccone *et al.*, 2021). In previous studies, it was reported that myocardial inflammation and fibrosis were present in up to 78% of patients who had COVID in the chronic phase of the disease (Unudurthi *et al.*, 2020). Although the role of COVID-19 in the development of LV diastolic dysfunction is beyond the scope of this study, the important question is what is the evidence that acute high-grade inflammatory events contribute to LV diastolic dysfunction? And more importantly, are these events compounded by pre-existing comorbid conditions, such as hypertension?

2.4.2 Acute high-grade systemic inflammation

Research indicates that cardiac structure and function may be negatively impacted by an acute onset of high-grade inflammation (Zhang *et al.*, 2017; Xiao *et al.*, 2021). Sepsis and other conditions marked by acute high-grade systemic inflammation can cause multiple organ failure, which commonly includes myocardial dysfunction (Angriman *et al.*, 2022). Previously, high-grade inflammation was shown to cause a decline in systolic function in a sepsis model, as indicated by decreased LVEF (Parker *et al.*, 1984). The role of high-grade inflammation in diastolic dysfunction has not been adequately studied (Davis *et al.*, 2011; Landesberg *et al.*, 2012). However, recent evidence suggests that high-grade inflammation causes diastolic abnormalities, in addition to subclinical systolic function decline (Mokotedi *et al.*, 2020). Based on these inconsistencies, the need to study mechanisms of cardiac dysfunction induced by acute high-grade inflammation as well as its long-term consequences is evident.

2.5 Effect of acute high-grade LPS-induced inflammation on cardiac function

Recent research has reported that patients who were hospitalised with severe sepsis were more likely than the general population to develop myocardial dysfunction,

at least one year post recovery (Kosyakovsky *et al.*, 2021). Comorbid conditions have been associated with sepsis development and severity (Wang *et al.*, 2012). Although no causal relationship was determined between hypertension and sepsis (Wang *et al.*, 2012), it was shown that they both present with endothelial dysfunction, which leads to the myocardial dysfunction (Bermejo-Martin *et al.*, 2018).

Animal models using lipopolysaccharide (LPS) administration have been used to investigate the processes driving cardiac dysfunction caused by acute high-grade inflammation (Table 2.1). Briefly, these studies highlight that despite the variations in LPS dosage, administration method and duration of exposure, LPS administration caused severe changes in cardiac structure and function. Gram-negative bacteria contain LPS, which triggers the host innate immune system to produce a high cytokine load via the activation of toll-like receptors (TLRs) (Lew *et al.*, 2013). The immune reaction to LPS is important in fighting off the infection, however, it may cause detrimental reactions within the host, which may ultimately lead to multiple-organ failure (Beheshti *et al.*, 2020). Once-off intraperitoneal injections of LPS have been shown to increase levels of TLR- 4 and nuclear factor (NF)-κB in the myocardium (Zhang *et al.*, 2017; Xiao *et al.*, 2021). LPS acts through toll-like receptor (TLR)- 4 to activate the NF-κB signalling pathway, thus resulting in the translocation of NF-κB from the cytoplasm into the nucleus, and leading to subsequent expression of several inflammatory cytokines, including IL- 1β (Figure 2.1) (Strand *et al.*, 2015; Xiao *et al.*, 2021). Increased levels of cardiac IL- 1β were reported to correlate with the level of cardiac injury in LPS-induced inflammation (Fairweather *et al.*, 2003).

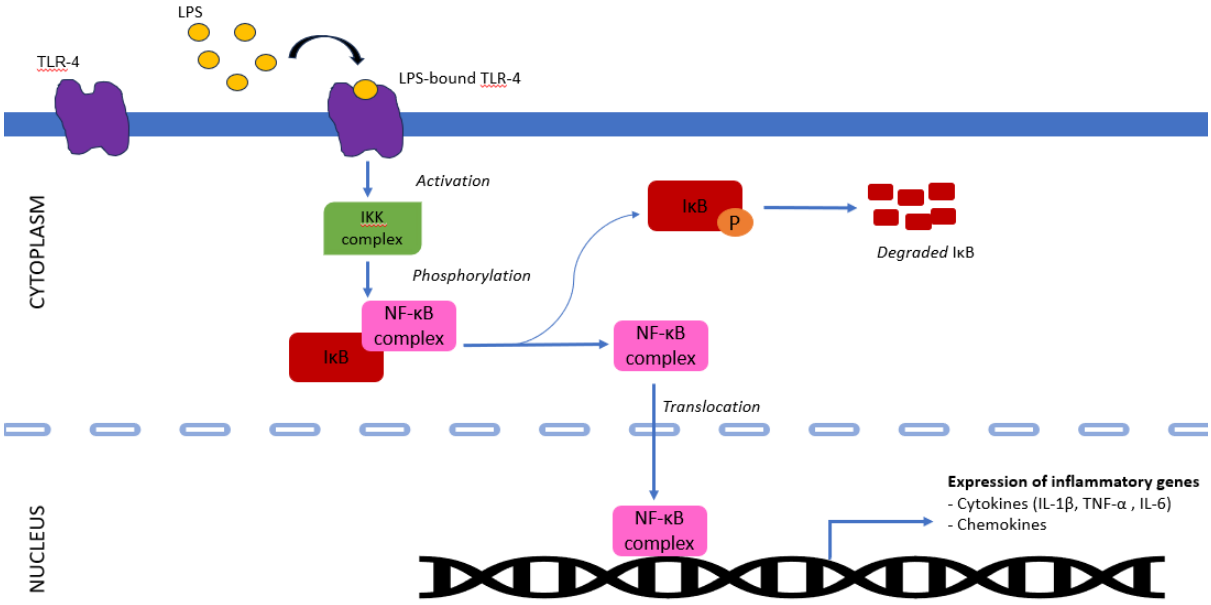

Figure 2. 1 Intracellular signalling pathways of LPS.

The binding of LPS to its membrane-bound receptor, TLR-4, leading to the activation of the IκB kinase (IKK) complex, which phosphorylates the IκB bound to and inhibiting NF-κB, resulting in the degradation of IκB. The unbound NF-κB translocates into the nucleus, and binds DNA to regulate the expression of inflammatory cytokines such as IL-1β. (Figure 2.1 modified from Hou and colleagues (2015)).

LPS-induced inflammation resulted in several myocardial alterations and subsequent acute decline in LV systolic and diastolic function, independent of prior cardiac injury (Clerc *et al.*, 2018; Cai *et al.*, 2020). In a chronic, recurrent LPS administration rat study, inflammation increased cardiac fibrosis (Lew *et al.*, 2014; Asgharzadeh *et al.*, 2018*b*). However, an acute study reported cardiomyocyte damage via increased interstitial oedema, cardiomyocyte cell attachment disruption and apoptosis without any cardiac fibrosis (Li *et al.*, 2014; Xianchu *et al.*, 2018). The absence of cardiac fibrosis in acute models of LPS-induced inflammation suggests that fibrosis is a long-term process that occurs in chronic models of inflammation only (Li *et al.*, 2021). Despite the contrasting evidence, studies have shown that acute high-grade inflammation causes immediate changes to myocardial structure and function (Landesberg *et al.*, 2012). However, whether a single bout of LPS-induced inflammation results in long-term fibrotic tissue development needs to be elucidated.

LPS exposure has been associated with global LV systolic dysfunction in the short-term, as measured by reduced fractional shortening (FS) and LVEF (Chu *et al.*, 2019). Chronic LPS-induced high-grade inflammation reduced the pump function (LVEF) and contractility (FS) of the heart (Wu *et al.*, 2018). However, an acute model of LPS-induced inflammation reported a reduction in FS 6 hours after LPS administration, which was ameliorated after 24 hours (Lew *et al.*, 2013). This finding suggests that the rats fully recovered from LPS-induced inflammation, and the LV pump function returned to baseline after 24 hours. Increased collagen volume, mitochondrial dysfunction and cardiomyocyte apoptosis were implicated in the development of the systolic dysfunction (Lew *et al.*, 2013; van der Poll *et al.*, 2017).

Although it has not been well studied in chronic LPS models, it is suggested that LV diastolic function is affected by acute LPS-induced inflammation (Sturgess *et al.*, 2021). Acute LPS-induced inflammation impaired LV relaxation, via dysfunction of the SERCA pump, resulting in impaired Ca^{2+} handling (Joulin *et al.*, 2009). Compared to chronic studies, fibrosis is not implicated as a mechanism in the development of diastolic dysfunction in acute LPS studies (Li *et al.*, 2021). However, LPS caused increased LV wall thickness 15 minutes after administration in rodents (Iwase *et al.*, 2001). Histopathological tests showed that the increased LV wall thickness was driven by myocardial oedema and capillary congestion (Iwase *et al.*, 2001). Together, acute myocardial oedema and the increased LV wall thickness results in increased LV passive stiffness and impaired diastolic dysfunction (Desai *et al.*, 2008). Despite the fact that myocardial function is acutely altered in response to acute LPS-induced inflammation, whether an acute onset of high-grade inflammation may cause long-term LV functional impairment is presently unknown. Therefore, it is essential to determine the mechanisms underlying the development of myocardial dysfunction in the long-term after exposure to acute high-grade inflammation. Additionally, whether pre-existing hypertension compounds the effects of LPS-induced inflammation should be investigated.

Table 2.1 Summary of LPS studies assessing the effects of LPS-induced inflammation on cardiac parameters

Author	Protocol	Echocardiographic measures	Main outcomes
Asgharzadeh_2018*a*	Weekly ip injections of 10 mg/kg LPS in Wistar rats. The rats were terminated after 4 weeks.	—	Inflammation induces cardiac fibrosis as a primary effect, leading to HFpEF.
Asgharzadeh_2018*b*	Daily ip injections of 1 mg/kg LPS in Wistar rats. The rats were terminated after 3 weeks.	—	LPS induced cardiac inflammation, which led to fibrosis
Zhao_2016	Once-off iv injection of 20 mg/kg LPS in Sprague-Dawley rats. The rats were terminated after 4 hours.	LVEDD, LVESD, FS	LPS induced inflammatory cells infiltration into myocardium, and Impaired systolic function (FS)
Chu_2016	Once-off ip injection of 10, 20 or 25 mg/kg LPS in C57BL/6J mice. The mice were terminated after 6 hours.	LVEDD, LVESD, LVEDV, LVESV, LVEF, FS, CS	LV dilation at 20 mg/kg, impaired systolic function (FS, LVEF) and worsened circumferential deformation after LPS administration.
Sturgess_2021	Once-off iv injection of 10 mg/ml LPS in Sprague-Dawley rats. The rats were terminated after 2 hours.	LVEDD, LVESD, FS, LVOT VTI, LVOT V_{max}, E, e', E/e'	LPS induced impaired LV diastolic function which was associated with infiltration of inflammatory cell.
Zhang_2017	Once-off ip injection of 10 mg/kg LPS in Sprague-Dawley rats. The rats were terminated after 24 hours.	LVEDD, LVESD, FS	LPS induced infiltration of immune cells, LV dilation, Impaired systolic function (FS)

Lew_2014	Weekly ip injections of 10 mg/kg LPS in C57B1/6 mice. The mice were terminated after 1, 2, 3 and 4 weeks.	LV mass/BW	LPS activated pro-fibrotic mediators days after administration, which induced fibrosis after 2 weeks, with no changes before then
Saiyang_2020	Once-off ip injection of 10 mg/mL LPS in C57/B6J mice. The mice were terminated after 6, 12 and 24 hours.	LVEDD, LVESD, LVEF, FS	LPS induced impaired systolic function (FS, LVEF).
Cai_2020	Once-off ip injection of 6 mg/kg LPS in C57BL/6 mice. The mice were terminated after 6 hours.	LVEDD, LVESD, LVEF, FS	LPS triggered cardiac inflammation and impaired systolic function (FS, LVEF)
Wei_2018	Once-off ip injection of 6 mg/kg LPS in C57BL/6. The mice were terminated after 6 hours.	LVEF, FS	LPS induced signs of septic shock in the rats and Impaired systolic function (FS, LVEF)
Wu_2018	Twice-a-week ip injections of 2.5 mg/kg LPS in BALB/c mice. The mice were terminated after 5 weeks.	Heart mass/BW, LVEDD, LVESD, LVEDV, LVESV, LVEF, FS	LPS induced LV dilation, impaired systolic function (FS, LVEF), infiltrating immune cells and presence of fibrosis
Xiao_2021	Once-off ip injection of 10 mg/kg LPS in Wistar rats. The rats were terminated after 12 hours.	LVPWs, LVEDV, LVESV, LVEF, FS	LPS induced cardiac inflammation and impaired systolic function (FS, LVEF)
Clerc_2016	Once-off intraperitoneal injection of 10 mg/kg LPS in Wistar rats. The rats were terminated after 4 hours.	LVEF, FS, E/A, CS, LS, LVEDV, LVESV	LPS induced delayed LV relaxation, Impaired systolic function (FS, LVEF, CS & LS)

Li_2021	Once-off intraperitoneal injection of 4 or 10 mg/kg LPS in Sprague-Dawley rats. The rats were terminated after 6 hours.	LVEF, FS	LPS impaired systolic function (FS, LVEF), caused diffuse interstitial oedema, cardiomyocyte damage and hypertrophy without cardiac fibrosis
Joulin_2009	Once-off intravenous injection of 10 mg/kg LPS in Sprague-Dawley rats. The rats were terminated after 4 hours.	LVEF, FS, E/A	LPS induced impaired LV relaxation and impaired systolic function (FS, LVEF)

LPS, lipopolysaccharide; ip, intraperitoneal; iv, intravenous; HFpEF, heart failure with preserved ejection fraction; LVEDD, left ventricular end-diastolic diameter; LVESD, left ventricular end-systolic diameter; FS, fractional shortening; LVEF, ejection fraction; LVEDV, left ventricular end-diastolic volume; LVESV, left ventricular end-systolic volume; LV mass/BW, left ventricular mass normalised to body weight; Heart mass/BW, heart mass normalised to body weight; CS, circumferential strain; LS, longitudinal strain; LVPWs, left ventricular posterior wall thickness in systole; LVOT VTI, left ventricular outflow tract velocity time integral; LVOT V_{max}, left ventricular outflow tract maximum velocity; E, early mitral valve inflow velocity; A, late mitral valve inflow velocity; e', early mitral annular motion velocity.

2.6 Problem statement

HFpEF accounts for 50% of all heart failure cases with prevalence that continues to increase across the world. Patients with HFpEF often present with impaired LV relaxation and passive stiffness, which are involved in the pathogenesis of LV diastolic dysfunction. There are several cellular and molecular pathways that are connected to the aetiology of LV diastolic dysfunction, and this heterogeneity limits our understanding of the development of HFpEF.

Comorbid conditions, such as hypertension, have a detrimental role in the pathogenesis of LV diastolic and systolic dysfunction. The long-standing increased blood pressure drives structural changes in the myocardium, leading to LV remodelling. However, as with HFpEF, the phenotype of hypertension is not consistent in all hypertensive patients. Some hypertensive patients present with LV remodelling and functional changes that are absent in other hypertensive patients. Therefore, the mechanisms of how hypertension-induced LV remodelling leads to HFpEF requires further elucidation.

Recently, it was shown that hypertension or other comorbid conditions did not fully account for all the changes shown in LV systolic and diastolic function. Indeed, inflammation was implicated in the progression of hypertension to LV diastolic dysfunction. It was established that inflammation drives cellular and molecular pathways that lead to LV diastolic and systolic dysfunction. Fibrotic tissue formation, as an underlying mechanism, has been shown to cause LV remodelling. These LV morphological changes resulted in impaired LV systolic and diastolic function in response to chronic low-grade inflammation.

The detrimental effects of inflammation on cardiac structure and function have been well described in chronic models of inflammation. However, the short-term effects of acute high-grade inflammation have been inconsistent and unclear, highlighting the need to investigate the short- and long-term consequences of exposure to acute high-grade inflammation.

Patients with severe sepsis developed myocardial dysfunction at least one year after recovery. The use of LPS, which activates sepsis, has allowed for the investigation of the effect of acute high-grade inflammation in animal models. The short-term effects of acute LPS-induced inflammation have been determined in rodent models; however, the long-term effects of acute LPS-induced inflammation have not been studied. Therefore, the mechanisms responsible for the development of myocardial dysfunction in the long-term post LPS administration need to be determined.

Additionally, sepsis patients who had comorbid conditions, such as hypertension, had a higher risk for developing myocardial dysfunction in the long-term. However, the underlying mechanisms of how hypertension influenced the development of sepsis-induced myocardial dysfunction in the long-term were not reported. Therefore, whether hypertension worsens myocardial dysfunction caused by inflammation ought to be investigated.

2.7 Aim

To compare the short- and long-term effects of acute high-grade inflammation on myocardial morphology and function in rats. In addition, the study aimed to determine whether the effects of acute high-grade inflammation on myocardial morphology and function is exacerbated in rats with hypertension.

Objectives

The objectives are to determine:

1. the changes in LV geometry, systolic and diastolic function using echocardiography 24 hours and 6 weeks after a single LPS administration in normotensive Wistar Kyoto (WKY) and Spontaneously Hypertensive rats (SHR).

2. serum concentrations of IL- 1β as inflammatory markers 24 hours and 6 weeks after a single LPS administration in WKY and SHR.

3. changes in LV fibrosis, using histology, in the heart tissue 24 hours and 6 weeks after a single LPS administration in WKY and SHR.

Chapter 3: Methods

3.1 Animals

Four-month-old male Wistar Kyoto (WKY, n=36) rats and spontaneously hypertensive rats (SHR, n=38) were used in this study. The rats were obtained from the Wits Research Animal Facility (WRAF), and they were housed in individual cages, in a temperature-controlled room. The rats were allowed unrestricted access to a standard rat chow diet and water. The experimental procedures were approved by the Animal Research and Ethics Committee (AREC) of the University of the Witwatersrand (AREC number: 2022/05/03/C).

3.2 Study design

The rats underwent a two-week adaptation period, where body weight and blood pressure were measured weekly. Following the adaptation period, the rats were randomly assigned to two groups per rat strain namely saline or LPS injection to obtain the following groups: WKY-control, WKY-LPS, SHR-control, SHR-LPS (Figure 1). To induce inflammation, the rats in the LPS groups received a single intraperitoneal injection of LPS (1 mg/kg, serotype 0111:B4, Merck KGaA, Darmstadt, Germany) derived through phenol extraction from *Escherichia coli* and reconstituted in saline. The rats in the control groups received a single intraperitoneal injection of saline (1 ml/kg). In each group, the rats were then further divided into the 24-hour group, where the rats were terminated 24 hours post LPS (or saline) administration, and the 6-week group, where the rats were terminated 6 weeks post LPS (or saline) administration.

To determine the short-term effects of LPS, the rats in the 24-hour groups for both rat strains had their blood pressure and body weight measured 24 hours post LPS or saline injections. Echocardiography was then performed under anaesthesia before termination and blood sampling by cardiac puncture. The rat heart was then

isolated and tissues were harvested and stored for histopathological analyses. In the long-term (6-week) groups, for both rat strains, sickness behaviour was monitored following LPS administration using a sickness behaviour assessment sheet (Appendix B) which included monitoring of signs of distress, lethargy, laboured breathing or a change in appearance, appetite or body weight. The animals were monitored for sickness behaviour twice daily for the first 3 days after LPS administration, then once daily for the rest of the week (4 days) and thereafter once a week for the remaining five weeks. In addition, in the long-term groups, body weight and blood pressure were measured once a week for the duration of the study. At the end of the 6-week period, echocardiography was performed under anaesthesia before termination and blood was sampled by cardiac puncture. The heart was isolated and tissues were harvested and stored for histopathological analyses. The rats that died following LPS injections were excluded from the sample (n=2).

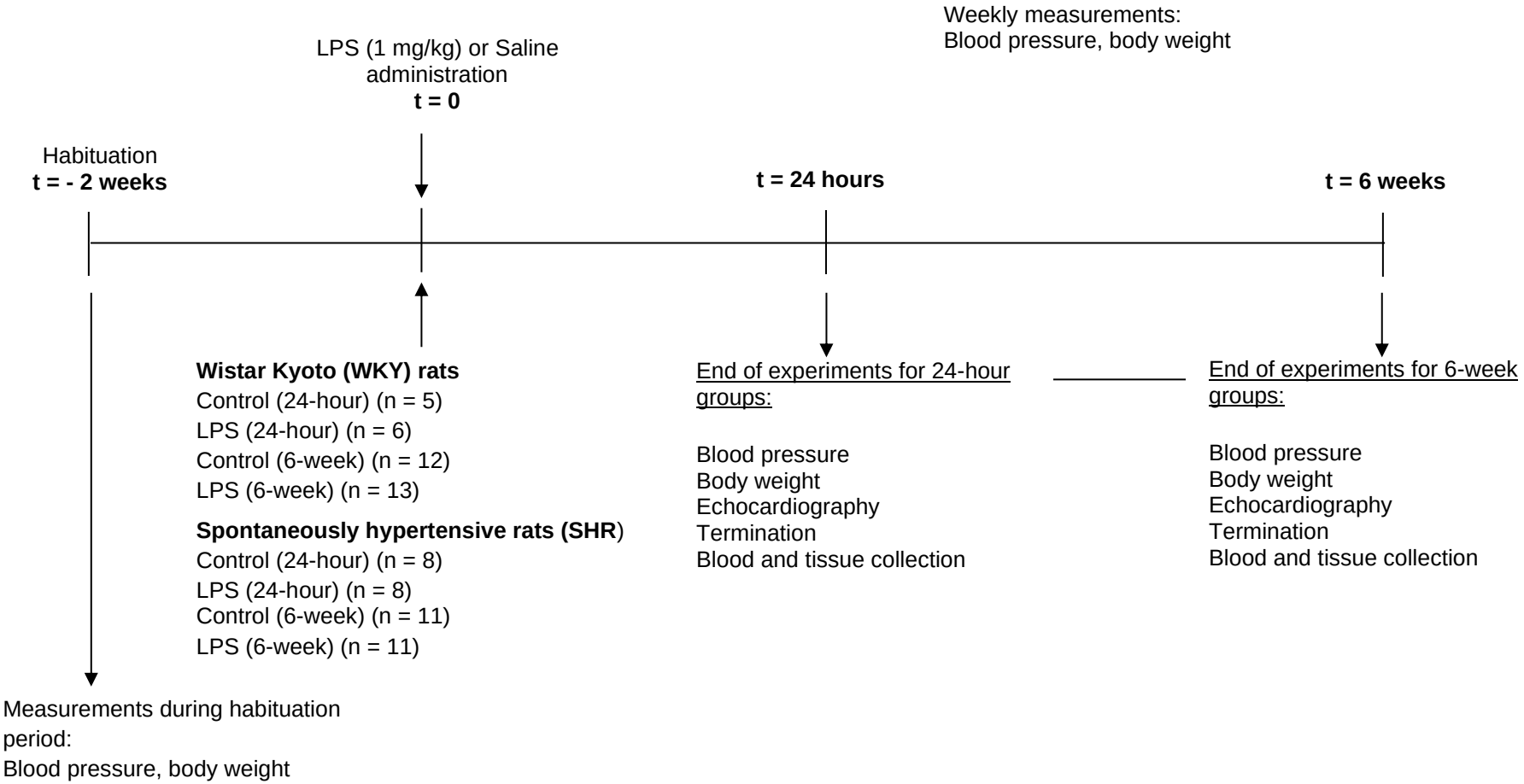

Figure 3.1 Experimental protocol for the study.

LPS, lipopolysaccharide

3.3 Measurements and procedures

3.3.1 Non-invasive blood pressure

Blood pressure was measured using the tail-cuff technique (Biopac Systems Inc, Goleta, CA, USA). Each rat was placed in a restrainer to allow access to the base of the tail. The rats were habituated to the restrainers during the habituation period. The tail was heated on a heating pad for 5 minutes prior to attaching the tail cuff. The tail cuff was coupled to a volume-pressure sensor which measured systolic and diastolic blood pressure. An average of two measures were taken as the blood pressure.

3.3.2 Echocardiography

3.3.2.1 Conventional *echocardiography*

Prior to termination, anaesthesia was induced using 2% isoflurane in oxygen in an induction chamber and maintained with continuous 1% isoflurane ventilation. The rats were placed in a left lateral decubitus position with their chest hair shaved. An experienced researcher blinded to the experimental groups performed echocardiography using a high-resolution ultrasound probe (15 MHz) coupled to a cardiology ultrasound system (Affiniti CVx, Philips Healthcare, Andover, Massachusetts). M-mode images were obtained in the parasternal long axis view to measure left ventricular (LV) dimensions, including LV end-diastolic diameter (LVEDD), end-systolic diameter (LVESD), posterior wall thickness (LVPW) and intraventricular septal wall thickness (IVS) in systole (s) and diastole (d) (Figure 3.2). Endocardial fractional shortening (FS_{end}) was calculated as [(LVEDD- LVESD) / LVEDD] x 100 (Saiyang *et al.*, 2021). LV relative wall thickness (RWT) was determined

as (IVSd + LVPWd)/LVEDD) (Mokotedi *et al.*, 2020). The Teichholz formula was used to determine LV end-diastolic volume (LVEDV) and end-systolic volume (LVESV) as; LVEDV= [7/ (2.4 + LVEDD)] x $LVEDD^3$ and as LVESV= [7/ (2.4 + LVESD)] x $LVESD^3$ (Teicholz *et al.*, 1976). LV ejection fraction (LVEF) was determined as [LVEF= (LVEDV – LVESV)/ LVEDV] (Teicholz *et al.*, 1976). An average of three measures were used for each variable.

Pulsed-wave Doppler was performed in apical four-chamber view to measure the transmitral inflow velocity at the level of the mitral valve leaflet tips during early (E) and late (A) diastole (Figure 3.3). LV relaxation was calculated as the E/A ratio. Pulsed-wave Doppler in the apical five chamber view was used to measure left ventricular outflow tract (LVOT) velocity time integral (VTI) as well as LVOT peak velocity (V_{max}) as measures of systolic flow (Figure 3.4).

Tissue Doppler Imaging (TDI) was used in apical four-chamber view to measure the myocardial tissue lengthening velocities of the mitral annulus of both the septal and lateral walls during early (e') and late (a') diastole (Figure 3.5). Early systolic mitral velocity (s') was also measured for the septal and lateral walls. Where necessary, the average of the lateral and septal velocities was calculated and reported as so. All three e' measures were used as indices of LV relaxation. LV passive stiffness was calculated as e'/a' and LV filling pressure was calculated as E/e'. All echocardiography images and videos obtained were viewed and analysed offline using IMAGE-COM software (TOMTEC Imaging Systems GmbH, Germany).

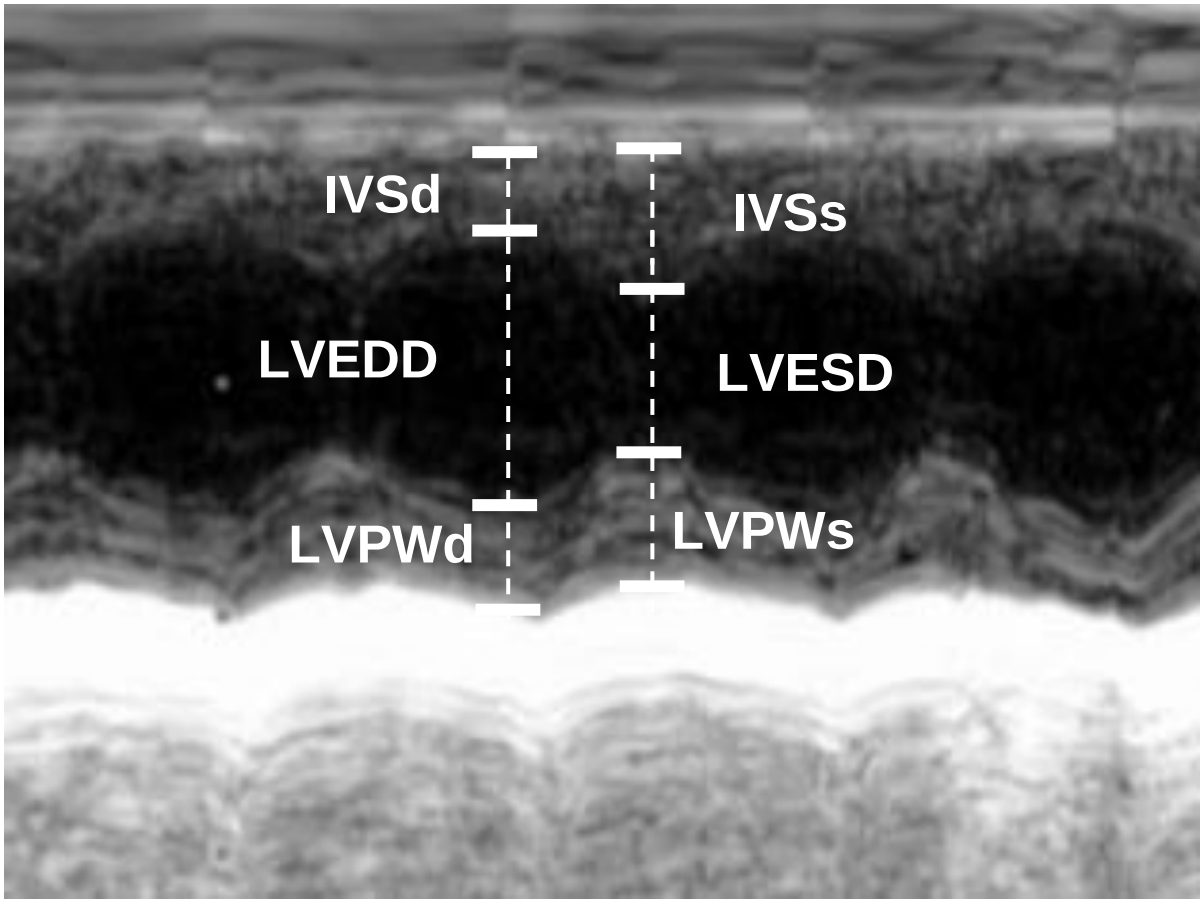

Figure 3.2 Representative M-mode image obtained in the parasternal long-axis view showing the left ventricular dimensions.

IVSd, interventricular septum in diastole; IVSs, interventricular septum in systole; LVEDD, left ventricular end-diastolic diameter; LVESD, left ventricular end-systolic diameter; LVPWd, left ventricular posterior wall thickness in diastole; LVPWs, left ventricular posterior wall thickness in systole.

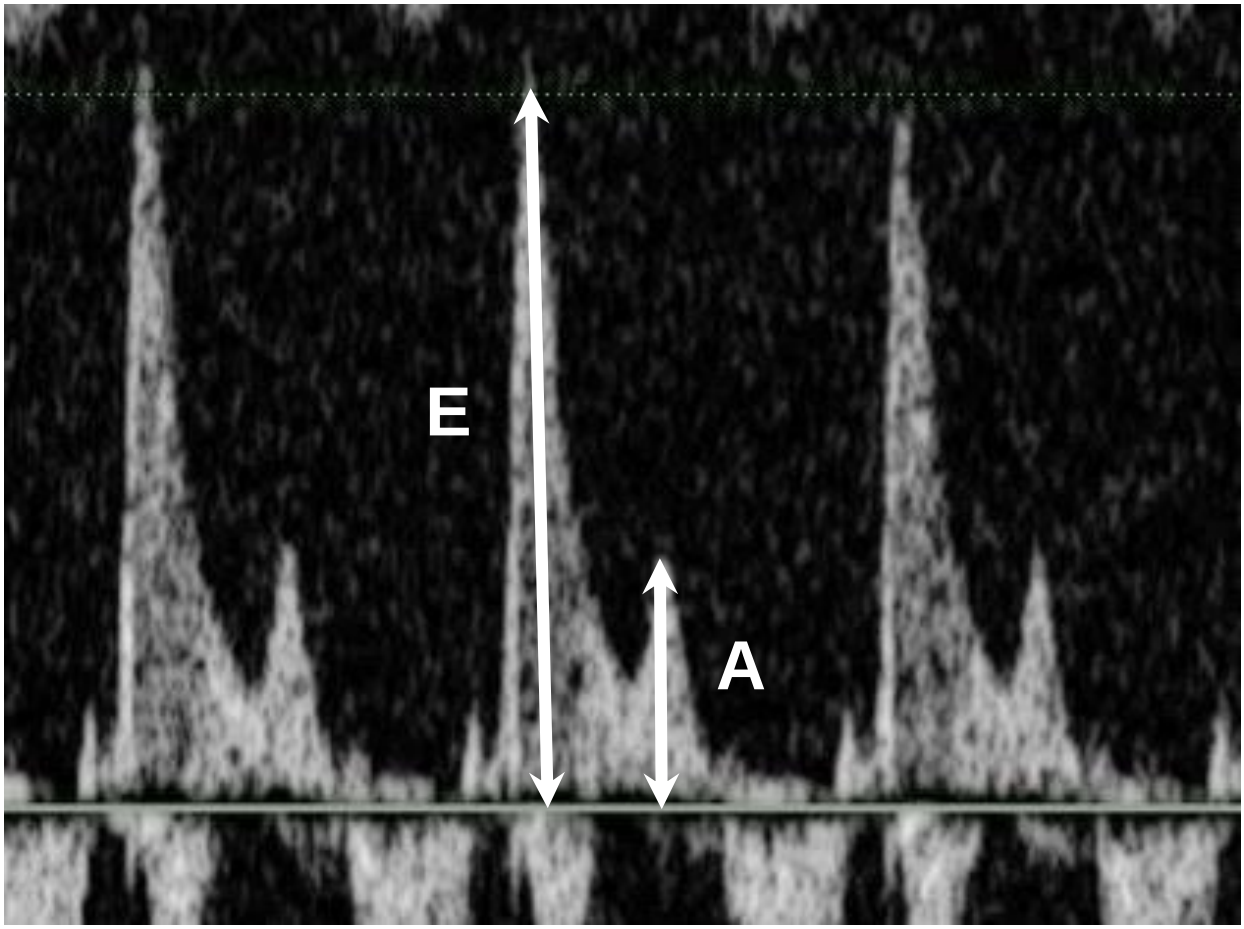

Figure 3.3 Representative pulsed-wave Doppler image obtained in apical four-chamber view showing mitral inflow velocities during diastole.

E, early mitral inflow velocity; A, late mitral inflow velocity.

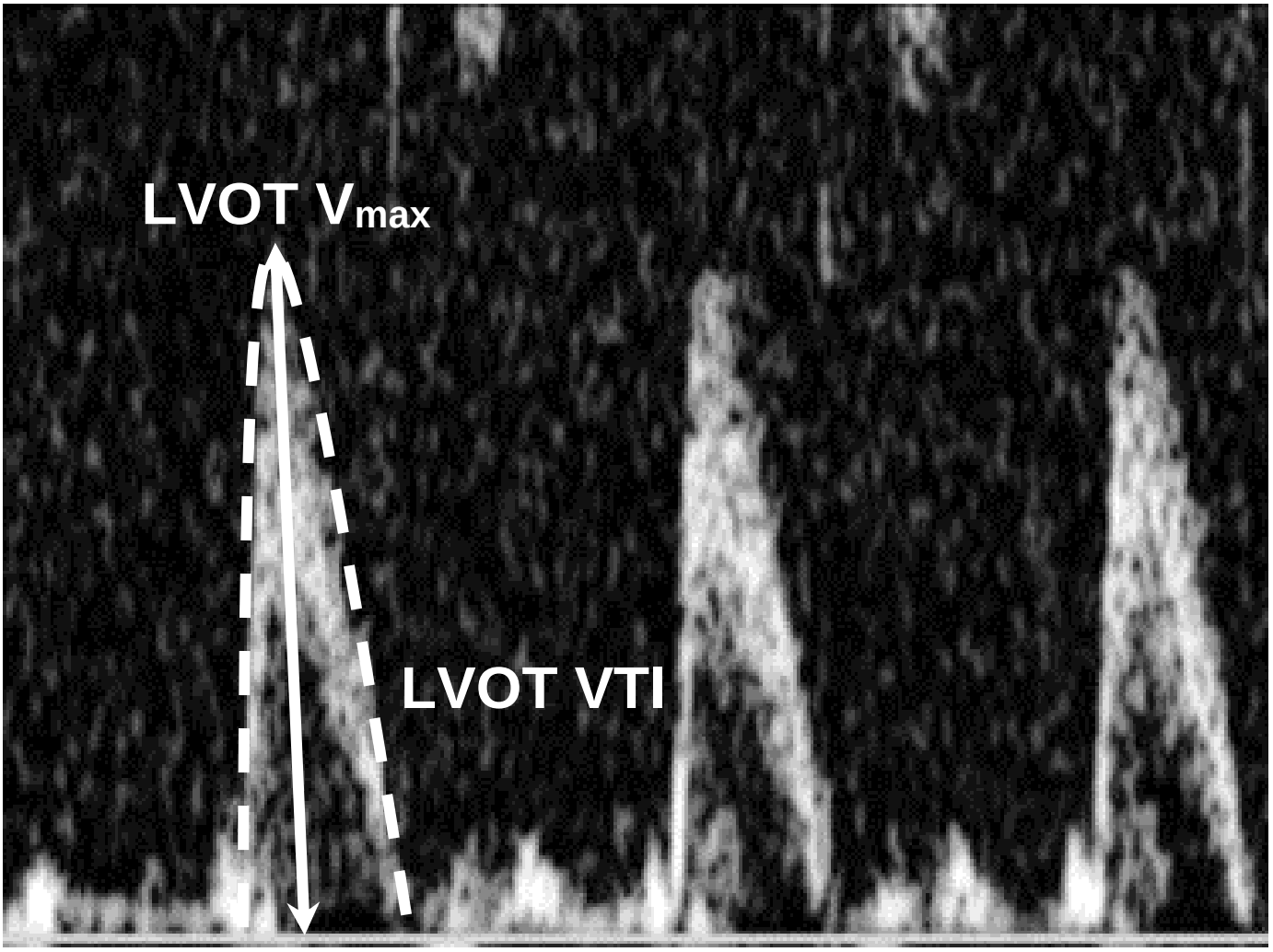

Figure 3.4 Representative pulsed-wave Doppler image obtained in apical four-chamber view showing LVOT VTI and LVOT V_{max}.

LVOT VTI, left ventricular outflow tract velocity time integral; LVOT V_{max}, left ventricular outflow tract peak velocity.

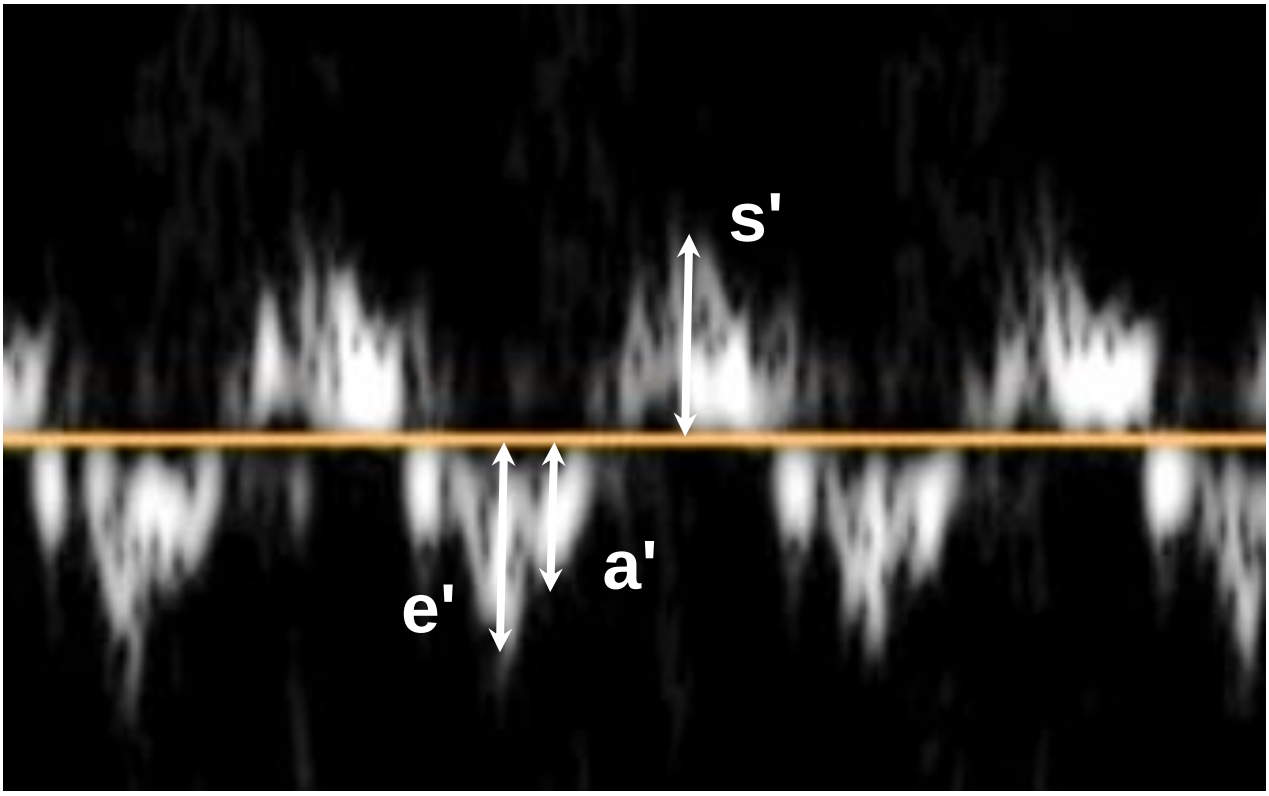

Figure 3.5 Representative tissue Doppler image obtained in the apical four-chamber view to measure tissue lengthening of the mitral annulus during diastole.

e', early annular tissue velocity; a', late annular tissue velocity, s', early systolic mitral annular velocity.

3.3.2.2 Speckle-tracking echocardiography (STE)

B-mode videos were obtained to assess LV systolic function by measuring myocardial strain in both the circumferential and longitudinal views. Two-dimensional (2D) speckle tracking echocardiography analyses were performed offline using TOMTEC-ARENA TTA2.51 ultrasound workspace software (2D CPA, TOMTEC Imaging Systems GmbH, Germany). For circumferential speckle tracking, three endocardial markers were placed in the end-systolic frame followed by the end-diastolic frame in the short-axis view. Similarly, for longitudinal speckle tracking, three endocardial markers were placed in the end-systolic frame followed by the end-diastolic frame in the apical four-chamber view. The automated border tracking software was used to trace the endocardial and epicardial borders of the LV myocardium, which were manually adjusted to accurately track the movement of the myocardium. The software tracked the frame-to-frame movement of the natural acoustic markers, also called speckles, to accurately track the movement of the myocardium (Figure 3.6 A & B). The software produced a 6-segmental myocardial strain of the chamber for both the longitudinal and the circumferential strains. Peak LV longitudinal and circumferential strain measurements were obtained and the average calculated from three consecutive cardiac cycles from the six anatomic regions. Myocardial strain is a measure of the degree of deformation of the LV during systole (Chu *et al.*, 2016).

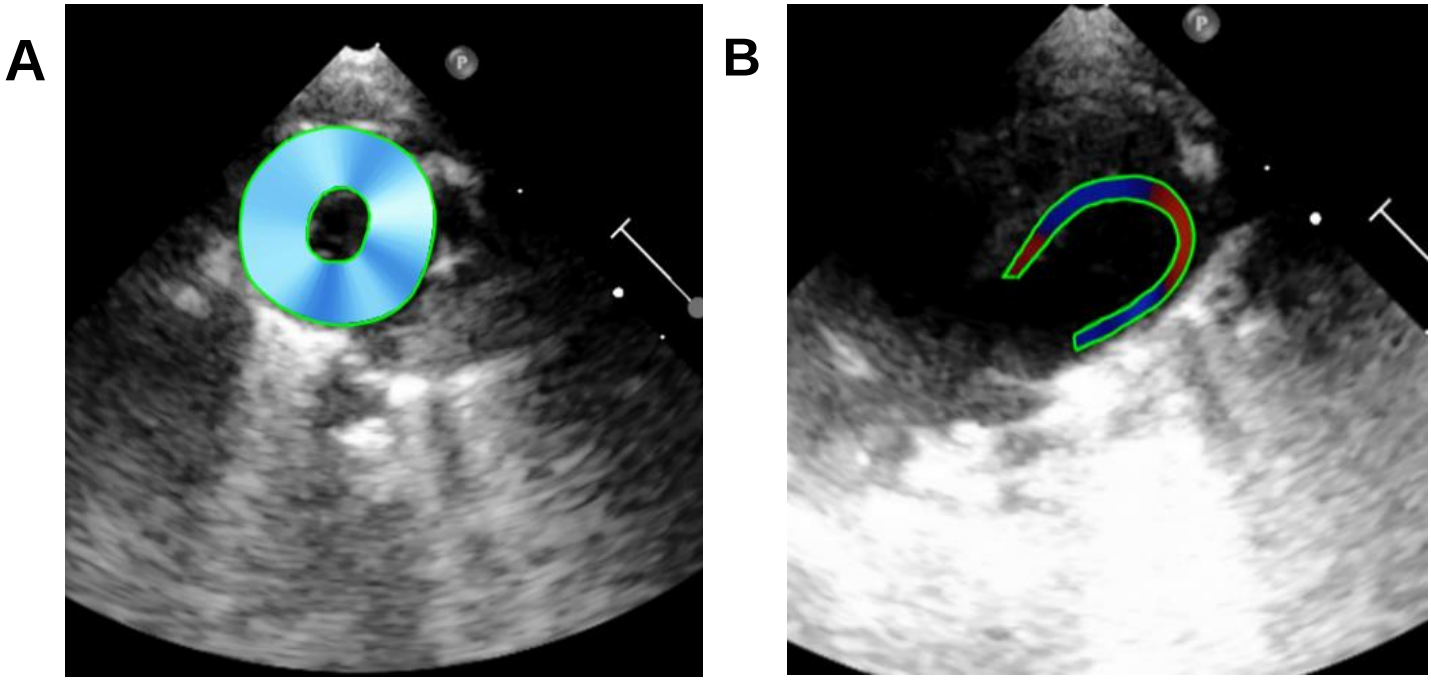

Figure 3.6 Representative B-mode images obtained to measure myocardial strain in the apical four-chamber view.

A) Circumferential strain trace in the short-axis view, and B) Longitudinal strain trace.

3.3. Inflammatory marker interleukin (IL)-1β concentration

Following echocardiography, the rats were terminated by cardiac puncture. The blood was collected and allowed to clot at room temperature, whereafter it was centrifuged at 3000 rpm for 15 minutes, and serum was collected and stored at – 80 °C. Serum concentrations of IL- 1β were measured in duplicate using Enzyme-linked Immunosorbent Essay (ELISA) as per the manufacturer's instructions (ABclonal Technology Co. Ltd, Ma, USA). The optical density of the reaction was detected using an automated microplate reader at 450 nm (Thermofisher Labsystems Multiskan Ascent, MA, USA). The lower detection limit for IL- 1β was 62.5 pg/ml.

3.3.4 Histology

Following blood collection, the heart was surgically removed and weighed. The LV was dissected along the septum and divided into three sections along the short axis. One of the three LV sections was immediately fixed in 10% buffered formalin for histological analysis. Following fixation, the LV sections for all the animals were placed in an automatic tissue processor (Shandon Citadel 1000, Thermofisher, MA, USA). In the processor, the LV sections were dehydrated using ascending concentrations of alcohol, cleared using chloroform and infiltrated using paraffin wax. Following infiltration, the LV sections were placed in a mould, embedded in wax and cooled to solidify. The embedded LV sections were cut in 4 µm sections using a microtome, and mounted onto standard glass slides. For the staining procedure, the sections were deparaffinized using xylene and rehydrated using varying concentrations of alcohol. The tissue sections were then stained with Picrosirius red for one hour, followed by differentiation in acidified water and dehydration. The dehydrated slides were mounted in Entellan and cover-slipped. The stained slides were examined for markers of

cardiac fibrosis. Representative images were acquired using a Zeiss Axioscope 2 brightfield microscope fitted with a high-resolution camera (Figure 3.7). All images were captured at 10x magnification. The myocardial collagen area was calculated as an average of three visual fields of view with a high density of collagen fibres and three fields of view with a low density of collagen fibres using the NIH ImageJ software (version 1.54). Collagen volume fraction (CVF) was calculated as the average myocardial collagen area / total myocardial tissue area x 100.

3.4 Data analysis

Data analysis was performed using SAS software, version 9.4 (SAS Institute Inc., USA). Continuous data are expressed as mean ± standard deviation (SD) for normally distributed data, and median ± interquartile range (IQR) for skewed data. The Shapiro-Wilk test was used to determine normality of the data distribution. Where data was non-normally distributed, it was log transformed prior to linear regression. Differences in echocardiographic parameters, CVF and serum concentrations of IL-1β were determined using a mixed model, analysis of variance (ANOVA), with rat strain (WKY vs SHR) and LPS administration (control vs LPS) as the main effects. Differences in body weight and blood pressure were determined using repeated-measures ANOVA. In the case of significant F-values, Tukey's *post hoc* tests were performed. Pearson's correlations were used to determine the associations between inflammatory markers, collagen volume and echocardiographic parameters. Statistical significance was considered at $p < 0.05$.

Chapter 4: Results

4.1 Changes in body weight and blood pressure

In the short-term groups, there were no significant differences in body weight between the different experimental groups at baseline or at 24 hours after LPS administration (all $p > 0.05$; Table 4.1). In the long-term groups, there was a significant change in body weight over time (all $p < 0.05$; Figure 4.1A). Compared to week 0, rats in the WKY-control group and the SHR-control group were significantly heavier at week 6 ($p = 0.011$ and $p = 0.02$, respectively) and rats in the WKY-LPS group at week 5 and 6 ($p = 0.04$ and $p = 0.004$, respectively). There were no significant differences in the body weight changes between the different rat strains or between the control and LPS-treated groups (all $p > 0.05$).

Regarding blood pressure in the short-term groups, there were no significant differences in systolic and diastolic blood pressure between baseline and 24 hours after LPS administration in any of the experimental groups (all $p > 0.05$; Table 4.1). There was a significant effect of rat strain, as both systolic and diastolic blood pressure were higher in the SHR groups compared to their respective WKY counterparts (all $p < 0.05$).

In the long-term groups, there were no significant changes in systolic or diastolic blood pressure over time in any of the experimental groups (all $p > 0.05$, Figure 4.1B). There were no significant differences between the groups that received LPS compared to their respective control groups in either systolic or diastolic blood pressure (all $p > 0.05$). However, there was a significant effect of rat strain, as both systolic and diastolic blood pressure were consistently higher in the SHR compared to the respective WKY groups (all $p < 0.05$).

Table 4.1 Body weight and blood pressure at baseline and termination in the short-term groups.

	Baseline				Termination			
	WKY-control	WKY-LPS	SHR-control	SHR-LPS	WKY-control	WKY-LPS	SHR-control	SHR-LPS
Body weight (g)	314.4 ± 34.7	309.3 ± 21.4	294.4 ± 27.4	316.6 ± 22.2	318.4 ± 34.9	296.5 ± 27.7	296.4 ± 27.3	301.4 ± 25.2
Systolic blood pressure (mmHg)	118 ± 3	119 ± 1	188 ± 3 #	188 ± 4 #	119 ± 2	120 ± 1	185 ± 5 #	185.0 ± 3 #
Diastolic blood pressure (mmHg)	77 ± 5	78 ± 5	117 ± 4 #	118 ± 5 #	76 ± 2	78 ± 2	121 ± 2 #	119 ± 4 #

Data expressed as means ± SD. Repeated measures two-way ANOVA was used to determine group or rat strain effects followed by Tukey's *post hoc* test# $P < 0.05$ in SHR-control group compared to WKY-control group or SHR-LPS group compared to WKY-LPS group. WKY, Wistar Kyoto rats; SHR, spontaneously hypertensive rats; LPS, lipopolysaccharide group.

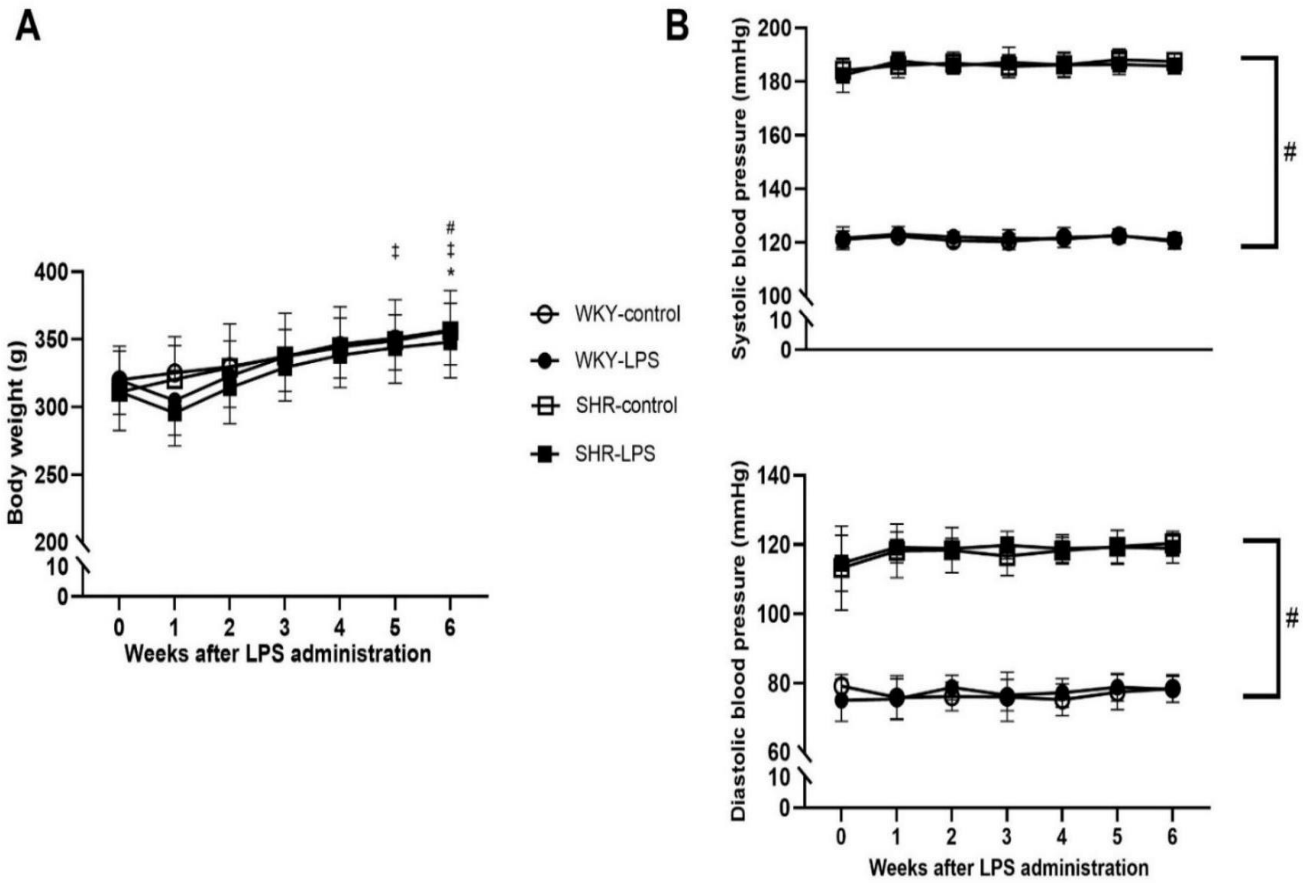

Figure 4.1 Changes in (A) body weight, as well as (B) systolic and diastolic blood pressure in response to LPS administration in control and LPS-treated rats over six weeks.

Data expressed as means ± SD. Repeated measures two-way ANOVA was used to determine group or rat strain effects followed by Tukey's *post hoc* test. * $P < 0.05$ for WKY-control week 6 vs week 0, ‡ $P < 0.05$ for WKY-LPS week 5 and 6 vs week 0 and # $P < 0.05$ for SHR-control week 6 vs week 0 for body weight. And # $P < 0.05$ for SHR (LPS and control) vs WKY (LPS and control) for blood pressure. WKY, Wistar Kyoto rats; SHR, spontaneously hypertensive rats; LPS, lipopolysaccharide group.

4.2 IL- 1β concentration

In the short-term group, there was a significant LPS administration effect on IL - 1β concentrations ($F = 12.59$, $p = 0.002$, Figure 4.2A). However, there was no significant effect of rat strain on IL- 1β ($F = 0.16$, $p = 0.69$).

In the long-term groups, there were no significant effects of LPS administration ($F = 0.08$, $p = 0.97$), or rat strain ($F = 0.23$, $p = 0.64$) on serum concentrations of IL-1β between the different experimental groups (Figure 4.2B).

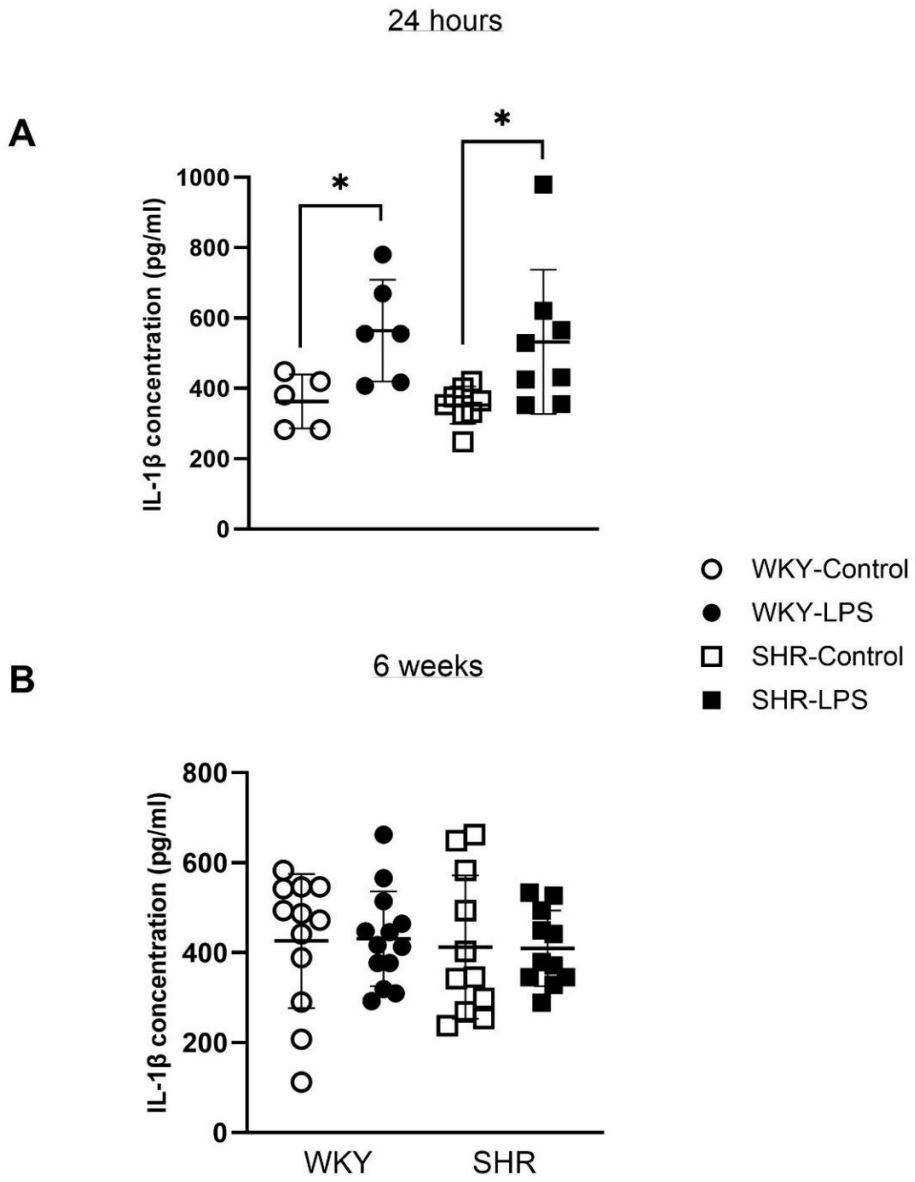

Figure 4.2 Serum concentration of IL- 1β in control and LPS-treated rats at (A) 24 hours and at (B) six weeks.

Data expressed as means ± SD. Two-way ANOVA was used to determine group or rat strain effects followed by Tukey's *post hoc* test. * $P < 0.05$ in WKY-LPS compared to WKY-control or SHR-LPS group compared to SHR-control group. WKY, Wistar Kyoto rat; SHR, spontaneously hypertensive rats; LPS, lipopolysaccharide group; IL-1β, interleukin - 1β.

4.3 Changes in cardiovascular parameters

4.3.1 Cardiac weight and left ventricular geometry

In the short-term groups, there was a significant effect of rat strain on heart weight ($F = 13.09$, $p = 0.001$, Table 4.2). Heart weight was significantly higher in the LPS-treated SHR compared to LPS-treated WKY rats ($p = 0.02$). There was a significant effect of LPS administration on heart weight ($F = 5.13$, $p = 0.03$) and normalised heart weight ($F = 8.27$, $p = 0.009$), but there were no interactions between the effects of rat strain and LPS administration.

There were no significant effects of LPS administration or rat strain on LV weight or normalised LV weight (all $p > 0.05$). Additionally, there were no significant differences in cardiac geometric measures in the control and LPS-treated rats after 24 hours (all $p > 0.05$).

In the long-term groups, there was no significant effect of LPS administration on heart weight and normalised heart weight (all $p > 0.05$, Table 4.2). However, there was a significant effect of rat strain on heart weight ($F = 17.53$, $p = 0.0001$), and normalised heart weight ($F = 27.63$, $p < 0.0001$), without interactions between the effects of rat strain and LPS administration. There were no significant differences in LV weight and normalised LV weight between the different experimental groups (all $p > 0.05$). There were no significant differences in cardiac geometry between the different experimental groups (all $p > 0.05$).

Table 4.2 Effect of LPS on cardiac weight and geometry in the short- and long-term groups.

	24 hours				6 weeks			
	WKY-control	**WKY-LPS**	**SHR-control**	**SHR-LPS**	**WKY-control**	**WKY-LPS**	**SHR-control**	**SHR-LPS**
Heart weight (g)	1.12 ± 0.07	1.18 ± 0.10	1.24 ± 0.09	1.39 ± 0.16 #	1.27 ± 0.11	1.23 ± 0.17	1.46 ± 0.16 #	1.43 ± 0.17 #
Heart weight/body weight x 10^3	3.54 ± 0.29	4.00 ± 0.59	4.08 ± 0.25	4.61 ± 0.51	3.60 ± 0.48	3.45 ± 0.34	4.09 ± 0.34 #	4.11 ± 0.32 #
LV weight (g)	0.52 ± 0.07	0.56 ± 0.14	0.56 ± 0.11	0.54 ± 0.09	0.57 ± 0.17	0.56 ± 0.15	0.69 ± 0.23	0.68 ± 0.22
LV weight/body weight x 10^3	1.65 ± 0.20	1.93 ± 0.59	1.76 ± 0.23	1.78 ± 0.18	1.61 ± 0.49	1.56 ± 0.42	1.92 ± 0.63	1.94 ± 0.56
LVEDD (mm)	6.46 ± 0.47	5.69 ± 0.29	5.87 ± 1.21	5.48 ± 0.68	6.86 ± 0.82	7.03 ± 0.70	6.49 ± 0.38	6.46 ± 0.62
LVPWd (mm)	1.73 ± 0.32	1.73 ± 0.41	1.81 ± 0.27	1.97 ± 0.38	1.72 ± 0.26	1.59 ± 0.27	1.95 ± 0.31	1.72 ± 0.23
IVSd (mm)	1.48 ± 0.28	1.75 ± 0.34	1.91 ± 0.31	2.05 ± 0.42	1.68 ± 0.28	1.65 ± 0.24	1.95 ± 0.34	1.75 ± 0.23
LVESD (mm)	3.02 ± 0.60	2.70 ± 0.35	3.47 ± 1.24	3.51 ± 0.87	3.52 ± 0.44	3.82 ± 0.45	3.86 ± 0.54	3.89 ± 0.59
LVPWs (mm)	2.84 ± 0.40	2.71 ± 0.46	2.49 ± 0.30	2.68 ± 0.15	2.71 ± 0.31	2.44 ± 0.36	2.80 ± 0.36	2.46 ± 0.26
IVSs (mm)	2.82 ± 0.38	2.88 ± 0.29	2.80 ± 0.40	2.67 ± 0.62	2.81 ± 0.27	2.78 ± 0.30	2.88 ± 0.43	2.63 ± 0.25
RWT (mm)	0.51 ± 0.12	0.62 ± 0.15	0.68 ± 0.25	0.75 ± 0.18	0.51 ± 0.12	0.47 ± 0.09	0.61 ± 0.10	0.55 ± 0.10

Data expressed as means ± SD. Two-way ANOVA was used to determine group or rat strain effects followed by Tukey's *post hoc* test. # $P < 0.05$ in SHR-control group compared to WKY-control group or SHR-LPS group compared to WKY-LPS group. WKY, Wistar Kyoto rat; SHR, spontaneously hypertensive rat; LPS, lipopolysaccharide group; LVEDD, left ventricular end-diastolic diameter; LVPWd, left ventricular posterior wall thickness at end-diastole; IVSd, interventricular septal wall thickness at end-diastole; LVESD, left ventricular end-systolic diameter; LVPWs, left ventricular posterior wall thickness at end-systole; IVSs, interventricular septal wall thickness at end-systole; RWT, relative wall thickness.

4.3.2 LV diastolic function

In the short-term groups, there was a significant effect of LPS administration on mitral inflow velocity in early diastole (E; $F = 22.68$, $p < 0.0001$, Table 4.3). There was also a significant interaction between LPS administration and rat strain ($F = 6.71$, $p = 0.02$). E was significantly reduced in LPS-treated SHR compared to its control group ($p = 0.0001$).

There was a significant effect of LPS administration on E/A ($F = 8.38$, $p = 0.008$), septal e' ($F = 16.8$, $p = 0.0004$), and average e' ($F = 14.9$, $p = 0.0008$), all indices of LV relaxation. There was also a significant effect of LPS administration on LV passive stiffness, as indicated by average e'/a' ($F = 8.41$, $p = 0.008$). However, there were no significant effects of LPS administration on E/e', an index of LV filling pressures, between the different experimental groups ($F = 1.29$, $p = 0.30$). There was also no significant effect of rat strain on the diastolic function variables (all $p > 0.05$).

In the long-term groups, there was no significant effect of LPS administration on any of the diastolic function variables (all $p > 0.05$, Table 4.3). However, there was a significant effect of rat strain on LV relaxation (septal e'; $F = 15.08$, $p = 0.0004$). There was no significant effect of rat strain on LV passive stiffness (e'/a') and LV filling pressure (E/e') (both $p > 0.05$).

Table 4.3 Effect of LPS-induced inflammation on LV diastolic function in the short- and long-term groups.

	24-hours				6-weeks			
	WKY-control	**WKY-LPS**	**SHR-control**	**SHR-LPS**	**WKY-control**	**WKY-LPS**	**SHR-control**	**SHR-LPS**
E (cm/s)	1.09 ± 0.13	0.98 ± 0.19	1.16 ± 0.15	0.73 ± 0.17 *	1.19 ± 0.16	1.16 ± 0.12	1.05 ± 0.17	1.07 ± 0.14
E/A	1.43 ± 0.40	1.10 ± 0.29	1.51 ± 0.63	0.90 ± 0.31 *	1.43 ± 0.23	1.49 ± 0.33	1.98 ± 0.90	1.78 ± 0.81
Septal e' (cm/s)	5.08 ± 0.98	3.32 ± 0.60 *	4.24 ± 0.84	3.20 ± 0.85 *	4.95 ± 0.97	5.02 ± 0.60	4.03 ± 0.81 #	4.08 ± 0.83 #
Lateral e’	4.04 ± 0.34	3.60 ± 0.42	4.24 ± 0.94	3.28 ± 0.85	4.83 ± 0.94	4.93 ± 1.08	4.61 ± 0.98	4.72 ± 0.90
Average e’ (cm/s)	4.56 ± 0.45	3.46 ± 0.17	4.23 ± 0.86	3.24 ± 0.83 *	4.90 ± 0.86	4.99 ± 0.75	4.32 ± 0.53	4.39 ± 0.65
Average e'/a’	1.38 ± 0.41	0.87 ± 0.24 *	1.04 ± 0.32	0.80 ± 0.19	1.29 ± 0.32	1.23 ± 0.24	1.18 ± 0.23	1.17 ± 0.29
E/e’	0.24 ± 0.04	0.29 ± 0.06	0.28 ± 0.04	0.24 ± 0.07	0.24 ± 0.05	0.22 ± 0.04	0.25 ± 0.05	0.23 ± 0.05

Data expressed as means ± SD. Two-way ANOVA was used to determine group or rat strain effects followed by Tukey’s post hoc test. * $P < 0.05$ in WKY-LPS group compared to WKY-control group or SHR-LPS group compared to SHR-control group. # $P < 0.05$ in SHR-control compared to WKY-control or SHR-LPS group compared to WKY-LPS group. WKY, Wistar Kyoto rat; SHR, spontaneously hypertensive rat; LPS, lipopolysaccharide group; E-wave, early mitral inflow velocity; E/A, ratio of early to late mitral inflow velocity; e’, early annular tissue velocity; e’/a’, ratio of early to late annular tissue velocity; E/e’, ratio of early mitral inflow velocity to early annular tissue velocity.

4.3.3 LV systolic function

In the short-term groups, there was a significant effect of rat strain on global systolic function, indicated by LV ejection fraction (LVEF; $F = 12.9$, $p = 0.002$) and endocardial fractional shortening (FS_{end}; $F = 12.71$, $p = 0.002$) (Table 4.4). However, there were no significant effects of LPS administration on LVEF and FS_{end}.

There was a significant effect of LPS administration on LVOT VTI ($F = 24.54$, $p < 0.0001$), and LVOT V_{max} ($F = 11.67$, $p = 0.0024$), indices of stroke volume. Additionally, there was a significant effect of rat strain on LVOT VTI ($F = 9.43$, $p = 0.005$), and LVOT V_{max} ($F = 8.01$, $p = 0.01$). We noted no significant effects of LPS administration and rat strain on longitudinal systolic function, as indicated by systolic mitral velocity (s', all $p > 0.05$).

In the long-term groups, there was a significant effect of rat strain on LVEF ($F = 11.55$, $p = 0.002$) and FS_{end} ($F = 10.81$, $p = 0.002$), indices of global systolic function (Table 4.4). There was no significant effect of LPS administration on global systolic function (all $p > 0.05$).

There was a significant effect of rat strain on LVOT VTI ($F = 6.45$, $p = 0.01$). There was no significant LPS administration effect on LVOT VTI after six weeks. Finally, there were no significant effects of LPS administration or rat strain on LVOT V_{max} and s' between the different experimental groups (all $p > 0.05$).

Table 4.4 Effects of LPS-induced inflammation on global systolic function in the short- and long-term groups.

	24 hours				6 weeks			
	WKY-control	**WKY-LPS**	**SHR-control**	**SHR-LPS**	**WKY-control**	**WKY-LPS**	**SHR-control**	**SHR-LPS**
LVEF (%)	87.59 ± 4.78	87.37 ± 3.99	77.33 ± 11.54	70.77 ± 12.20 $^{\#}$	82.84 ± 3.87	79.93 ± 4.96	75.87 ± 6.62 $^{\#}$	75.48 ± 7.13
FS_{end} (%)	53.54 ± 7.21	52.68 ± 5.77	42.87 ± 12.47	36.64 ± 9.86 $^{\#}$	46.95 ± 4.01	44.07 ± 4.60	40.69 ± 6.33 $^{\#}$	40.02 ± 6.30
LVOT VTI (cm)	7.22 ± 0.89	5.92 ± 1.14	6.61 ± 0.94	4.13 ± 1.08 $^{*\#}$	6.67 ± 0.53	6.41 ± 0.68	5.84 ± 0.75 $^{\#}$	6.17 ± 0.89
LVOT V_{max} (m/s)	1.31 ± 0.17	1.17 ± 0.15	1.20 ± 0.19	0.87 ± 0.22 $^{*\#}$	1.17 ± 0.16	1.17 ± 0.16	1.05 ± 0.13	1.12 ± 0.21
Average s' (cm/s)	4.50 ± 0.46	4.52 ± 0.40	4.33 ± 0.52	3.89 ± 0.36	5.07 ± 0.83	5.05 ± 0.74	4.32 ± 0.84	4.70 ± 0.69

Data expressed as means ± SD. Two-way ANOVA was used to determine group or rat strain effects followed by Tukey's post hoc test. * $P < 0.05$ in SHR-LPS group compared to SHR-control group. $^{\#}$ $P < 0.05$ in SHR-control compared to WKY-control or SHR-LPS group compared to WKY-LPS group. WKY, Wistar Kyoto rat; SHR, spontaneously hypertensive rat; LPS, lipopolysaccharide group; LVEF, left ventricular ejection fraction; FS_{end}, endocardial fractional shortening; LVOT VTI, left ventricular outflow tract velocity time integral; LVOT V_{max}, left ventricular outflow tract peak velocity; s', systolic mitral annular velocity.

4.4 Speckle-tracking echocardiography (STE)

In the short-term groups, there was a significant effect of LPS administration on myocardial deformation, as shown by circumferential strain ($F = 6.06$, $p = 0.02$, Figure 4.3A) and longitudinal strain ($F = 10.56$, $p < 0.0001$, Figure 4.4A). There was a significant effect of rat strain on circumferential strain ($F = 49.32$, $p < 0.0001$) and longitudinal strain ($F = 47.59$, $p < 0.0001$).

Although there was no significant effect of LPS administration (all $p > 0.05$), there was a significant effect of rat strain on the rate of myocardial deformation, as indicated by circumferential strain rate ($F = 39.58$, $p < 0.0001$, Figure 4.3C) and longitudinal strain rate ($F = 26$, $p < 0.0001$, Figure 4.4C).

In the long-term groups, there was a significant effect of rat strain on circumferential strain ($F = 13.02$, $p = 0.0008$, Figure 4.3B), longitudinal strain ($F = 37.63$, $p < 0.0001$, Figure 4.4B), circumferential strain rate ($F = 11.87$, $p = 0.0013$, Figure 4.3D) and longitudinal strain rate ($F = 42.33$, $P < 0.0001$, Figure 4.4D). LPS administration had no significant effect on myocardial deformation and the rate of deformation in the long-term groups.

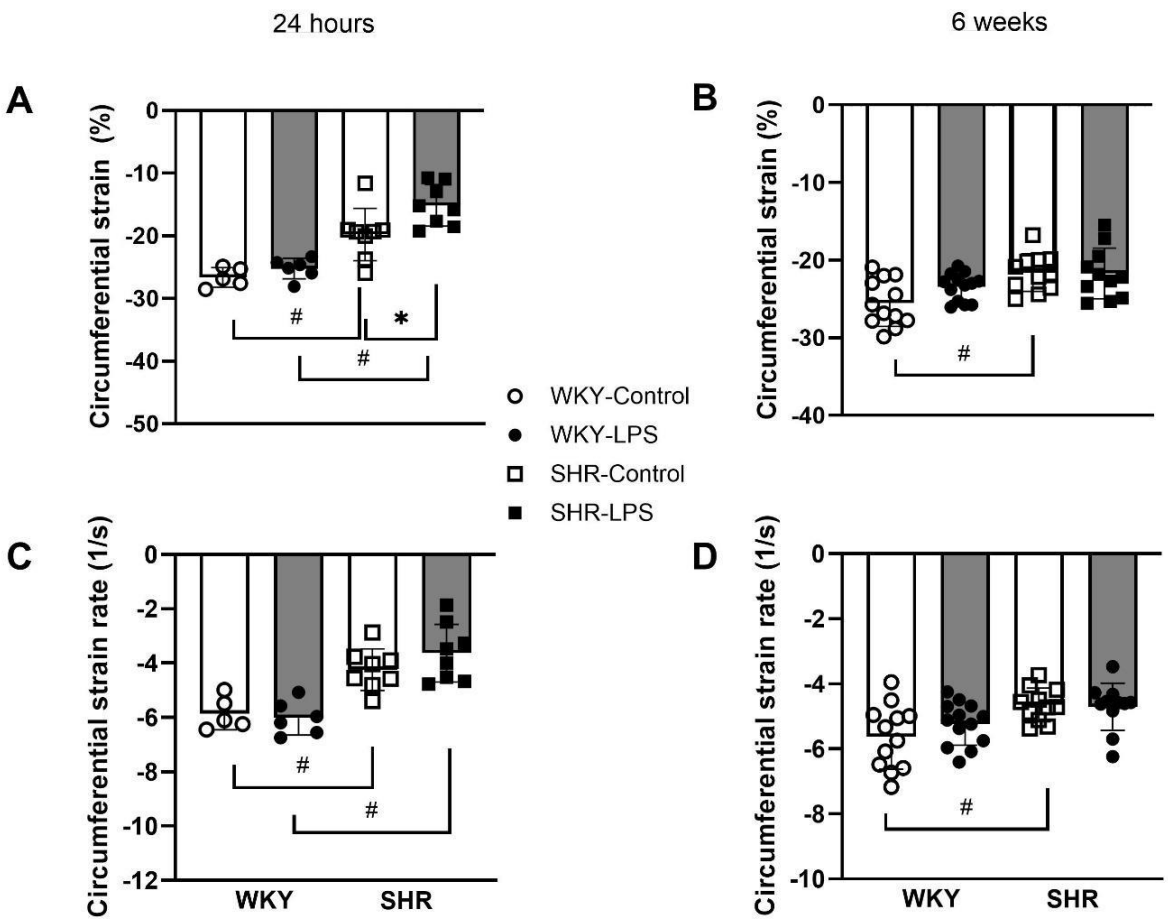

Figure 4.3 Circumferential strain and strain rate in control and LPS-treated animals at (A & C) 24 hours and at (B & D) six weeks.

Data expressed as means ± SD. Two-way ANOVA was used to determine group or rat strain effects followed by Tukey's post hoc test. * $P < 0.05$ in SHR-LPS group compared to SHR-control group. # $P < 0.05$ in SHR-control compared to WKY-control or SHR-LPS group compared to WKY-LPS group. WKY, Wistar Kyoto rat; SHR, spontaneously hypertensive rat; LPS, lipopolysaccharide group.

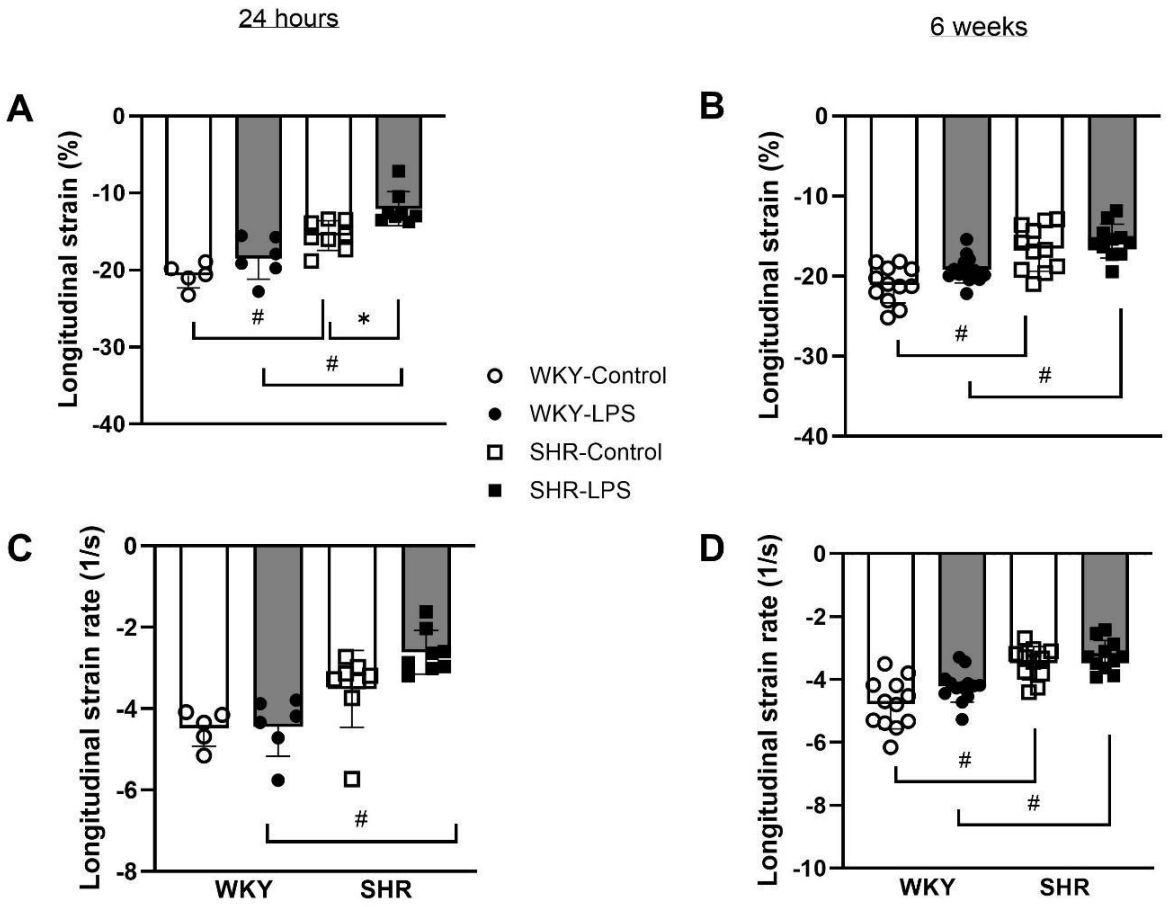

Figure 4.4 Longitudinal strain and strain rate in control and LPS-treated rats at (A & C) 24 hours and at (B & D) six weeks.

Data expressed as means ± SD. Two-way ANOVA was used to determine group or rat strain effects followed by Tukey's post hoc test. * $P < 0.05$ in SHR-LPS group compared to SHR-control group. # $P < 0.05$ in SHR-control compared to WKY-control or SHR-LPS group compared to WKY-LPS group. WKY, Wistar Kyoto rat; SHR, spontaneously hypertensive rat; LPS, lipopolysaccharide group.

4.5 Collagen volume fraction (CVF)

In the short-term groups, LPS administration significantly increased CVF ($F = 5.5$, $p = 0.02$, Figure 4.5A). Although there was a significant effect of rat strain on CVF ($F = 4.88$, $p = 0.04$), there were no significant interaction effects.

In the long-term groups, there was a significant interaction between LPS administration and rat strain effects on CVF ($F = 4.1$, $p = 0.049$). CVF was significantly greater in SHR-LPS compared to the WKY-LPS ($p = 0.049$) group (Figure 4.5B).

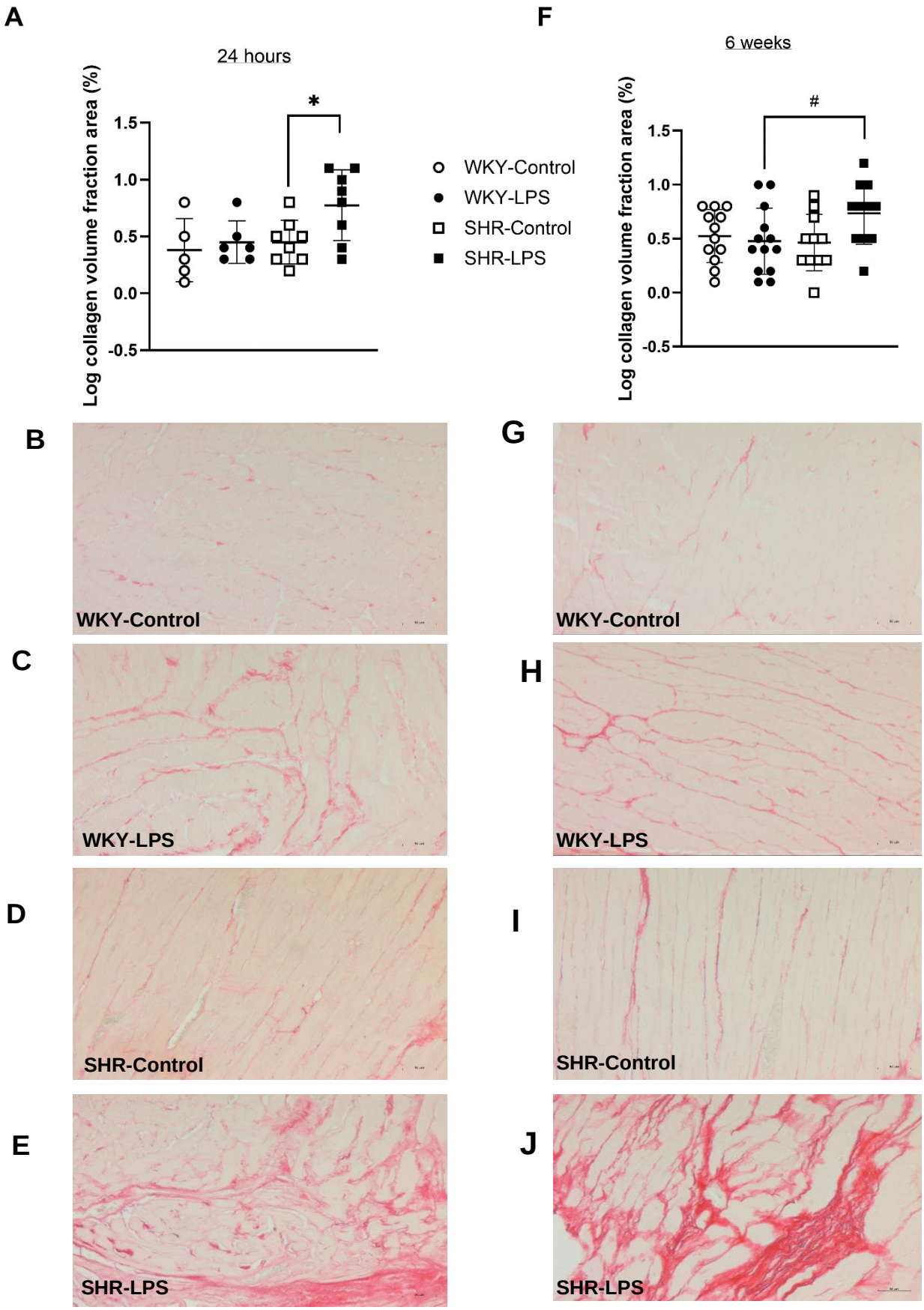

Figure 4.5 Collagen volume fraction area and representative images of the left

ventricle stained with Picrosirius red staining under a brightfield microscope in control and LPS-treated rats at (A-E) 24 hours and at (F-J) six weeks.

Data expressed as means ± SD. Two-way ANOVA was used to determine group or rat strain effects on the log transformed data followed by Tukey's *post hoc* test. * $P < 0.05$ in SHR-LPS group compared to SHR-control group and $^{\#}$ $P < 0.05$ in SHR-LPS compared to WKY-LPS. WKY, Wistar Kyoto rat; SHR, spontaneously hypertensive rats; LPS, lipopolysaccharide group.

4.6 Relationship between IL- 1β concentration and echocardiographic markers of LV structure and function

To determine whether inflammatory cytokines were associated with changes in the echocardiographic parameters, a Pearson's correlation analysis was performed. In the short-term groups (Figure 4.6A), IL- 1β was associated with impaired relaxation (septal e': r = -0.36, p = 0.04; average e': r = -0.33, p = 0.046) and LV passive stiffness (e'/a' : r = -0.36, p = 0.04), but not with myocardial deformation (CS: r = 0.14, p = 0.49; CSR: r = 0.01, p = 0.95; LS: r = 0.19, p = 0.36); LSR: r = 0.10, p = 0.61), RWT (r = 0.14, p = 0.50) or fibrosis (CVF: r = 0.03, p = 0.87).

In the long-term groups (Figure 4.6B), IL- 1β was associated with impaired relaxation (E/A: r = 0.35, p = 0.01; average e': r = 0.29, p = 0.047), increased LV passive stiffness (e'/a': r = 0.34, p = 0.02), impaired myocardial deformation (r = -0.32, p = 0.03) and fibrosis (CVF: r = 0.38, p = 0.008), but not with RWT (r = -0.05, p = 0.75), LV filling pressure (E/e': r = -0.08, p = 0.60) or the other markers of myocardial strain (CS: r = 0.05, p = 0.70; CSR: r = 0.18, p = 0.22; LSR: r = -0.13, p = 0.38).

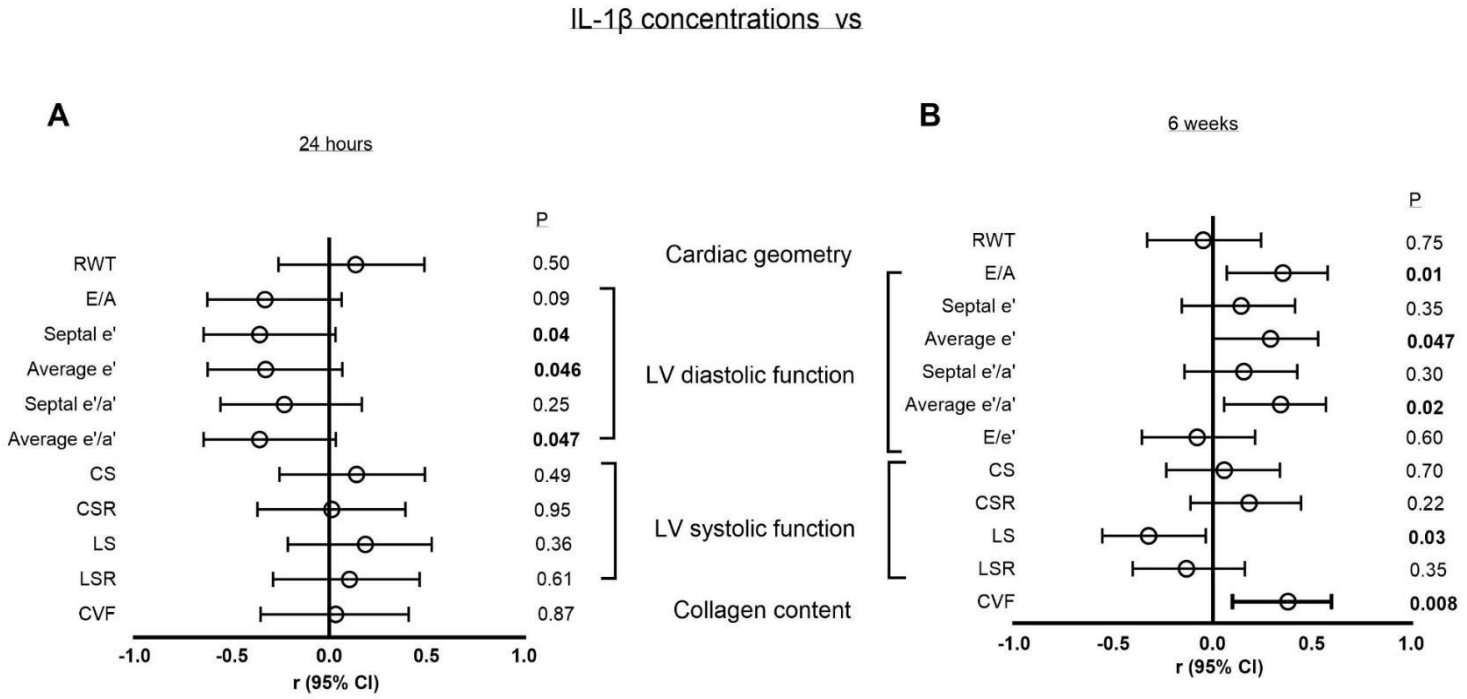

Figure 4.6 Associations between inflammatory cytokine IL- 1β and measures of cardiac geometry, LV diastolic function and systolic function in the (A) short-term and (B) long-term groups.

Pearson's correlation analysis was performed to determine the associations. IL- 1β, interleukin- 1β; RWT, relative wall thickness; E/A, ratio of early to late mitral inflow velocity; e', early annular tissue velocity; e'/a', ratio of early to late annular tissue velocity; E/e', ratio of early mitral inflow velocity to early annular tissue velocity; CS, circumferential strain; CSR, circumferential strain rate; LS, longitudinal strain; LSR, longitudinal strain rate; CVF, collagen volume fraction area.

4.7 Relationship between collagen volume and echocardiographic markers of LV structure and function

To determine whether changes in the structural properties of the LV were associated with changes in the echocardiographic parameters, a Pearson's correlation analysis was performed. In the short-term groups (Figure 4.7A), CVF was associated with impaired relaxation (e': ($r = -0.51$, $p = 0.006$) and impairments in myocardial deformation (CS: $r = 0.53$, $p = 0.004$; CSR: $r = 0.44$, $p = 0.02$; and LS: $r = 0.42$, $p =$ 003), but not with RWT ($r = 0.3282$, $p = 0.095$).

In the long-term groups (Figure 4.7B), CVF was only associated with impaired relaxation (E/A: $r = 0.33$, $p = 0.02$), but not with RWT ($r = 0.0944$, $p = 0.53$) or any marker of myocardial strain (CS: $r = 0.10$, $p = 0.49$; CSR: $r = 0.21$, $p = 0.15$; LS: $r = -$ 0.04, $p = 0.75$; LSR: $r = 0.04$, $p = 0.77$).

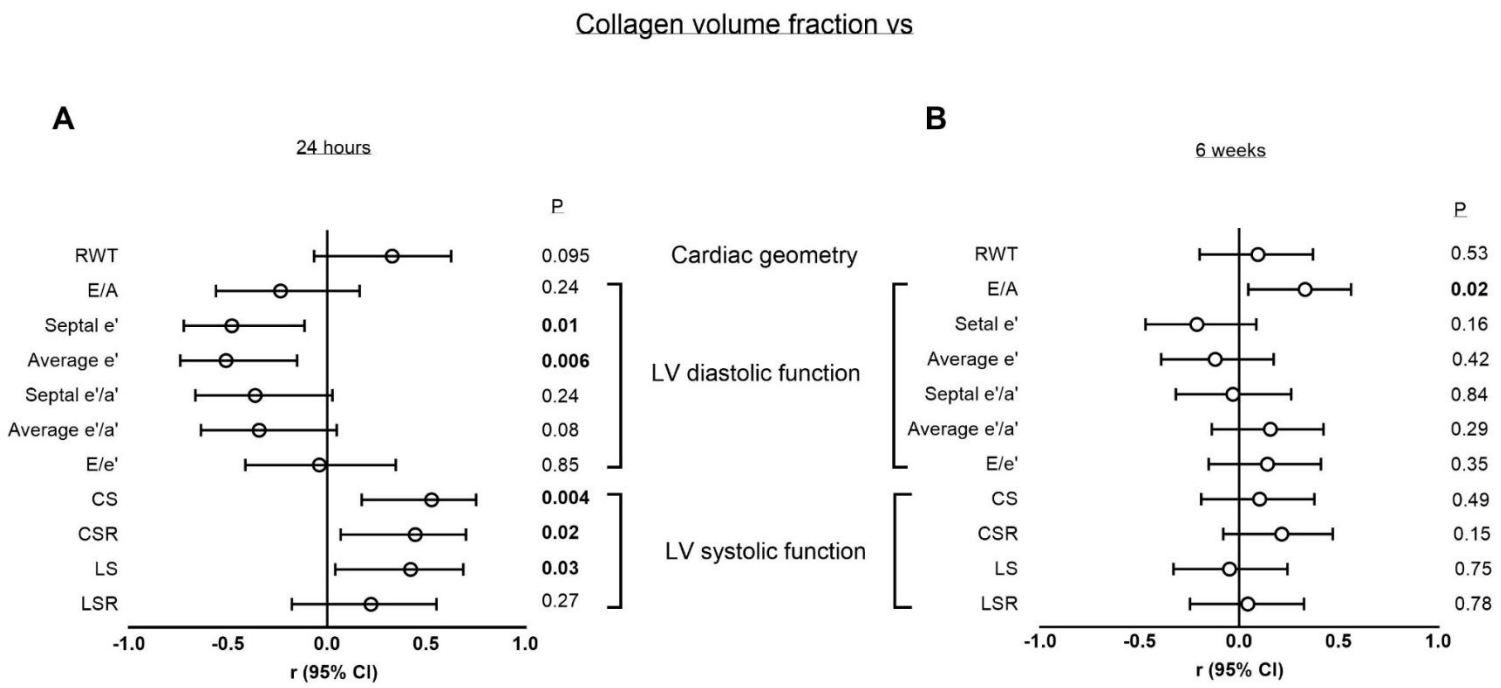

Figure 4.7 Associations between collagen volume fraction and measures of cardiac geometry, LV diastolic function and systolic function in the (A) short-term and (B) long-term groups.

Pearson's correlation analysis was performed to determine the associations. RWT, relative wall thickness; E/A, ratio of early to late mitral inflow velocity; e', early annular tissue velocity; e'/a', ratio of early to late annular tissue velocity; E/e', ratio of early mitral inflow velocity to early annular tissue velocity; CS, circumferential strain; CSR, circumferential strain rate; LS, longitudinal strain; LSR, longitudinal strain rate.

Chapter 5: Discussion

The present study investigated the short- and long-term effects of acute LPS-induced inflammation on cardiac geometry and function as well as whether pre-existing hypertension was exacerbated by the effects of inflammation on cardiac function. Our main results are that in both normotensive and hypertensive rats, after 24 hours, there was increased inflammation as indicated by increased IL- 1β concentrations. The increased concentrations of IL- 1β was associated with impaired LV relaxation (decreased E/A and e') and increased LV passive stiffness (decreased e'/a'), independent of changes in body weight or blood pressure. In the hypertensive rats, only LPS administration resulted in additional impairments in LV systolic function, as measured by decreased pump function (reduced LVEF and FS_{end}) as well as global myocardial deformation (decreased circumferential and longitudinal strain). Impaired systolic function measures mentioned above were related to the change in collagen volume.

In the long-term, a single LPS administration did not result in persistent systemic inflammation, as IL- 1β concentrations were no different from control rats after six weeks. Furthermore, there were no differences in body weight, blood pressure or any of the echocardiographic parameters between the LPS and control rats in either of the rat strains. However, in the hypertensive rats there were increased heart weight and heart weight normalised to body weight, impaired systolic function (decreased LVEF, LVOT VTI and FS_{end}) and impaired myocardial deformation (decreased circumferential strain, circumferential strain rate, longitudinal strain and longitudinal strain rate), compared to the normotensive rats. Interestingly, there were no differences in LV diastolic parameters between normotensive and hypertensive rats. Although exposure to acute LPS-induced inflammation with pre-existing hypertension did not compound

the hypertension-induced changes in LV systolic function, it did contribute to increased fibrosis (collagen content). Taken together, these results suggest that in the short-term, acute exposure to high-grade inflammation impacts both LV systolic and diastolic function. In addition, rats predisposed to hypertension have a more pronounced inflammation-induced cardiac dysfunction. An acute exposure to high-grade inflammation did not have significant effects on the rats, beyond the impact of hypertension, on cardiac function. However, an acute exposure to high-grade inflammation may cause structural changes in the long-term that may be associated with impaired myocardial deformation, an early subclinical change in systolic function.

5.1 The effects of acute LPS administration on systemic inflammation, body weight and blood pressure

LPS triggers inflammation in a receptor-mediated manner, resulting in the activation of downstream signalling pathways (Zhang *et al.*, 2017). LPS binds to toll-like receptor (TLR)- 4, which in turn activates the nuclear factor- κB (NF- κB) signalling pathway (Ghosh & Hayden, 2008). Activation of these pathways increases the cellular inflammatory response, which is mainly responsible for the release of pro-inflammatory cytokines (Wang *et al.*, 2017). NF- κB exists as a complex and is localised in the cytosol, bound to its inhibitor, IκB, in healthy cells (Ghosh & Hayden, 2008). LPS-induced injury triggers phosphorylation of the NF- κB complex mediated by IκB kinase complex (IKK), which degrades IκB, and releases the NF- κB complex to translocate into the nucleus and promote expression of target genes, including IL-1β (Hou *et al.*, 2015). Indeed, in the present study, a single dose of LPS induced inflammation, as seen by increased IL- 1β concentrations in the short-term. These results are in line with previous studies where the effects of LPS were determined

within 24 hours of administration *in vivo* (Weil *et al.*, 2011; Zhao *et al.*, 2016; Zhang *et al.*, 2017; Zhang *et al.*, 2018; Li *et al.*, 2018; Xiao *et al.*, 2021). The increases in systemic inflammation in the present study had no effect on either body weight or blood pressure within 24 hours. In previous animal models of septic shock, it was shown that cardiac output and systemic vascular resistance were decreased (Mulligan *et al.*, 2012; Clerc *et al.*, 2018). Sepsis initially results in vasodilation and increased capillary permeability due to the inflammatory mediators released as part of the immune reaction (Ince *et al.*, 2016; Bermejo-Martin *et al.*, 2018). The hypovolemia and reduced peripheral resistance occur as a result of the vasodilation, leading to a reduction in stroke volume and the increase in heart rate as a compensatory mechanism (Clerc *et al.*, 2018). Nevertheless, it is probable that the reduced cardiac output was due to the depleted intravascular volume which was associated with the lack of fluid replacement (Clerc *et al.*, 2018). Therefore, it has been suggested that LPS causes LV dysfunction mainly via temporary haemodynamic changes (Lew *et al.*, 2013). In the present study, the dose of LPS was low (1 mg/kg) compared to the majority of previous studies that used 10 mg/kg, which may not have resulted in the typical septic shock symptoms previously observed. Despite the impairments in cardiac function induced by inflammation that will be discussed later, it may be that blood pressure was maintained by an increase in the sympathetic nervous system activity (Clerc *et al.*, 2018).

Despite the short-term effects of LPS administration being similar to previous reports (Weil *et al.*, 2011; Zhang *et al.*, 2017; Xiao *et al.*, 2021), when the animals in the present study recovered for six weeks after a single dose of LPS, there were no differences in serum IL- 1β concentrations between the LPS and control groups. This

suggests that the acute inflammatory response was resolved after six weeks. Indeed, it is well accepted that LPS-induced sickness behaviour resolves within 72 hours (Ortega-Gómez *et al.*, 2013). Similarly in the present study, when monitoring the animals for sickness behaviour, all rats recovered and showed no sickness behaviour (appendix A) within 3-5 days after the LPS administration.

In the present study, one week after LPS administration, body weight did tend to decrease in both normotensive and hypertensive rats. It has been well accepted that in animals with an acute infection, there is a decrease in food and water intake during the acute sickness response (Harden *et al.*, 2006). Nevertheless, once the sickness behaviour was resolved, increases in body weight were similar between the groups for the duration of the study. Chronic injections of LPS did not change body weight compared to the control group (Asgharzadeh *et al.*, 2018*a*). Similarly, there were no differences in blood pressure between the LPS and control groups of the respective rat strains. However, as expected, the blood pressure in the SHR were significantly higher compared to their WKY counterparts.

5.2 The short- and long-term effects of LPS administration and hypertension on LV geometry and myocardial fibrosis

In the present study, exposure to LPS for 24 hours had limited effects on any changes in cardiac structure. Although there were trends towards an increased septal wall thickness and a decreased LV internal diameter, these differences were not significant. Nevertheless, LPS administration did increase the heart weight, even after adjusting for body weight. Interestingly, in the SHR that received LPS, there was a significant increase in the collagen volume fraction compared to the control SHR. These results suggest that LPS may lead to structural changes in the heart that may

be worsened by the effects of pressure overload induced by hypertension. Additionally, we did not show any rat strain-specific effects in the cardiac geometry variables in the short-term groups. These results are inconsistent with previous evidence that showed significant differences in cardiac geometry (increased LV mass, interventricular septal wall thickness at end-diastole, LV posterior wall thickness at end-diastole and relative wall thickness) in 11-week-old SHR compared to age-matched WKY rats (He *et al.*, 2021). Changes in cardiac geometry were shown to begin from 12 weeks after birth (Kokubo *et al.*, 2005), which we did not observe in our 4-month-old SHR. A previous study suggested that the development of LV hypertrophy, which is responsible for the increased LV wall thickness, begins from five months (Li *et al.*, 2019). It is possible that the changes in LV wall thickness in the present study may have required an extended study duration beyond six weeks.

In the long-term rats, there were overall significant rat strain effects on the heart weight and normalised heart weight. These results are consistent with several previous studies showing similar effects in SHR compared to WKY rats in cardiac weight (Miguel-Carrasco *et al.*, 2010; Eiler *et al.*, 2011; He *et al.*, 2021). Interestingly, CVF was increased in the SHR exposed to LPS compared to their WKY counterparts and compared to their control SHR. Furthermore, there were no differences in CVF between the SHR-Control and WKY-Control rats. These results suggest that the initial exposure to inflammation may have initiated adverse cardiac remodelling in the hypertensive, but not normotensive rats.

It is well established that pressure overload induced by hypertension drives significant changes in myocardial structure, leading to the development of myocardial hypertrophy (increased relative wall thickness and increased LV mass) or fibrosis

(Wachtell *et al.*, 2000). However, in the present study we did not observe an increase in CVF in the hypertensive control rats compared to normotensive rats in the long-term groups. Hence, it is likely that this response was triggered by the initial inflammatory response. Indeed, LPS-induced inflammation causes cardiac fibrosis as a primary effect, without pre-existing cardiac injury (Lew *et al.*, 2013; Asgharzadeh *et al.*, 2018*b*). Systemic inflammation causes the migration and infiltration of leukocytes into the endothelium, as well as increased production of tumour growth factor- β, resulting in the differentiation of cardiac fibroblasts into myofibroblasts that produce collagen (Paulus & Tschöpe, 2013). Through the action of TLR- 4, LPS triggers the expression of collagen type I and III, with more expression of the rigid type I compared to the more compliant type III, resulting in increased fibrosis (Kasner *et al.*, 2011). In addition to increased collagen type I expression, inflammation promotes increased collagen fibre cross-linking, which contributes to fibrosis and is positively associated impaired LV diastolic function (López *et al.*, 2012).

There are two main patterns of how collagen accumulates to form myocardial fibrosis; reparative fibrosis which replaces dead cardiomyocytes and forms fibrotic scars as well as reactive fibrosis which occurs without cell loss (López *et al.*, 2015). Although reparative fibrosis occurs to repair the myocardium and prevent further damage, apoptosis has been reported to play a role in wound healing processes (Johnson & DiPietro, 2013). Apoptosis is responsible for eliminating damaged cells and maintaining tissue homeostasis (Chen & Lau, 2010). High levels of apoptosis have been reported in several cases of fibrosis (Johnson & DiPietro, 2013). However, in the present study, we did not measure apoptosis and hence we are unable to make firm conclusions on the type of fibrosis. Although it was not statistically significant, in the

SHR that received LPS in the long-term, there was a decreased RWT compared to the SHR-Control rats. These results suggest a more eccentric remodelling pattern, which is characterised by decreased relative wall thickness (Nistri *et al.*, 2008), instead of a concentric pattern.

Although previous studies used repeated administrations of LPS, they showed similar CVF results as the present long-term SHR-LPS rats (Lew *et al.*, 2013; Asgharzadeh *et al.*, 2018*a*, 2018*b*; Wu *et al.*, 2018; Katare *et al.*, 2020), others have reported no changes in CVF in the first week after LPS administration (Lew *et al.*, 2014). Similarly, others have shown that daily LPS administration increased CVF after two weeks (Katare *et al.*, 2020). Although another study reported increased expression of fibrotic-related genes in the short-term (Xianchu *et al.*, 2018), it is unlikely that this would translate into collagen changes after 24 hours. In this regard, sepsis patients usually present with increased permeability of the vessels and tissue oedema in various organs due to the initial inflammatory cell infiltration (Lee & Slutsky, 2010). Hence, in the present study, the initial changes in wall thickness and heart weight in the rats in the short-term groups may be explained by myocardial oedema, a common but underexplored feature of sepsis. Future studies should investigate the potential causes of the changes in cardiac remodelling after acute, short-term LPS administration.

Taken together, the present study showed that acute LPS administration resulted in adverse cardiac remodelling that may be due to oedema in the short-term, and fibrosis in the long-term. However, only in rats predisposed to hypertension did the inflammation cause the adverse effects. It is well established that adverse ECM remodelling contributes to impaired LV diastolic and systolic dysfunction (Zhang *et al.*,

2024). However, several studies have also shown that LV diastolic dysfunction may develop without myocardial hypertrophy (Zile *et al.*, 2011). Therefore, we further explored the acute and chronic effects of acute LPS administration on LV diastolic and systolic function.

5.3 The short- and long-term effects of LPS administration and hypertension on LV diastolic function

It is well accepted that systemic inflammation impacts cardiac function, both in acute and chronic inflammatory conditions (Peng *et al.*, 2021). Indeed LPS-induced inflammatory mediators, including IL- 1β, have been shown to impact cardiac function (Xiao *et al.*, 2021). In the present study, acute LPS administration resulted in impaired LV relaxation as measured by a reduced E/A and decreased mitral annular lengthening velocity in early diastole (e') in the short-term. A decreased e' is considered one of the earliest markers of impaired LV relaxation, and unlike the E/A ratio, is not dependent on filling pressures (Nagueh *et al.*, 1997). Several studies reported impaired relaxation as indicated by decreased e' (Sturgess *et al.*, 2021; Soni *et al.*, 2022). Similar to our results, previous studies have consistently reported LV diastolic dysfunction in response to LPS administration (Joulin *et al.*, 2009; Clerc *et al.*, 2018). Furthermore, LPS administration resulted in an increase in LV passive stiffness, as indexed by a decreased e'/a' in the short-term. Interestingly, these changes did not translate into changes in LV filling pressure (E/e'). In contrast, a study reported no differences in LV passive stiffness as indexed by e'/a' in the LPS group compared to the control group (Soni *et al.*, 2022). The younger mice used in the previous study (Soni *et al.*, 2022), had not been exposed to hypertension, possibly explaining the inconsistency with our results. It is well established that hypertension

causes increased LV passive stiffness via LV hypertrophy (Lundin *et al.*, 1983). As previously mentioned, inflammation may be a trigger for hypertension-induced cardiac structural and functional changes. Importantly, the impairments in LV diastolic function were more pronounced in hypertensive animals that received LPS compared to their WKY counterparts. This result is not surprising, as we have already explained that hypertension is one of the main driving factors for the development of LV diastolic dysfunction (Lundin *et al.*, 1983).

In the long-term rats, acute LPS-administration did not impact LV diastolic function. This is not surprising as the IL- 1β concentrations returned to baseline levels at the time of termination. Indeed, others have suggested that the acute changes in LV diastolic function resulting from acute inflammation are reversed once the inflammation has resolved (Van Tassell *et al.*, 2013). Nevertheless, in hypertensive rats, LV relaxation (septal e') was impaired compared to the normotensive rats. However, there were no differences in LV passive stiffness (e'/a') or LV filling pressures (E/e'), between the hypertensive and normotensive rats. These results contrast with previous animal studies where SHR demonstrated increased LV passive stiffness and impaired LV filling pressures compared to WKY rats associated with concentric hypertrophy (Lundin *et al.*, 1983; Conrad *et al.*, 1995). However, in the present study, we did not show an increase in RWT in hypertensive rats, which may explain the lack of increases in LV passive stiffness and filling pressure, as previously mentioned. Even so, it is well accepted that long standing hypertension is associated with abnormal LV relaxation, which may be due to functional, not just structural changes (De Simone *et al.*, 2005).

LV diastolic dysfunction is driven by impairments in both active relaxation and LV passive stiffness (Franssen & González Miqueo, 2016). In active relaxation, Ca^{2+} handling plays a key role in maintaining diastolic function (Biesiadecki *et al.*, 2014). Evidence suggests that inflammation impairs relaxation by reducing the expression of Ca^{2+} regulation proteins *in vitro*, including the SERCA pump, which directly results in impaired relaxation (Combes *et al.*, 2002). Changes in the ECM, largely driven by changes in collagen volume and change in the phosphorylation of titin, contribute to passive LV stiffness (Zile *et al.*, 2015). In this regard, in a rat model of HFpEF, it has been shown that inflammation resulted in titin hypophosphorylation, thus resulting in increased LV passive stiffness (Franssen *et al.*, 2016). Additionally, inflammation triggered collagen gene expression and dysregulated collagen turnover, resulting in the accumulation of collagen in human and animal studies of LV diastolic dysfunction (Westermann *et al.*, 2011; Manilall *et al.*, 2021).

In the present study we showed similar associations between inflammation and LV diastolic dysfunction markers. Even in the acute inflammatory response, the present study shows that inflammation contributes to these mechanisms of impaired LV diastolic function. We showed significant associations between IL- 1β concentrations and impaired relaxation (e') and increased LV passive stiffness (e'/a') in the short-term rats. Interestingly, we also showed that CVF was associated with impaired relaxation (e'), but not with LV passive stiffness (e'/a'). As previously mentioned, it is unlikely that after 24 hours collagen content would change, and hence it may be that the fluid shifts and cardiac oedema induced by the inflammation may be responsible for the impaired relaxation.

In long-standing comorbid conditions such as hypertension, the induction of a systemic proinflammatory state has been associated with LV diastolic dysfunction (Paulus & Tschöpe, 2013). Although in the present study there were no differences in the IL- 1β concentrations between the WKY and SHR rats in the long-term, we showed a significant association between IL- 1β concentrations and impaired relaxation (E/A and e') and increased LV passive stiffness (e'/a'), but not increased filling pressure (E/e'). Interestingly, the CVF was associated only with relaxation (E/A), and not LV passive stiffness or filling pressure. These results suggest mechanisms other than inflammation- induced changes in ECM remodelling may contribute to hypertension-induced LV diastolic dysfunction. In this regard, in other models of chronic inflammation in our laboratory, we have shown changes in the molecular pathways involved in titin phosphorylation in response to inflammatory stimuli (Manilall *et al.*, 2022). Further studies are needed to explore the molecular pathways involved in hypertension-induced LV diastolic dysfunction, and the mediating role of inflammation.

5.4 The short- and long-term effects of LPS administration and hypertension of LV systolic function

The relationship between hypertension, inflammation and impaired LV diastolic dysfunction is well established (Paulus & Tschöpe, 2013). However, in hypertension-induced LV diastolic dysfunction, it is presumed that systolic function is preserved, as indicated in the diagnosis of HFpEF (Borlaug, 2020). In our laboratory we have previously shown that in chronic inflammation, despite maintaining an adequate systolic pump function, there are impairments in myocardial deformation, a preclinical measure of systolic dysfunction (Mokotedi *et al.*, 2020; Manilall *et al.*, 2023). Moreover, in severe sepsis, often due to myocardial apoptosis, pump function may be impaired

(Sturgess *et al.*, 2010). Therefore, in this model of acute high-grade inflammation we also investigated the LV systolic function.

The present study showed that in the short-term, hypertension reduced global systolic function as indexed by a decreased LVEF and FS_{end}. Although there were no differences in LVEF between SHR and WKY rats at five and seven months in a single study (Fu *et al.*, 2022), other studies reported that hypertension significantly reduced LVEF and FS at 5 months (Kokubo *et al.*, 2005; He *et al.*, 2021). However, LVEF and FS_{end} are load-dependent indices of systolic function and can be influenced by cardiac geometry (Balija & Lowry, 2011; Marwick, 2018).

Nevertheless, these global systolic dysfunction changes in the hypertensive rats translated to a reduced ejection of blood into the aorta, as shown by a reduced LVOT VTI and V_{max}. LVOT VTI is a marker of cardiac output and a determinant of adequate systemic tissue perfusion (Gola *et al.*, 1996). An animal model showed that pressure overload drives the development of concentric hypertrophy to compensate for the increased wall stress caused by the long-standing increased blood pressure (Sasayama *et al.*, 1976). However, in chronic hypertension, concentric hypertrophy often progresses to ventricular dilation, which results in impaired pump function and reduced cardiac output (Grossman, 1991; Drazner, 2011; Tan *et al.*, 2017). Our results suggest that in addition to systolic dysfunction, hypertension reduced the ability of the heart to meet the metabolic demands of the body by reducing systemic tissue perfusion. However, these changes were likely accelerated by the initial inflammatory stimulus as observed in the short-term rats.

Cardiac muscles contain fibres extending in three different planes, longitudinal, helically and in rings (Chu *et al.*, 2016). These fibres are important for the different

ways the heart can undergo deformation during systole, as LV contraction involves reducing the diameter of both the short- and long-axis of the LV chamber (Alam *et al.*, 2000; Li *et al.*, 2014). Therefore, STE is able to detect myocardial deformation in different planes and axes, and can recognise LV longitudinal and circumferential motion (Chu *et al.*, 2016).

In the present study, acute LPS-induced inflammation reduced myocardial deformation (longitudinal and circumferential strain) in SHR-LPS compared to control in the short-term. Previous studies have reported contradictory results, where one reported a decline in myocardial deformation (Chu *et al.*, 2016), in line with our results, and another study reported no differences in both longitudinal and circumferential deformation in response to LPS (Clerc *et al.*, 2018). Previous studies showed that myocardial strain measurements can be used to detect early changes in systolic function compared to LVEF or FS, showing dysfunction at 6 hours after LPS treatment (Chu *et al.*, 2015). Indeed, myocardial strain analysis has been used to report reduced systolic deformation with normal LVEF that indicated normal systolic function, demonstrating the sensitivity and precision of myocardial strain measurements (Stokke *et al.*, 2017). Although they were both affected in our study after 24 hours, it was previously shown that LV deformation is first impaired in the longitudinal direction, as demonstrated by impaired longitudinal strain, compared to circumferential strain (Miyoshi *et al.*, 2013). However, another study reported that circumferential strain was better associated with LVEF than longitudinal strain (Fu *et al.*, 2022).

Interestingly in the short-term, IL- 1β concentrations were not associated with changes in myocardial deformation or motion. However, CVF was significantly associated with circumferential and longitudinal strain. As previously mentioned, it is

unlikely that the changes in CVF are attributed to fibrosis, but rather to cardiac oedema. Indeed, others who have reported acute decreases in global longitudinal strain deformation also attributed the marked systolic dysfunction to acute oedema (Hestenes *et al.*, 2014; Sun *et al.*, 2021). Furthermore, our results showed that acute LPS-induced inflammation had no effect on LV systolic function in the long-term, which suggested that inflammation-induced LV systolic dysfunction was reversed once the inflammation was resolved (Van Tassell *et al.*, 2013).

Nevertheless, we showed that hypertension caused a decrease in both global systolic function as indicated by a decreased LVEF, FS_{end} and LVOT VTI in the long-term groups. In addition, in hypertensive rats, there was also a reduced longitudinal and circumferential strain compared to normotensive controls. Previous evidence showed that longitudinal and circumferential strain was similar in 3-month-old SHR compared to the WKY rats, but significantly decreased in 5-month-old SHR compared to WKY rats (Fu *et al.*, 2022). In the present study, we showed that hypertension-induced impaired myocardial strain, which was observed in 4-month-old SHR compared to WKY rats of the same age. Together, these results suggest that hypertension may begin to drive myocardial deformation from four months of age in SHR.

Hypertension and inflammation have been associated with increased collagen volume and cross-linking as well as myocardial fibrosis in the myocardium (Kasner *et al.*, 2011; Westermann *et al.*, 2011). It has been suggested that increased fibrosis is responsible for the early systolic dysfunction as measured by reduced myocardial strain (He *et al.*, 2021). Interestingly, the changes in myocardial strain seen in SHR occurred without changes in cardiac geometry or LV passive stiffness. In this regard,

although inflammation was strongly associated with change in the CVF in the long-term rats, it was not associated with changes in RWT or with changes in longitudinal or circumferential strain. However, IL- 1β concentrations were associated with impairments in longitudinal strain. These results suggest that inflammation may contribute to impaired myocardial deformation, independent of ECM remodelling. Indeed, we have previously shown in chronic inflammation that changes in myocardial strain may be related to functional changes in the myosin heavy chain responsible for myocardial contractions (Manilall *et al.*, 2021). Nevertheless, further investigations are needed to determine the molecular mechanisms responsible for systolic functional changes in inflammation and hypertension.

5.5 Study limitations and future perspectives

LPS levels in the serum were not measured, as such, we cannot compare our results with human sepsis studies. As a result, our data cannot be interpretated in the human context. Although rats have allowed us to study the effects of LPS, according to our study designs, these rats have small heart sizes which limit adequate STE measurements. STE has numerous analysis indexes and includes multiple motion indicators. Many indicators could be considered in the present study without the information of global myocardial strain in all planes and axes. Although associations were demonstrated between circulating inflammatory markers and impaired cardiac function, the direct casual effect of inflammation on impaired cardiac function can only be implied. Future studies should consider the measurement the several mediators in the inflammatory pathways involved in LPS-induced inflammation. Similarly, the measurement of fibrosis using CVF needs to be reevaluated, especially in short-term cases. Although we nominate oedema to be the primary effect in the short-term, future

studies ought to investigate the possible reasons for cardiac remodelling in the short-term, or find well-established methods in measuring the extent of the oedema.

Chapter 6: Conclusion

Our results provide us with understanding of how LPS-induced inflammation hypertension collaborate to induce significant impact on cardiac structure and function. We showed that LPS induced inflammation in the short-term, which reduced mitral filling patterns, LV relaxation and LV passive stiffness without alterations in LV filling pressure. Furthermore, the LPS-induced inflammation impaired systolic function by reducing stroke volume measures and reducing myocardial deformation. The diastolic and systolic dysfunction driven by inflammation that we observed occurred independent of alterations in cardiac geometry. Concentrations of IL- 1β were associated with impaired LV relaxation and passive stiffness, measures of LV diastolic dysfunction. Additionally, we conclude that LPS-induced inflammation may have caused the development of myocardial oedema in the short-term, which resulted in the structural alterations seen with the increased heart weight.

Although we showed increased CVF in our results, we conclude that there is no fibrosis present in the short-term groups, as the process takes 1-2 weeks to complete. The acute changes in increased CVF are therefore, not a result of fibrosis and may be attributed to other mechanisms such as oedema, oxidative stress and apoptosis. Myocardial oedema affects the ECM, resulting in the impairments in LV diastolic and systolic function we see in the short-term groups. Hypertension, which may have been maintained by the sympathetic nervous system, together with the inflammation, reduced LV diastolic and systolic function without structural remodelling. Hypertension is, therefore, the main driver of diastolic dysfunction, and subsequent heart failure with a preserved LVEF. Additionally, hypertension may be driving these effects via ECM changes with or without an inflammation trigger. In contrast to existing evidence of

heart failure with a preserved LVEF, we showed that hypertension and inflammation reduce systolic function, which is detected using early detection measures.

In the long-term, we showed that the inflammatory process is resolved after six weeks, which also reduced the inflammation-induced decline in LV diastolic and systolic function seen in the short-term groups. However, we observed changes to LV structural and functional changes, which we attribute to hypertension and hypertension-induced ECM remodelling. Hypertension independently caused impaired myocardial strain in the short-term, which was accompanied by changes to cardiac structure as well as impaired systolic function in the long-term. Although inflammation is associated with the impaired LV diastolic and systolic function in the long-term, LPS-induced inflammation may have triggered the hypertension-induced changes seen in cardiac structure and function in the long-term.

In conclusion, we demonstrated that acute inflammation caused by LPS led to detrimental remodelling of the heart, which may have been the result of oedema in the short-term and fibrosis in the long-term. Furthermore, the negative consequences of inflammation were limited to rats who were predisposed to hypertension.

References

Abhayaratna WP, Marwick TH, Smith WT & Becker NG (2006). Characteristics of left ventricular diastolic dysfunction in the community: an echocardiographic survey. *Heart* **92,** 1259–1264. https://doi.org/10.1136/hrt.2005.080150

Alam MB, Wardell JB, Andersson EB, Samad BA & Nordlander R (2000). Effects of first myocardial infarction on left ventricular systolic and diastolic function with the use of mitral annular velocity determined by pulsed wave doppler tissue imaging. *Journal of the American Society of Echocardiography* **13,** 343-352. https://doi.org/10.1016/s0894-7317(00)70003-4

Andersen OS, Smiseth OA, Dokainish H, Abudiab MM, Schutt RC, Kumar A & Nagueh SF (2017). Estimating left ventricular filling pressure by echocardiography. *Journal of the American College of Cardiology* **69,** 1937–1948. https://doi.org/10.1016/j.jacc.2017.01.058

Angriman F, Rosella LC, Lawler PR, Ko DT, Wunsch H & Scales DC (2022). Sepsis hospitalization and risk of subsequent cardiovascular events in adults: a population-based matched cohort study. *Intensive Care Medicine* **48,** 448–457. https://doi.org/10.1007/s00134-022-06634-z

Asgharzadeh F, Bargi R, Beheshti F, Hosseini M, Farzadnia M & Khazaei M (2018*a*). Thymoquinone prevents myocardial and perivascular fibrosis induced by chronic lipopolysaccharide exposure in male rats. *Journal of Pharmacopuncture* **21,** 284–293. https://doi.org/10.3831/kpi.2018.21.032

Asgharzadeh F, Bargi R, Hosseini M, Farzadnia M & Khazaei M (2018*b*). Cardiac and renal fibrosis and oxidative stress balance in lipopolysaccharideinduced

inflammation in male rats. *ARYA Atherosclerosis* **14,** 71–77. https://doi.org/10.22122/arya.v14i2.1550

Balija TM & Lowry SF (2011). Lipopolysaccharide and sepsis-associated myocardial dysfunction. *Current Opinion in Infectious Diseases* **24,** 248–253. https://doi.org/10.1097/qco.0b013e32834536ce

Balmforth C, Simpson J, Shen L, Jhund PS, Lefkowitz M, Rizkala AR & McMurray JJV (2019). Outcomes and effect of treatment according to etiology in HFrEF: An analysis of PARADIGM-HF. *Journal of the American College of Cardiology: Heart Failure* **7,** 457–465. https://doi.org/10.1016/j.jchf.2019.02.015

Beheshti F, Hosseini M, Hashemzehi M, Hadipanah MR & Mahmoudabady M (2020). The cardioprotective effects of aminoguanidine on lipopolysaccharide induced inflammation in rats. *Cardiovascular Toxicology* **20,** 474–481. https://doi.org/10.1007/s12012-020-09570-w

Bellenger NG, Burgess MI, Ray SG, Lahiri A, Coats AJS, Cleland JGF & Pennell DJ (2000). Comparison of left ventricular ejection fraction and volumes in heart failure by echocardiography, radionuclide ventriculography and cardiovascular magnetic resonance. Are they interchangeable? *European Heart Journal* **21,** 1387–1396. https://doi.org/10.1053/euhj.2000.2011

Berk BC, Fujiwara K & Lehoux S (2007). ECM remodeling in hypertensive heart disease. J*ournal of Clinical Investigation* **117,** 568–575. https://doi.org/10.1172/jcI31044

Bermejo-Martin JF, Martín-Fernandez M, López-Mestanza C, Duque P & Almansa R (2018). Shared features of endothelial dysfunction between sepsis and its

preceding risk factors (Aging and Chronic Disease). *Journal of Clinical Medicine* **7,** 400. https://doi.org/10.3390/jcm7110400

Biesiadecki BJ, Davis JP, Ziolo MT & Janssen PML (2014). Tri-modal regulation of cardiac muscle relaxation; intracellular calcium decline, thin filament deactivation, and cross-bridge cycling kinetics. *Biophysical Reviews* **6,** 273–289. https://doi.org/10.1007/s12551-014-0143-5

Borbély A, Falcao-Pires I, Van Heerebeek L, Hamdani N, Édes I, Gavina C, Leite-Moreira AF & Paulus WJ (2009). Hypophosphorylation of the stiff N2B titin isoform raises cardiomyocyte resting tension in failing human myocardium. *Circulation Research* **104,** 780–786. https://doi.org/10.1161/circresaha.108.193326

Borbély A, Van Der Velden J, Papp Z, Bronzwaer JGF, Edes I, Stienen GJM & Paulus WJ (2005). Cardiomyocyte stiffness in diastolic heart failure. *Circulation* **111,** 774–781. https://doi.org/10.1161/01.cir.0000155257.33485.6d

Border WL, Kimball TR, Witt SA, Glascock BJ, Khoury P & Daniels SR (2007). Diastolic filling abnormalities in children with essential hypertension. *Journal of Pediatrics* **150,** 503–509. https://doi.org/10.1016/j.jpeds.2007.01.038

Borlaug BA (2020). Evaluation and management of heart failure with preserved ejection fraction. *Nature Reviews Cardiology* **17,** 559–573. https://doi.org/10.1038/s41569-020-0363-2

Borlaug BA & Kass DA (2006). Mechanisms of diastolic dysfunction in heart failure. *Trends in Cardiovascular Medicine* **16,** 273–279. https://doi.org/10.1016/j.tcm.2006.05.003

Bozkurt B, Coats AJ, Tsutsui H, Abdelhamid M, Adamopoulos S, Albert N & Zieroth S

(2021). Universal definition and classification of heart failure: a report of the heart failure society of america, heart failure association of the european society of cardiology, japanese heart failure society and writing committee of the universal definition of heart failure. *European Journal of Heart Failure* **27,** 387-413. https://doi.org/10.1016/j.cardfail.2021.01.022

Breunig M, Morbach C, Kleinert S, Tony HP, Angermann CE & Stoerk S (2018). Cardiovascular risk and death in patients with rheumatic diseases and heart failure with preserved ejection fraction. *European Heart Journal* **39.** https://doi.org/10.1093/eurheartj/ehy566.P5422

Brower GL, Gardner JD, Forman MF, Murray DB, Voloshenyuk T, Levick SP & Janicki JS (2006). The relationship between myocardial extracellular matrix remodeling and ventricular function. *European Journal of Cardio-thoracic Surgery* **30,** 604–610. https://doi.org/10.1016/j.ejcts.2006.07.006

Cai ZL, Shen B, Yuan Y, Liu C, Xie QW, Hu TT & Tang QZ (2020). The effect of HMGA1 in LPS-induced myocardial inflammation. *International Journal of Biological Sciences* **16,** 1798–1810. 1798–1810. https://doi.org/10.7150/ijbs.39947

Chen CC & Lau LF (2010) Deadly liaisons: fatal attraction between CCN matricellular proteins and the tumor necrosis factor family of cytokines. *Journal of Cell Communication and Signaling* **4**, 63–69. https://doi.org/10.1007/s12079-009-0080-4

Chinnaiyan KM, Alexander D, Maddens M & McCullough PA (2007). Curriculum in cardiology: Integrated diagnosis and management of diastolic heart failure.

American Heart Journal **153,** 189–200. https://doi.org/10.1016/j.ahj.2006.10.022

Chu M, Gao Y, Zhang Y, Zhou B, Wu B, Yao J & Xu D (2015). The role of speckle tracking echocardiography in assessment of lipopolysaccharide-induced myocardial dysfunction in mice. *Journal of Thoracic Disease* **7,** 2253–2261. https://doi.org/10.3978/j.issn.2072-1439.2015.12.37

Chu M, Gao Y, Zhou B, Wu B, Wang J & Xu D (2016). Circumferential strain can be used to detect lipopolysaccharide-induced myocardial dysfunction and predict the mortality of severe sepsis in mice. *PLOS ONE* **11**. https://doi.org/10.1371/journal.pone.0155346

Chu M, Gao Y, Zhou B, Wu B, Wang J & Xu D (2019). Circumferential strain can be used to detect lipopolysaccharide-induced myocardial dysfunction and predict the mortality of severe sepsis in mice. *Quantitative Imaging In Medicine And Surgery* **9,** 151–159. https://doi.org/10.21037/qims.2018.11.03

Clerc R, Doll S, Riou LM, Perret P, Broisat A, Soubies A & Ghezzi C (2018). Sympathetic cardiac function in early sepsis: Noninvasive evaluation with [123I]-meta-iodobenzylguanidine (123I-MIBG) in vivo SPECT imaging. *Journal of Nuclear Cardiology* **25,** 483–491. https://doi.org/10.1007/s12350-016-0619-8

Collier P, Watson CJ, Voon V, Phelan D, Jan A, Mak G & McDonald KM (2011). Can emerging biomarkers of myocardial remodelling identify asymptomatic hypertensive patients at risk for diastolic dysfunction and diastolic heart failure? *European Journal of Heart Failure* **13,** 1087–1095. https://doi.org/10.1093/eurjhf/hfr079

Combes A, Frye CS, Lemster BH, Brooks SS, Watkins SC, Feldman AM & McTiernan

CF (2002). Chronic exposure to interleukin 1β induces a delayed and reversible alteration in excitation-contraction coupling of cultured cardiomyocytes. *Pflugers Archiv European Journal of Physiology* **445,** 246–256. https://doi.org/10.1007/s00424-002-0921-y

Conrad CH, Brooks WW, Hayes JA, Sen S, Robinson KG & Bing OHL (1995). Myocardial fibrosis and stiffness with hypertrophy and heart failure in the spontaneously hypertensive rat. *Circulation* **91,** 161–170. https://doi.org/10.1161/01.cir.91.1.161

Cuspidi C, Macca G, Michev I, Fusi V, Severgnini B, Corti C & Zanchetti A (2002). Left ventricular concentric remodelling and extracardiac target organ damage in essential hypertension. *Journal of Human Hypertension* **16,** 385–390. https://doi.org/10.1038/sj.jhh.1001420

Davis JM, Knutson KL, Strausbauch MA, Crowson CS, Therneau TM, Wettstein PJ & Gabriel SE (2011). A signature of aberrant immune responsiveness identifies myocardial dysfunction in rheumatoid arthritis. *Arthritis and Rheumatism* **63,** 1497–1506. https://doi.org/10.1002/art.30323

De Simone G, Kitzman DW, Chinali M, Oberman A, Hopkins PN, Rao DC & Devereux RB (2005). Left ventricular concentric geometry is associated with impaired relaxation in hypertension: The HyperGEN study. *European Heart Journal* **26,** 1039–1045. https://doi.org/10.1093/eurheartj/ehi019

Denga TM, Gunter S, Fourie S, Manilall A, Millen AME & Mokotedi L (2023). Interleukin-6 blockers improve inflammation-induced lipid metabolism impairments but induce liver fibrosis in collagen-induced arthritis. *Endocrine,*

Metabolic & Immune Disorders-Drug Targets **23,** 548–557. https://doi.org/10.2174/1871530323666221017153157

Desai KV, Laine GA, Stewart RH, Cox CS, Quick CM, Allen SJ & Fischer UM (2008). Mechanics of the left ventricular myocardial interstitium: Effects of acute and chronic myocardial edema. *American Journal of Physiology Heart and Circulatory Physiology* **294,** 2428–2434. https://doi.org/10.1152/ajpheart.00860.2007

Deswal A, Petersen NJ, Feldman AM, Young JB, White BG & Mann DL (2001). Cytokines and cytokine receptors in advanced heart failure: An analysis of the cytokine database from the Vesnarinone Trial (VEST). *Circulation* **103,** 2055–2059. https://doi.org/10.1161/01.cir.103.16.2055

Drazner MH (2011). The progression of hypertensive heart disease. *Circulation* **123,** 327–334. https://doi.org/10.1161/circulationaha.108.845792

Dunlay SM, Roger VL & Redfield MM (2017). Epidemiology of heart failure with preserved ejection fraction. *Nature Reviews Cardiology* **14,** 591–602. https://doi.org/10.1038/nrcardio.2017.65

Eissler R, Schmaderer C, Rusai K, Kühne L, Sollinger D, Lahmer T & Baumann M (2011). Hypertension augments cardiac toll-like receptor 4 expression and activity. *Hypertension Research* **34,** 551–558. https://doi.org/10.1038/hr.2010.270

Fairweather D, Yusung S, Frisancho S, Barrett M, Gatewood S, Steele R & Rose NR (2003). IL-12 receptor β1 and toll-like receptor 4 increase il-1β- and il-18-associated myocarditis and coxsackievirus replication. *Journal of Immunology* **170,** 4731–4737. https://doi.org/10.4049/jimmunol.170.9.4731

Frangogiannis NG (2021). Cardiac fibrosis. *Cardiovasvular research* **117,** 1450–1488. https://doi.org/10.1093/cvr/cvaa324

Franssen C, Chen S, Unger A, Korkmaz HI, De Keulenaer GW, Tschöpe C & Hamdani N (2016). Myocardial microvascular inflammatory endothelial activation in heart failure with preserved ejection fraction. *Journal of the American College of Cardiology Heart Failure* **4,** 312–324. https://doi.org/10.1016/j.jchf.2015.10.007

Franssen C & González Miqueo A (2016). The role of titin and extracellular matrix remodelling in heart failure with preserved ejection fraction. *Netherlands Heart Journal* **24,** 259–267. https://doi.org/10.1007/s12471-016-0812-z

Fu L, Ruan Q, You Z, Huang H, Chen Y, Cheng S & Huang C (2022). Investigation of left ventricular strain and its morphological basis during different stages of diastolic and systolic dysfunction in spontaneously hypertensive rat. *American Journal of Hypertension* **35,** 423–432. https://doi.org/10.1093/ajh/hpac008

Fukuda N, Wu Y, Nair P & Granzier HL (2005). Phosphorylation of titin modulates passive stiffness of cardiac muscle in a titin isoform-dependent manner. *Journal of General Physiology* **125,** 257–271. https://doi.org/10.1085/jgp.200409177

Fukuta H & Little WC (2007). Contribution of systolic and diastolic abnormalities to heart failure with a normal and a reduced ejection fraction. *Progress in Cardiovascular Diseases* **49,** 229–240. https://doi.org/10.1016/j.pcad.2006.08.009

Ganau A, Devereux RB, Roman MJ, de Simone G, Pickering TG, Saba PS & Laragh JH (1992). Patterns of left ventricular hypertrophy and geometric remodeling in essential hypertension. *Journal of the American College of Cardiology* **19,** 1550–

1558. https://doi.org/10.1016/0735-1097(92)90617-v

Geneva: World Health Organization (WHO) (2023). *Global Report on Hypertension: the race against the silent killer*. Licence: CC BY-NC-SA 3.0 IGO. Available at: https://www.who.int/publications/i/item/9789240081062 [Accessed March, 27 2024]

Ghosh S & Hayden MS (2008). New regulators of NF-κB in inflammation. *Nature Reviews Immunology* **8,** 837–848. https://doi.org/10.1038/nri2423

Gola A, Pozzoli M, Capomolla S, Traversi E, Sanarico M, Cobelli F & Tavazzi L (1996). Comparison of doppler echocardiography with thermodilution for assessing cardiac output in advanced congestive heart failure. *American Journal of Cardiology* **78,** 708–712. https://doi.org/10.1016/s0002-9149(96)00406-7

González A, Ravassa S, Beaumont J, López B & Díez J (2011). New targets to treat the structural remodeling of the myocardium. *Journal of the American College of Cardiology* **58,** 1833–1843. https://doi.org/10.1016/j.jacc.2011.06.058

González A, Ravassa S, López B, Moreno MU, Beaumont J, San José G & Díez J (2018*a*). Myocardial remodeling in hypertension toward a new view of hypertensive heart disease. *Hypertension* **72,** 549–558. https://doi.org/10.1161/hypertensionaha.118.11125

González A, Schelbert EB, Díez J & Butler J (2018*b*). myocardial interstitial fibrosis in heart failure: biological and translational perspectives. *Journal of the American College of Cardiology* **71,** 1696–1706. https://doi.org/10.1016/j.jacc.2018.02.021

Griffiths EJ & Rutter GA (2009). Mitochondrial calcium as a key regulator of mitochondrial ATP production in mammalian cells. *Biochimica et Biophysica Acta*

Bioenergetics **1787,** 1324–1333. https://doi.org/10.1016/j.bbabio.2009.01.019

Groenewegen A, Rutten FH, Mosterd A & Hoes AW (2020). Epidemiology of heart failure. *European Journal of Heart Failure* **22,** 1342–1356. https://doi.org/10.1002/ejhf.1858

Grossman W (1991). Diastolic dysfunction in congestive heart failure. *New England Journal of Medicine* **325,** 1557–1564. https://doi.org/10.1056/nejm199111283252206

Grossman W, Jones D & McLaurin LP (1975). Wall stress and patterns of hypertrophy in the human left ventricle. *Journal of Clinical Investigation* **56,** 56–64. https://doi.org/10.1172/jci108079

Guan Z, Liu S, Wang Y, Meng P, Zheng X, Jia D & Ma C (2019). Left ventricular systolic dysfunction potentially contributes to the symptoms in heart failure with preserved ejection fraction. *Echocardiography* **36,** 1825–1833. https://doi.org/10.1111/echo.14496

Hamdani N, Franssen C, Lourenço A, Falca o-Pires I, Fontoura D, Leite S & Paulus WJ (2013). Myocardial titin hypophosphorylation importantly contributes to heart failure with preserved ejection fraction in a rat metabolic risk model. *Circulation Heart Failure* **6,** 1239–1249. https://doi.org/10.1161/circheartfailure.113.000539

Harden LM, du Plessis I, Poole S & Laburn HP (2006). Interleukin-6 and leptin mediate lipopolysaccharide-induced fever and sickness behavior. *Physiology and Behavior* **89,** 146–155. https://doi.org/10.1016/j.physbeh.2006.05.016

Harouki N, Nicol L, Remy-Jouet I, Henry JP, Dumesnil A, Lejeune A & Mulder P (2017). The IL-1β antibody gevokizumab limits cardiac remodeling and coronary

dysfunction in rats with heart failure. *Journal of the American College of Cardiology Basic to Translational Science* **2,** 418–430. https://doi.org/10.1016/j.jacbts.2017.06.005

He A, Qian L, Yan S, Zhu M, Zhao X, Ma W & Xu D (2021). Speckle tracking echocardiography verified the efficacy of qianyangyuyin granules in alleviating left ventricular remodeling in a hypertensive rat model. *Evidence-based Complementary and Alternative Medicine*. https://doi.org/10.1155/2021/5862361

Van Heerebeek L, Borbély A, Niessen HWM, Bronzwaer JGF, Van Der Velden J, Stienen GJM & Paulus WJ (2006). Myocardial structure and function differ in systolic and diastolic heart failure. *Circulation* **113,** 1966–1973. https://doi.org/10.1161/circulationaha.105.587519

Van Heerebeek L, Hamdani N, Falcão-Pires I, Leite-Moreira AF, Begieneman MPV, Bronzwaer JGF & Paulus WJ (2012). Low myocardial protein kinase G activity in heart failure with preserved ejection fraction. *Circulation* **126,** 830–839. https://doi.org/10.1161/circulationaha.111.076075

Hestenes SM, Halvorsen PS, Skulstad H, Remme EW, Espinoza A, Hyler S & Edvardsen T (2014). Advantages of strain echocardiography in assessment of myocardial function in severe sepsis: An experimental study. *Critical Care Medicine* **42,** 432–440. https://doi.org/10.1097/ccm.0000000000000310

Hicklin HE, Gilbert ON, Ye F, Brooks JE & Upadhya B (2020). Hypertension as a road to treatment of heart failure with preserved ejection fraction. *Current Hypertension Reports* **22,** 82. https://doi.org/10.1007/s11906-020-01093-7

Hou XL, Tong Q, Wang WQ, Shi CY, Xiong W, Chen J & Fang JG (2015). Suppression

of inflammatory responses by dihydromyricetin, a flavonoid from ampelopsis grossedentata, via inhibiting the activation of nf-κb and mapk signaling pathways. *Journal of Natural Products* **78,** 1689–1696. https://doi.org/10.1021/acs.jnatprod.5b00275

Ikonomidis I, Tzortzis S, Lekakis J, Paraskevaidis I, Andreadou I, Nikolaou M & Kremastinos DT (2009). Lowering interleukin-1 activity with anakinra improves myocardial deformation in rheumatoid arthritis. *Heart* **95,** 1502–1507. https://doi.org/10.1136/hrt.2009.168971

Ince C, Mayeux PR, Nguyen T, Gomez H, Kellum JA, Ospina-Tascón GA & De Backer D (2016). The endothelium in sepsis. *Shock* **45,** 259–270. https://doi.org/10.1097/shk.0000000000000473

Iwase M, Yokota M, Kitaichi K, Wang L, Takagi K, Nagasaka T & Hasegawa T (2001). Cardiac functional and structural alterations induced by endotoxin in rats: Importance of platelet-activating factor. *Critical Care Medicine* **29,** 609–617. https://doi.org/10.1097/00003246-200103000-00025

Izzo JL & Gradman AH (2004). Mechanisms and management of hypertensive heart disease: From left ventricular hypertrophy to heart failure. *Medical Clinics of North America* **88,** 1257–1271. https://doi.org/10.1016/j.mcna.2004.06.002

Johnson A & DiPietro LA (2013) Apoptosis and angiogenesis: an evolving mechanism for fibrosis. *The Fedaration of American Societies for Experimental Biology Journal* **27**, 3893-3901. https://doi.org/10.1096/fj.12-214189

Joulin O, Marechaux S, Hassoun S, Montaigne D, Lancel S & Neviere R (2009). Cardiac force-frequency relationship and frequency-dependent acceleration of

relaxation are impaired in LPS-treated rats. *Critical Care* **13**. https://doi.org/10.1186/cc7712

Kang C, Choi S, Jang EJ, Joo S, Jeong JH, Oh SY & Lee H (2024). Prevalence and outcomes of chronic comorbid conditions in patients with sepsis in Korea: a nationwide cohort study from 2011 to 2016. *Biomed Central Infectious Diseases* **24**, 184. https://doi.org/10.1186/s12879-024-09081-x

Kapila R & Mahajan RP (2009). Diastolic dysfunction. *Continuing Education in Anaesthesia, Critical Care and Pain* **9,** 29–33. https://doi.org/10.1093/bjaceaccp/mkn046

Kasner M, Westermann D, Lopez B, Gaub R, Escher F, Kühl U & Tschöpe C (2011). Diastolic tissue doppler indexes correlate with the degree of collagen expression and cross-linking in heart failure and normal ejection fraction. *Journal of the American College of Cardiology* **57,** 977-985. https://doi.org/10.1016/j.jacc.2010.10.024

Katare PB, Nizami HL, Paramesha B, Dinda AK & Banerjee SK (2020). Activation of toll like receptor 4 (TLR4) promotes cardiomyocyte apoptosis through SIRT2 dependent p53 deacetylation. *Scientific Reports* **10.** https://doi.org/10.1038/s41598-020-75301-4

Kemp CD & Conte J V. (2012). The pathophysiology of heart failure. *Cardiovascular Pathology* **21,** 365–371. https://doi.org/10.1016/j.carpath.2011.11.007

Kilfoil PJ, Lotteau S, Zhang R, Yue X, Aynaszyan S, Solymani RE & Goldhaber JI (2020). Distinct features of calcium handling and β-adrenergic sensitivity in heart failure with preserved versus reduced ejection fraction. *Journal of Physiology* **598,**

5091–5108. https://doi.org/10.1113/jp280425

Kokubo M, Uemura A, Matsubara T & Murohara T (2005). Noninvasive evaluation of the time course of change in cardiac function in spontaneously hypertensive rats by echocardiography. *Hypertension Research* **28,** 601–609. https://doi.org/10.1291/hypres.28.601

Kong P, Christia P & Frangogiannis NG (2014). The pathogenesis of cardiac fibrosis. *Cellular and Molecular Life Sciences* **71,** 549–574. https://doi.org/10.1007/s00018-013-1349-6

Kosyakovsky LB, Angriman F, Katz E, Adhikari NK, Godoy LC, Marshall JC & Lawler PR (2021). Association between sepsis survivorship and long-term cardiovascular outcomes in adults: a systematic review and meta-analysis. *Intensive Care Medicine* **47,** 931–942. https://doi.org/10.1007/s00134-021-06479-y

Krüger M, Kötter S, Grützner A, Lang P, Andresen C, Redfield MM & Linke WA (2009). Protein kinase G modulates human myocardial passive stiffness by phosphorylation of the titin springs. *Circulation Research* **104,** 87–94. https://doi.org/10.1161/circresaha.108.184408

Landesberg G, Gilon D, Meroz Y, Georgieva M, Levin PD, Goodman S & Sprung CL (2012). Diastolic dysfunction and mortality in severe sepsis and septic shock. *European Heart Journal* **33,** 895–903. https://doi.org/10.1093/eurheartj/ehr351

Le Roux R, Mokotedi L, Fourie S, Manilall A, Gunter S & Millen AME (2022). TNF-α inhibitors reduce inflammation-induced concentric remodelling, but not diastolic dysfunction in collagen-induced arthritis. *Clinical and experimental rheumatology*

40, 24–32. https://doi.org/10.55563/clinexprheumatol/l4nnv0

Lee H, Kong Y-H, Kim K-H, Huh J, Kang I-S & Song J (2015). Left ventricular hypertrophy and diastolic function in children and adolescents with essential hypertension. *Clinical Hypertension* **21,** 21. https://doi.org/10.1186/s40885-015-0031-8

Lee WL & Slutsky AS (2010). Sepsis and endothelial permeability. *New England Journal of Medicine* **363,** 689–691. https://doi.org/10.1056/NEJMcibr1007320

Lew WYW, Bayna E, Dalle Molle E, Contu R, Condorelli G & Tang T (2014). Myocardial fibrosis induced by exposure to subclinical lipopolysaccharide is associated with decreased miR-29c and enhanced NOX2 expression in mice. *PLOS ONE* **9**. https://doi.org/10.1371/journal.pone.0107556

Lew WYW, Bayna E, Molle ED, Dalton ND, Lai NC, Bhargava V & Tang T (2013). Recurrent exposure to subclinical lipopolysaccharide increases mortality and induces cardiac fibrosis in mice. *PLOS ONE* **8.** https://doi.org/10.1371/journal.pone.0061057

Lewis GA, Schelbert EB, Williams SG, Cunnington C, Ahmed F, McDonagh TA & Miller CA (2017). Biological phenotypes of heart failure with preserved ejection fraction. *Journal of the American College of Cardiology* **70,** 2186–2200. https://doi.org/10.1016/j.jacc.2017.09.006

Li J, Kemp BA, Howell NL, Massey J, Mińczuk K, Huang Q, & Kundu BK (2019). Metabolic changes in spontaneously hypertensive rat hearts precede cardiac dysfunction and left ventricular hypertrophy. *Journal of the American Heart Association*, **8**. https://doi.org/10.1161/JAHA.118.010926

Li P, Chen XR, Xu F, Liu C, Li C, Liu H & Kong XQ (2018). Alamandine attenuates sepsis-associated cardiac dysfunction via inhibiting MAPKs signaling pathways. *Life Sciences* **206,** 106–116. https://doi.org/10.1016/j.lfs.2018.04.010

Li T, Liu J, Du W, Wang X, Chen Z & Zhang L (2014). 2D speckle tracking imaging to assess sepsis induced early systolic myocardial dysfunction and its underlying mechanisms. *European Review for Medical and Pharmacological Science* **18,** 3105–3114. Available at: https://www.europeanreview.org/article/7967 [Accessed March 20, 2024]

Li YY, McTiernan CF & Feldman AM (2000). Interplay of matrix metalloproteinases, tissue inhibitors of metalloproteinases and their regulators in cardiac matrix remodeling. *Cardiovascular Research* **46,** 214–224. https://doi.org/10.1016/s0008-6363(00)00003-1

Li Z, Meng Y, Liu C, Liu H, Cao W, Tong C & Peng L (2021). Kcnh2 mediates FAK/AKT-FOXO3A pathway to attenuate sepsis-induced cardiac dysfunction. *Cell Proliferation* **54.** https://doi.org/10.1111/cpr.12962

López B, González A, Ravassa S, Beaumont J, Moreno MU, San José G & Javier D (2015). Circulating biomarkers of myocardial fibrosis. *Journal of the American College of Cardiology* **65,** 2449–2456. https://doi.org/10.1016/j.jacc.2015.04.026

López B, Querejeta R, González A, Larman M & Díez J (2012). Collagen cross-linking but not collagen amount associates with elevated filling pressures in hypertensive patients with stage C heart failure: Potential role of lysyl oxidase. *Hypertension* **60,** 677–683. https://doi.org/10.1161/hypertensionaha.112.196113

Lundin S, Friberg P & Ricksten S -E (1983). Diastolic properties of the hypertrophied

left ventricle in spontaneously hypertensive rats. *Acta Physiologica Scandinavica* **118,** 1–9. https://doi.org/10.1111/j.1748-1716.1983.tb07233.x

Manilall A, Mokotedi L, Gunter S, Le Roux R, Fourie S, Flanagan CA & Millen AME (2021). Inflammation-induced left ventricular fibrosis is partially mediated by tumor necrosis factor-α. *Physiological Reports* **9.** https://doi.org/10.14814/phy2.15062

Manilall A, Mokotedi L, Gunter S, Le Roux R, Fourie S, Flanagan CA, & Millen AME (2022). Increased protein phosphatase 5 expression in inflammation-induced left ventricular dysfunction in rats. *Biomed Central Cardiovascular Disorders* **22,** 539. https://doi.org/10.1186/s12872-022-02977-z

Manilall A, Mokotedi L, Gunter S, Le Roux R, Fourie S, Flanagan CA & Millen AME (2023). Tumor Necrosis factor-α mediates inflammation-induced early-stage left ventricular systolic dysfunction. *Journal of Cardiovascular Pharmacology* **81,** 411–422. https://doi.org/10.1097/fjc.0000000000001428

Maragiannis D, Alvarez PA, Ghosn MG, Chin K, Hinojosa JJ, Buergler JM & Nagueh SF (2018). Left ventricular function in patients with hypertrophic cardiomyopathy and its relation to myocardial fibrosis and exercise tolerance. *International Journal of Cardiovascular Imaging* **34,** 121–129. https://doi.org/10.1007/s10554-017-1214-z

Marwick TH (2018). Ejection fraction pros and cons: jacc state-of-the-art review. *Journal of the American College of Cardiology* **72,** 2360–2379. https://doi.org/10.1016/j.jacc.2018.08.2162

Matsusaka H, Ide T, Matsushima S, Ikeuchi M, Kubota T, Sunagawa K & Tsutsui H

(2006). Targeted deletion of matrix metalloproteinase 2 ameliorates myocardial remodeling in mice with chronic pressure overload. *Hypertension* **47,** 711–717. https://doi.org/10.1161/01.hyp.0000208840.30778.00

Micklesfield LK, Kolkenbeck-Ruh A, Mukoma G, Prioreschi A, Said-Mohamed R, Ware LJ, & Norris SA (2022). The healthy aging adult south africa report card: a systematic review of the evidence between 2013 and 2020 for middle-aged south african men and women. *Cardiovascular Journal of Africa* **33,** 200–219. https://doi.org/10.5830/cvja-2022-015

Miguel-Carrasco JL, Zambrano S, Blanca AJ, Mate A & Vázquez CM (2010). Captopril reduces cardiac inflammatory markers in spontaneously hypertensive rats by inactivation of NF-kB. *Journal of Inflammation* **7.** https://doi.org/10.1186/1476-9255-7-21

Mills KT, Stefanescu A & He J (2020). The global epidemiology of hypertension. *Nature Reviews Nephrology* **16,** 223–237. https://doi.org/10.1038/s41581-019-0244-2

Miyoshi H, Oishi Y, Mizuguchi Y, Iuchi A, Nagase N, Ara N & Oki T (2013). Effect of an increase in left ventricular pressure overload on left atrial-left ventricular coupling in patients with hypertension: A two-dimensional speckle tracking echocardiographic study. *Echocardiography* **30,** 658–666. https://doi.org/10.1111/echo.12117

Mokotedi L, Michel FS, Mogane C, Gomes M, Woodiwiss AJ, Norton GR & Millen AME (2020). Associations of inflammatory markers with impaired left ventricular diastolic and systolic function in collagen-induced arthritis. *PLOS ONE* **15**.

https://doi.org/10.1371/journal.pone.0230657

Mulligan KX, Morris RT, Otero YF, Wasserman DH & McGuinness OP (2012). Disassociation of muscle insulin signaling and insulin-stimulated glucose uptake during endotoxemia. *PLOS ONE*, **7.** https://doi.org/10.1371/journal.pone.0030160

Nagueh SF (2021). Heart failure with preserved ejection fraction: Insights into diagnosis and pathophysiology. *Cardiovascular Research* **117,** 999–1014. https://doi.org/10.1093/cvr/cvaa228

Nagueh SF, Middleton KJ, Kopelen HA, Zoghbi WA & Quiñones MA (1997). Doppler tissue imaging: A noninvasive technique for evaluation of left ventricular relaxation and estimation of filling pressures. *Journal of the American College of Cardiology* **30,** 1527–1533. https://doi.org/10.1016/s0735-1097(97)00344-6

Nair N (2020). Epidemiology and pathogenesis of heart failure with preserved ejection fraction. *Reviews in Cardiovascular Medicine* **21,** 531–540. https://doi.org/10.31083/j.rcm.2020.04.154

Nistri S, Galderisi M, Faggiano P, Antonini-canterin F, Ansalone G, Lloyd F & Marino PN (2008). Practical echocardiography in aortic valve stenosis. *Journal of Cardiovascular Medicine* **9,** 653–665. https://doi.org/10.2459/jcm.0b013e3282f27d49

Omote K, Nagai T, Iwano H, Tsujinaga S, Kamiya K, Aikawa T & Anzai T (2020). Left ventricular outflow tract velocity time integral in hospitalized heart failure with preserved ejection fraction. *European Society of Cardiology Heart Failure* **7,** 167–175. https://doi.org/10.1002/ehf2.12541

Ortega-Gómez A, Perretti M & Soehnlein O (2013). Resolution of inflammation: An integrated view. *EMBO Molecular Medicine* **5,** 661–674. https://doi.org/10.1002/emmm.201202382

Parker MM, Shelhamer JH, Bacharach SL, Green MV, Natanson C, Frederick TM & Parrillo JE (1984). Profound but reversible myocardial depression in patients with septic shock. *Annals of Internal Medicine* **100,** 483–490. https://doi.org/10.7326/0003-4819-100-4-483

Paulus WJ & Tschöpe C (2013). A novel paradigm for heart failure with preserved ejection fraction: Comorbidities drive myocardial dysfunction and remodeling through coronary microvascular endothelial inflammation. *Journal of the American College of Cardiology* **62,** 263–271. https://doi.org/10.1016/j.jacc.2013.02.092

Paulus WJ & Zile MR (2021). from systemic inflammation to myocardial fibrosis: the heart failure with preserved ejection fraction paradigm revisited. *Circulation Research* **128,** 1451–1467. https://doi.org/10.1161/circresaha.121.318159

Pauschinger M, Knopf D, Petschauer S, Doerner A, Poller W, Schwimmbeck PL & Schultheiss HP (1999). Dilated cardiomyopathy is associated with significant changes in collagen type I/III ratio. *Circulation* **99,** 2750–2756. https://doi.org/10.1161/01.cir.99.21.2750

Peng X, Wang Y, Xi X, Jia Y, Tian J, Yu B & Tian J (2021). Promising therapy for heart failure in patients with severe covid-19: calming the cytokine storm. *Cardiovascular Drugs and Therapy* **35,** 231–247. https://doi.org/10.1007/s10557-020-07120-8

Pironti G, Bersellini-Farinotti A, Agalave NM, Sandor K, Fernandez-Zafra T, Jurczak A & Andersson DC (2018). Cardiomyopathy, oxidative stress and impaired contractility in a rheumatoid arthritis mouse model. *Heart* **104,** 2026–2034. https://doi.org/10.1136/heartjnl-2018-312979

Rayner B (2010). Hypertension: Detection and management in South Africa. *Nephron - Clinical Practice* **116,** 269–273. https://doi.org/10.1159/000318788

Redfield MM, Jacobsen SJ, Burnett JC, Mahoney DW, Bailey KR & Rodeheffer RJ (2003). Burden of systolic and diastolic ventricular dysfunction in the community: appreciating the scope of the heart failure epidemic. *Journal of the American Medical Association* **289,** 194–202. https://doi.org/10.1001/jama.289.2.194

Saiyang X, Qingqing W, Man X, Chen L, Min Z, Yun X & Qizhu T (2021). Activation of Toll-like receptor 7 provides cardioprotection in septic cardiomyopathy-induced systolic dysfunction. *Clinical and Translational Medicine* **11.** https://doi.org/10.1002/ctm2.266

Sakata Y, Ohtani T, Takeda Y, Yamamoto K & Mano T (2013). Left ventricular stiffening as therapeutic target for heart failure with preserved ejection fraction. *Circulation Journal* **77,** 886–892. https://doi.org/10.1253/circj.cj-13-0214

Sasayama S, Ross J, Franklin D, Bloor CM, Bishop S & Dilley RB (1976). Adaptations of the left ventricle to chronic pressure overload. *Circulation Research* **38,** 172–178. https://doi.org/10.1161/01.res.38.3.172

Savarese G, Becher PM, Lund LH, Seferovic P, Rosano GMC & Coats AJS (2022). Global burden of heart failure: a comprehensive and updated review of epidemiology. *Cardiovascular Research* **118,** 3272-3287.

https://doi.org/10.1093/cvr/cvac013

Schussheim AE, Diamond JA, Jhang JS & Phillips RA (1998). Midwall fractional shortening is an independent predictor of left ventricular diastolic dysfunction in asymptomatic patients with systemic hypertension. *American Journal of Cardiology* **82,** 1056–1059. https://doi.org/10.1016/s0002-9149(98)00558-x

Schutte AE, Srinivasapura Venkateshmurthy N, Mohan S & Prabhakaran D (2021). Hypertension in low- and middle-income countries. *Circulation Research* **128,** 808–826. https://doi.org/10.1161/circresaha.120.318729

Selby DE, Palmer BM, Lewinter MM & Meyer M (2011). Tachycardia-induced diastolic dysfunction and resting tone in myocardium from patients with a normal ejection fraction. *Journal of the American College of Cardiology* **58,** 147–154. https://doi.org/10.1016/j.jacc.2010.10.069

Shah AM, Cikes M, Prasad N, Li G, Getchevski S, Claggett B & Solomon SD (2019). Echocardiographic features of patients with heart failure and preserved left ventricular ejection fraction. *Journal of the American College of Cardiology* **74,** 2858–2873. https://doi.org/10.1016/j.jacc.2019.09.063

Shvilkina T & Shapiro N (2023). Sepsis-Induced myocardial dysfunction: heterogeneity of functional effects and clinical significance. *Frontiers in Cardiovascular Medicine* **10.** https://doi.org/10.3389/fcvm.2023.1200441

Simmonds SJ, Cuijpers I & Heymans S (2020). Cellular and molecular differences between HFpEF and HFrEF : A step ahead in an improved. *Cells* **9,** 242. https://doi.org/10.3390/cells9010242

Singer M, Deutschman CS, Seymour C, Shankar-Hari M, Annane D, Bauer M & Angus

DC (2016). The third international consensus definitions for sepsis and septic shock (sepsis-3). *Journal of the American Medical Association* **315,** 801–810. https://doi:10.1001/jama.2016.0287

Soni S, Martens MD, Takahara S, Silver HL, Maayah ZH, Ussher JR & Dyck JRB (2022). Exogenous ketone ester administration attenuates systemic inflammation and reduces organ damage in a lipopolysaccharide model of sepsis. *Biochimica et Biophysica Acta Molecular Basis of Disease* **1868.** https://doi.org/10.1016/j.bbadis.2022.166507

Stokke TM, Hasselberg NE, Smedsrud MK, Sarvari SI, Haugaa KH, Smiseth OA & Remme EW (2017). Geometry as a confounder when assessing ventricular systolic function: comparison between ejection fraction and strain. *Journal of the American College of Cardiology* **70,** 942–954. https://doi.org/10.1016/j.jacc.2017.06.046

Strand ME, Aronsen JM, Braathen B, Sjaastad I, Kvaløy H, Tønnessen T & Lunde IG (2015). Shedding of syndecan-4 promotes immune cell recruitment and mitigates cardiac dysfunction after lipopolysaccharide challenge in mice. *Journal of Molecular and Cellular Cardiology* **88,** 133–144. https://doi.org/10.1016/j.yjmcc.2015.10.003

Sturgess DJ, Marwick TH, Joyce C, Jenkins C, Jones M, Masci P & Venkatesh B (2010). Prediction of hospital outcome in septic shock: A prospective comparison of tissue Doppler and cardiac biomarkers. *Critical Care* **14.** https://doi.org/10.1186/cc8931

Sturgess DJ, Morrison S, Haluska B, Gobe GC, Jones MA, Volante S & Venkatesh B

(2021). Left ventricular impaired relaxation and interstitial myocarditis identified in sepsis-associated cardiac dysfunction: Use of a rodent model. *Medical Science Monitor* **27**. https://doi.org/10.12659/msm.929512

Sun R, Zhang Y, Li X, Zhang Q, Xie T, Li Z & Wang J (2021). Investigation of effects of traditional Chinese medicine astragalus heart-protecting decoction on rats with dilated cardiomyopathy. *All Life* **14,** 846–854. https://doi.org/10.1080/26895293.2021.1977724

Szelényi Z, Fazakas Á, Szénási G, Kiss M, Tegze N, Csaba B & Vereckei A (2015). Inflammation and oxidative stress caused by nitric oxide synthase uncoupling might lead to left ventricular diastolic and systolic dysfunction in patients with hypertension. *Journal of geriatric cardiology* **12,** 1-10. https://doi.org/10.11909/j.issn.1671-5411.2015.01.001

Tan C, Rubenson D, Srivastava A, Mohan R, Smith MR, Billick K & Thomas Heywood J (2017). Left ventricular outflow tract velocity time integral outperforms ejection fraction and Doppler-derived cardiac output for predicting outcomes in a select advanced heart failure cohort. *Cardiovascular Ultrasound* **15,** 18. https://doi.org/10.1186/s12947-017-0109-4

Teicholz L, Kreulen T, Herman M & Gorlin R (1976). Problems in echocardiographic-angiographic correlations in the presence or absence of asynergy. *American Journal of Cardiology* **37,** 7–11. https://doi.org/10.1016/0002-9149(76)90491-4

Torre-Amione G, Kapadia S, Lee J, Durand J-B, Bies RD, Young JB & Mann DL (1996). Tumor necrosis factor-α and tumor necrosis factor receptors in the failing human heart. *Circulation* **93,** 704–711. https://doi.org/10.1161/01.cir.93.4.704

Tschöpe C & Van Linthout S (2014). New insights in (inter)cellular mechanisms by heart failure with preserved ejection fraction. *Current Heart Failure Reports* **11,** 436–444. https://doi.org/10.1007/s11897-014-0219-3

Tyagi SC (2000). Physiology and homeostasis of extracellular matrix: Cardiovascular adaptation and remodeling. *Pathophysiology* **7,** 177–182. https://doi.org/10.1016/s0928-4680(00)00046-8

Unudurthi SD, Luthra P, Bose RJC, McCarthy J & Kontaridis MI (2020). Cardiac inflammation in COVID-19: Lessons from heart failure. *Life Sciences* **260.** https://doi.org/10.1016/j.lfs.2020.118482

Van der Poll T, Shankar-Hari M & Wiersinga WJ (2021). The immunology of sepsis. *Immunity* **54,** 2450–2464. https://doi.org/10.1016/j.immuni.2021.10.012

Van der Poll T, van de Veerdonk FL, Scicluna BP & Netea MG (2017). The immunopathology of sepsis and potential therapeutic targets. *Nature Reviews Immunology* **17,** 407–420. https://doi.org/10.1038/nri.2017.36

Van Tassell BW, Seropian IM, Toldo S, Mezzaroma E & Abbate A (2013). Interleukin-1β induces a reversible cardiomyopathy in the mouse. *Inflammation Research* **62,** 637–640. https://doi.org/10.1007/s00011-013-0625-0

Wachtell K, Smith G, Gerdts E, Dahlöf B, Nieminen MS, Papademetriou V & Devereux RB (2000). Left ventricular filling patterns in patients with systemic hypertension and left ventricular hypertrophy (the LIFE study). *American Journal of Cardiology* **85,** 466–472. https://doi.org/10.1016/s0002-9149(99)00773-0

Wang HE, Shapiro NI, Griffin R, Safford MM, Judd S & Howard G (2012). Chronic medical conditions and risk of sepsis. *PLOS ONE* **7.**

https://doi.org/10.1371/journal.pone.0048307

Wang W, Hu X, Shen P, Zhang N & Fu Y (2017). Sodium houttuyfonate inhibits LPS-induced inflammatory response via suppressing TLR4/NF-κB signaling pathway in bovine mammary epithelial cells. *Microbial Pathogenesis* **107,** 12–16. https://doi.org/10.1016/j.micpath.2017.03.011

Weil BR, Herrmann JL, Abarbanell AM, Manukyan MC, Poynter JA & Meldrum DR (2011). Intravenous infusion of mesenchymal stem cells is associated with improved myocardial function during endotoxemia. *Shock* **36,** 235–241. https://doi.org/10.1097/SHK.0b013e318225f6ae

Westermann D, Lindner D, Kasner M, Zietsch C, Savvatis K, Escher F & Tschope C (2011). Cardiac inflammation contributes to changes in the extracellular matrix in patients with heart failure and normal ejection fraction. *Circulation: Heart Failure* **4,** 44–52. https://doi.org/10.1161/circheartfailure.109.931451

Wu B, Li J, Ni H, Zhuang X, Qi Z, Chen Q & Jin B (2018). TLR4 activation promotes the progression of experimental autoimmune myocarditis to dilated cardiomyopathy by inducing mitochondrial dynamic imbalance. *Oxidative Medicine and Cellular Longevity* **2018**. https://doi.org/10.1155/2018/3181278

Xianchu L, Lan Z, Ming L & Yanzhi M (2018). Protective effects of rutin on lipopolysaccharide-induced heart injury in mice. *Journal of Toxicological Sciences* **43,** 329–337. https://doi.org/10.2131/jts.43.329

Xiao Z, Kong B, Fang J, Qin T, Dai C, Shuai W & Huang H (2021). Ferrostatin-1 alleviates lipopolysaccharide-induced cardiac dysfunction. *Bioengineered* **12,** 9367–9376. https://doi.org/10.1080/21655979.2021.2001913

Yamamoto K, Masuyama T, Sakata Y, Nishikawa N, Mano T, Yoshida J & Hori M (2002). Myocardial stiffness is determined by ventricular fibrosis, but not by compensatory or excessive hypertrophy in hypertensive heart. *Cardiovascular Research* **55,** 76–82. https://doi.org/10.1016/s0008-6363(02)00341-3

Yucel C, Demir S, Demir M, Tufenk M, Nas K, Molnar F & Acarturk E (2015). Left ventricular hypertrophy and arterial stiffness in essential hypertension. *Bratislava Medical Journal* **116,** 714–718. https://doi.org/10.4149/bll_2015_140

Zaccone G, Tomasoni D, Italia L, Lombardi CM & Metra M (2021). Myocardial involvement in COVID-19: an interaction between comorbidities and heart failure with preserved ejection fraction. a further indication of the role of inflammation. *Current Heart Failure Reports* **18,** 99–106. https://doi.org/10.1007/s11897-021-00509-y

Zhang N, Feng H, Liao HH, Chen S, Yang Z, Deng W & Tang QZ (2018). Myricetin attenuated LPS induced cardiac injury in vivo and in vitro. *Phytotherapy Research* **32,** 459–470. https://doi.org/10.1002/ptr.5989

Zhang N, Tang L, Zhang L, Wang Q, Zhao L, Liu X & Wang C (2024). Evaluation of left ventricular stiffness with echocardiography. *Echocardiography* **41.** https://doi.org/10.1111/echo.15737

Zhang WB, Zhang HY, Zhang Q, Jiao FZ, Zhang H, Wang LW & Gong ZJ (2017). Glutamine ameliorates lipopolysaccharide-induced cardiac dysfunction by regulating the toll-like receptor 4/mitogen-activated protein kinase/nuclear factor-κB signaling pathway. *Experimental and Therapeutic Medicine* **14,** 5825–5832. https://doi.org/10.3892/etm.2017.5324

Zhao H, Zhang M, Zhou F, Cao W, Bi L, Xie Y & Wang S (2016). Cinnamaldehyde ameliorates LPS-induced cardiac dysfunction via TLR4-NOX4 pathway: The regulation of autophagy and ROS production. *Journal of Molecular and Cellular Cardiology* **101,** 11–24. https://doi.org/10.1016/j.yjmcc.2016.10.017

Zile MR, Baicu CF & Gaasch WH (2004). Diastolic heart failure — abnormalities in active relaxation and passive stiffness of the left ventricle. *New England Journal of Medicine* **350,** 1953–1959. https://doi.org/10.1056/nejmoa032566

Zile MR, Baicu CF, Ikonomidis JS, Stroud RE, Nietert PJ, Bradshaw AD & LeWinter MM (2015). Myocardial stiffness in patients with heart failure and a preserved ejection fraction contributions of collagen and titin. *Circulation* **131,** 1247–1259. https://doi.org/10.1161/circulationaha.114.013215

Zile MR, Gottdiener JS, Hetzel SJ, McMurray JJ, Komajda M, McKelvie R & Carson PE (2011). Prevalence and significance of alterations in cardiac structure and function in patients with heart failure and a preserved ejection fraction. *Circulation* **124,** 2491–2501. https://doi.org/10.1161/circulationaha.110.011031

Appendices

Appendix A Animal research ethics clearance certificate

ANIMALS RESEARCH ETHICS COMMITTEE (AREC)

UNIVERSITY OF THE WITWATERSRAND, JOHANNESBURG

STRICTLY CONFIDENTIAL

CLEARANCE CERTIFICATE NUMBER: 2022/05/03/C

APPLICANT: Ms K Fako
School: School of Physiology; Department: N/A; Location: WRAF

PROJECT TITLE: The effects of acute LPS-induced sepsis on cardiac morphology and function in a Wistar Kyoto and Spontaneously Hypertensive rats
Category: C; Species and Numbers involved: *48X 4-month-old, Male, Wistar Kyoto (WKY) Rats and 48X 4-month-old, Male, Spontaneously hypertensive rats (SHR)*

Approval is hereby given for the use of animals for the research project named above and described in the application reviewed by a quorate meeting of the AREC held on 31 May 2022. This approval remains valid until 29 Jun 2024 and is conditional to the following (if blank there are no special conditions):

Condition 1	Condition 2	Condition 3	Condition 4

All material changes to the approved research must be reported to the AREC before they are implemented. Failure to do so will invalidate this clearance certificate.

An annual progress report must be provided to the AREC.

The use of these animals is subject to AREC guidelines on the use and care of laboratory animals, is limited to the procedures described in the application and is subject to additional conditions listed below:

I, the Chair of the AREC (or my designated representative) am satisfied that the proposed research is ethical as judged by local law, international standards and University policy.

Signed: _____ Date: 30 June 2022
(Chairperson of the AREC)

I am satisfied that the persons listed in this application are competent to perform the procedures described in the application, in the context of Section 23 (1) (c) of the veterinary and Para-veterinary Professions Act (19 of 1982).

Signed: ___ _____ Date: __1/07/2022_____
(Registered Veterinarian)

CC: Student supervisor: «Title1» «Initials1» «Supervisor_surname»
Director Wits Research Animal Facility (WRAF): Dr Kim Jardine

Appendix B Assessment sheet used when monitoring animal sickness behaviour during the habituation period and after LPS administration.

	Score
Behavioural observations	
Activity	
Reluctant to move	1
Lethargy/apathy	2
Persistent immobility	3
Posture	
Normal	0
Huddled	1
Breathing	
Normal	0
Laboured	1
Gasping	2
Grooming	
Lack of grooming	1
Rough coat, nasal discharge	2
Very rough coat	3
Orbital tightening	
Orbital tightening not present	0
Orbital tightening moderately present	1
Orbital tightening obviously present	2
Vocalisation	
Vocalisation on handling	1
Vocalisation, tense and nervous on handling	2
Vocalisation on moving/spontaneous	3
Stool	

Normal	0
Diarrhoea	1
Blood on bedding	2
Eating / drinking	
Yes	0
No	1
Clinical signs	
Body weight	
Normal <3% weight loss	0
3-7% weight loss	1
8-11% weight loss	2
12-15% weight loss	3
>15% weight loss for longer than 5 days	HEP
Eyes	
Bright	0
Red rimmed	1
Dim	2
Nose	
Clear	0
Discharge	1

HEP: humane endpoint implemented. Animals will be humanely killed when the total assessment score is ≥ 22 for more than 3 consecutive days. In case of severe weight loss (>15%), the animal will be humanely killed.